Enhanced Optical Filter Design

Library of Congress Cataloging-in-Publication Data

Cushing, David.
Enhanced optical filter design / David Cushing.
p. cm. – (Press monograph ; 201)
Includes bibliographical references and index.
ISBN 978-0-8194-8358-4
1. Optical coatings. 2. Light filters. 3. Optical films. I. Title.
TS517.2.C87 2011
621.36'9–dc23

2011025875

Published by

SPIE
P.O. Box 10
Bellingham, Washington 98227-0010 USA
Phone: +1 360.676.3290
Fax: +1 360.647.1445
Email: Books@spie.org
Web: http://spie.org

Printed in the United States of America.

First Printing

Enhanced Optical Filter Design

David Cushing

SPIE PRESS

Bellingham, Washington USA

This book is dedicated to my wife, Helen,
who has helped me make the most of my life.

Contents

Foreword

The University of Arizona College of Optical Sciences got really lucky the day that Dave Cushing found us.

Dave and his wife, Helen, came to Tucson in 2004. It took them a while to pick a house in the area, though. Dave was insisting on finding one zoned for three-phase wiring, so he could install a custom-built coating machine in the garage. He planned to tinker with it as his retirement project. Unfortunately for Dave (maybe fortunately for Helen), the heavy-duty electrical setup in the new place just didn't work out.

That bad news turned into good news for us at COS. Not long after his arrival in Arizona, Dave met up with our director of development at an industry conference. Dave decided to take his coating machine out of storage and donate it to the college. According to Helen, he wanted students "to have hands-on experience, so they knew what they were doing."

We installed that machine on the fifth floor of the Meinel Building, where it rests today. Thus began a brief but extraordinarily meaningful friendship.

* * * * *

David Henry Cushing was born in Boston, Massachusetts, in 1940. He didn't talk much about his life growing up, but from what friends and family could tell, it wasn't great. "He grew up without anything," his wife said. "How he got to where he got is a mystery."

Dave and Helen met through friends and got married in 1961. They started their family right around the time Dave started college, so he chose to find a job to support the household while taking night classes. In a stroke of good luck, he ended up working with thin films pioneer Edgar Barr as a production technician at Baird Atomic, Inc.

It took him ten years to get his degree. By 1969, Dave Cushing had a staff of fifty workers, a BS in electrical engineering from Northeastern University, three children (with a fourth on the way) — and a passion for optical coatings research that would last for the rest of his life.

His next move was bold: he and a partner founded MicroCoatings, Inc. to produce filters for medical electronics and defense purposes. They used vacuum chambers to manufacture laser range finders, semiconductor lithography systems, printers, flame photometers, and supermarket scanners.

Over the next seventeen years, MicroCoatings Inc. became well known for the quality of its work — NASA used their filters in the Galileo and Voyager spacecrafts. When the company was acquired in 1986 by the Optical Corporation of America, Dave stayed on as technical director.

When he left OCA in 1990, he was immediately snapped up by JDS Fitel Inc. for their operation in Canada. According to Helen, JDS Fitel called every David Cushing in the phonebook until they found the right one, and they came to Dave and Helen's home the next day. So, with the kids all mostly grown, the pair headed off to Ottawa. At JDS Fitel, Dave designed equipment for the production of telecom filters and set up the first truly successful production shop for dense wavelength-division multiplexing filters.

In 2001, Dave and Helen moved to Cincinnati, Ohio, where he headed thin films research and development for Corning Precision Lenses. Then, after seven US patents, several worldwide patents, numerous publications, and forty-five years in thin films, David H. Cushing retired in 2004. He and Helen elected to spend their golden years in sunny Tucson, where he had attended many pleasant conferences during his career.

* * * * *

After donating his coating machine to the College of Optical Sciences, Dave came on board as a visiting scientist. He went into the lab for several hours each week, working with students and performing his own research. During his days in the Meinel Building, he spent more time with professor emeritus and fellow optical coatings expert H. Angus Macleod, whom he had known through most of his career.

"He was just an awfully nice person," Angus said, "really a very approachable guy who didn't mind sharing things he knew with people." The college was understandably shocked and saddened, then, by Dave's sudden death on Friday, November 20, 2009.

The last project that Dave worked on at OSC was a decorative Spectralonic coating using aluminum foil as a substrate, wherein vaporized materials were deposited on the metal in a vacuum chamber, forming a permanent layer that was nanometers thick. Dave and fellow artists Henry El Kaim and George Hubbard used the treated foil to make vivid, highly saturated wall sculptures that changed color with the angle of view.

An art gallery here in Tucson displayed a few of these pieces in a posthumous "Aurora Show," held in December 2009. Several more decorate the halls of the Meinel Building, including a place of honor on the sixth floor, not too far from Dave's coating machine. In my office, I keep one of his creations, which he gave me shortly before he died.

One of David's most lasting legacies, however, is the scholarship that Helen created at the College of Optical Sciences in his name, in memory of the many years they spent together and his passion for thin films. Each year, the award goes to an undergraduate student, preferably one interested in optical coatings, for

use toward tuition. Dave knew from his own experiences, after all, how important undergraduate training could be, and how much of a challenge it was to fund that training.

On April 25, 2011, with Helen Cushing present, we named Gregory Jacob the first winner of the David H. Cushing Endowed Scholarship in Optical Sciences. With the Cushings' generous support, the College of Optical Sciences looks forward to educating the next generation of passionate and personable engineers and optical scholars according to Dave's incredible example.

James C. Wyant, Dean
University of Arizona College of Optical Sciences
September 2011

From left, Carl Maes, Gregory Jacob, Helen Cushing, and James Wyant.

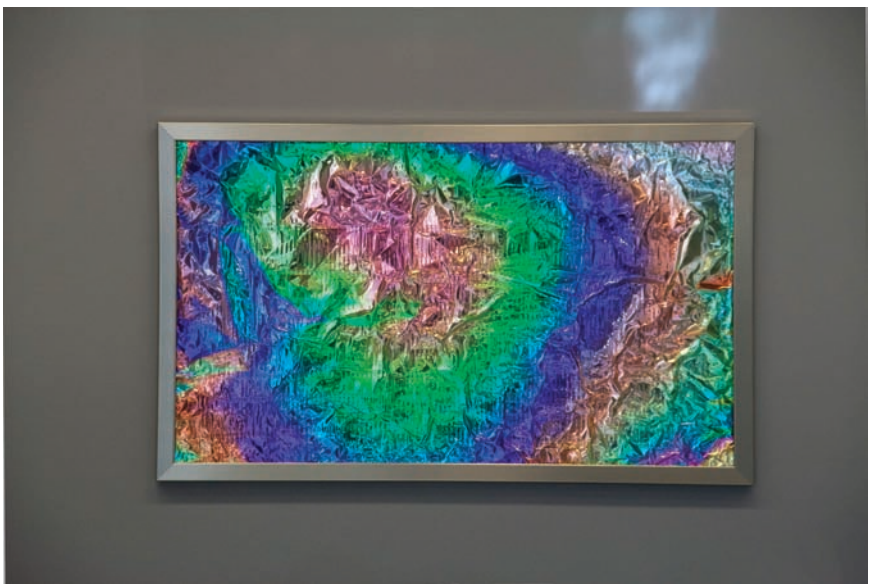

David Cushing's artwork, *Untitled*, on display at the University of Arizona College of Optical Sciences.

David Cushing's artwork, *Untitled*, on display at the University of Arizona College of Optical Sciences.

Preface

This book started as a short supplement to demonstrate how to improve the performance of coatings beyond the techniques described in the standard texts by Macleod and Baumeister. The coatings are designed with TFCalc®, but any of the available programs provide similar answers. The approach to designing is not mathematical in nature, but intuitive. I have more than 40 years experience building coatings and filters, and I mostly used an optical monitor as the primary control because the desired results were optical coatings, and other available methods of monitoring were unreliable. Early work used thermal sources without ion assistance, and the results for crystal monitoring were inconsistent. The stability of crystal monitoring has vastly improved with the energetic sources now available. This allows for nonquarterwave layers that can be counted on to be within a reasonable tolerance. I have made edge filters with 30 layers that follow the theoretical curves within a few nanometers of cutoff tolerance.

I have not manufactured many of the films described in this book; the concepts were originally depicted for papers presented at conferences. One can only present what is allowed by the employer(s). Typically, one cannot talk about the work that is currently being pursued, and the equipment for producing the described coatings may not be available when moving on to a new job. I anticipate that the designs are fairly easy to accomplish based on the work that I was able to do.

The designs were produced using TFCalc; copies of the designs, materials, and targets are supplied in the TFCalc format. I have also copied the designs into a new freeware program called OpenFilters. This program is available from École Polytechnique de Montréal, described in *Applied Optics* (Vol. 13, May 2008, p. c219). It is freely available on the website http://www.polymtl.ca/larfis.

The materials I used are also provided and need to be added to those given in the program. For the most part I have not supplied targets for these designs.

David Cushing
Tucson, Arizona
September 2009

Chapter 1
Basics

1.1 Introduction

Optical films are applied to surfaces and have the property of modifying the reflection (R) or transmission (T) of light at those surfaces. We observe a range of electromagnetic energy called visible light, but the full electromagnetic *spectrum* extends below to the ultraviolet spectrum, above to the infrared spectrum, and also beyond in both directions. Rules developed for optical filters work in these three spectral areas. Maxwell developed equations that explain the field theory for this branch of physics.

Places along the electromagnetic spectrum are identified in terms of wavelengths. The visible spectrum (the range of light that we see) extends from 380–780 nm (for color calculations). Higher-number wavelengths are in the infrared spectrum; lower-number wavelengths are in the ultraviolet spectrum (Fig. 1.1). The most prominent colors associated with these wavelengths are defined as

Violet	410 nm
Blue	460 nm
Green	515 nm
Yellow	570 nm
Orange	595 nm
Red	620 nm

Each color exists in a range (for example, red extends to about 750 nm), and as these ranges reach each other, what we think of as basic colors combine.

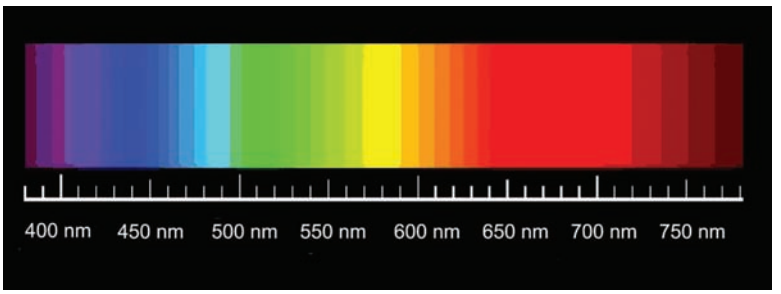

Figure 1.1 The visible spectrum.

An optical coating will typically have properties controlled for only one spectral area or aspect. An optical filter is one that passes some wavelengths of light and reflects or (hopefully) absorbs all others that can be detected. The opposite—when the optical filter reflects some wavelengths of light and passes all others—can also be required, but these are less likely to be achieved. In most cases, the filters discussed in this book are made by applying a multilayer film with a vacuum process onto a clear medium. A sheet of glass with transparency in the wavelength range that we wish to pass is used as a *substrate* on which to assemble the film. The films are used to either reduce or increase reflection for a limited range of wavelengths. Energetic plasmas may be added to the vacuum process for enhancement of the film properties.

1.2 Mathematical Models

Later in the book I will discuss *simple* equations for calculating $\%T$ (percent of transmission) or $\%R$ (percent of reflection) at a single wavelength. Excellent thin-film physics textbooks[1–3] are available that describe the mathematical methods of finding reflection and transmission. One method calculates the Fresnel coefficients and then relates them to reflection and transmission characteristics of the films. I will discuss only the optical properties of the solutions for this matrix math. A number of commercial programs are available to solve for the reflection and transmission of optical films. I use TFCalc to obtain the answers.

All materials have an effect on light. The *index of refraction n* for the material is derived by examining the reflection of the surface of the material. If light is absorbed, then the index derived is a complex number. See the above-referenced textbooks for more information about absorption. The reflection of a surface is defined by

$$\sqrt{R} = \frac{(n_s - n_i)}{(n_s + n_i)}.$$

The derivation is available in many physics books. n_i represents the index of air, which is assigned a value of 1. (If the coating were to be immersed in water, the index n_i would be 1.33.) For conventional glass the index of refraction n_s is generally 1.52, and the surface reflects ~4%. The index of substrates can range from 1.3–4. Glasses are usually between 1.45 and 1.9. Adding a film with index n_f to the substrate, the reflection at the quarterwave position is given by

$$\sqrt{R} = \frac{(n_i n_s - n_f^2)}{(n_i n_s + n_f^2)}. \text{ (Use the absolute value of the fraction.)}$$

1.3 Lower-Index Films

The case for a film examined in air deposited on a glass with an index of 1.52 is examined. If a film with an index of less than 1.52 is applied to the surface, the reflection will be reduced. If the index is equal to the square root of 1.52, the

reflection will disappear for one wavelength, and it will be very low for a large portion of the spectrum. Generally, the index values allowed by nature will not be this low (1.233 for glass).* For values between 1.233 and 1.52, the reflection is reduced, but not perfectly—how well depends on the ratio. For one wavelength the reflection value is a constant equal to the reflection of the bare glass. The film is defined as a *halfwave* thick at this point (400 nm for the curve). The curves in Fig. 1.2 illustrate this and also demonstrate the area of the low reflection, with maximum effect occurring at the quarterwave position (800 nm for the curve). The top curve is for the glass substrate with no coating. The value of *%R* changes with wavelength because the index of refraction used is from the real world. It has *dispersion*; that is, the index of refraction changes with wavelength. The lowest curve represents adding an index of 1.233 with a quarterwave thickness at 800 nm (in the near IR). The next higher curve represents a popular material used as a single-layer antireflection (AR) coating since the 1930s, magnesium fluoride ($n = 1.38$). The thick line is for a layer of quartz ($n = 1.46$), demonstrating that on its own, SiO_2 is not a good material for AR coating on glass.

1.4 High-Index Coatings

A series of curves for adding a high-index layer to a glass substrate is instructive (Fig. 1.3). The index varies by 0.10 increments at 2.06–1.66, and the lowest curve is the uncoated substrate. Reflection increases at the quarterwave position as the index increases and also for a significant part of the spectrum, but again, there is no change in reflection at the halfwave position. Even higher index values increase

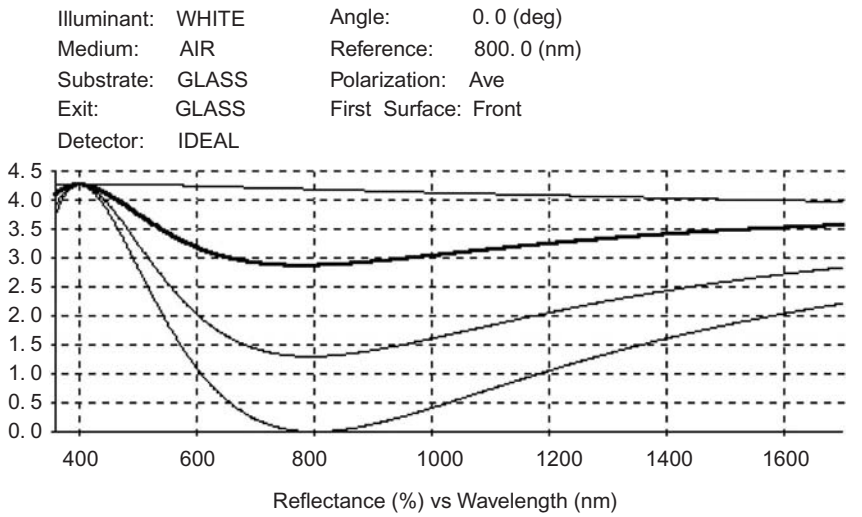

Figure 1.2 Low-index coatings.

*Lower index values can be produced with porous films. The indices for SiO_2 can be as low as 1.1. The techniques for making these films are beyond the scope of this book.

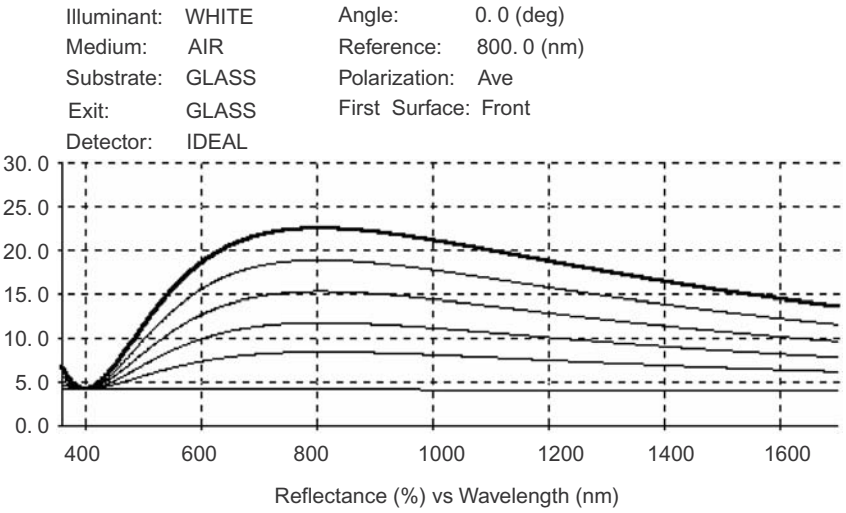

Figure 1.3 High-index coatings. From top to bottom, n = 2.06, 1.96, 1.86, 1.76, 1.66; The bottom line has no coating.

the reflection at the peak, but the curve follows a definite shape, and so the limits of performance need to be considered.

Much-higher-index materials are available for the infrared spectrum. The reflection from a single layer can be 40–80%. Multilayers are required to obtain higher reflections in the visible region.

1.5 Adding Layers

Using more than one material can allow for very low reflection for a small wavelength band. Quarterwave films of two materials will give no reflection if the proper materials are available. Nonquarterwave designs are possible for a wide range of index values. For the infrared spectrum, monitoring quarterwaves with a low-precision visible range optical monitor can easily make this type of AR coating. I will use Ta_2O_5 and SiO_2 for this demonstration. The first layer is high index, so the value can be between 2.0 and 2.5 and still yield $\ll$1% reflection. Altering the thickness ratio slightly would produce ~0% R. Real materials introduce dispersion, and the monitoring wavelength would be altered slightly to produce the desired results (Fig. 1.4).

The AR coating consists of one quarterwave of a high-index layer and four quarterwaves of low-index layer centered at *one-third of the desired wavelength* for the zero %R zone. For example, dividing a 1350-nm AR coating by 3 gives a 450-nm wavelength. Monitoring this is easily accomplished by stopping the layers at the maximum %R point (at 450 nm) twice—once for each material. A typical graph of the reflection for the film development is shown in Fig. 1.5. The high-index layer (n = 2.06) stops as the maximum %R is reached, and then the low-index layer (n = 1.46) starts. The first minimum is one quarterwave thick. The next

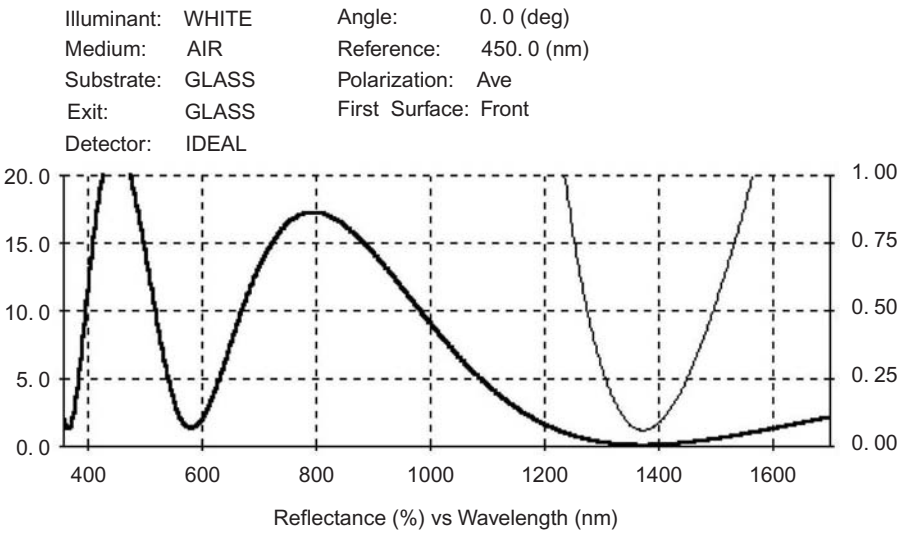

Figure 1.4 A two-layer AR coating (V-coat). Thick line: 20%R full scale; thin line: 1%R full scale.

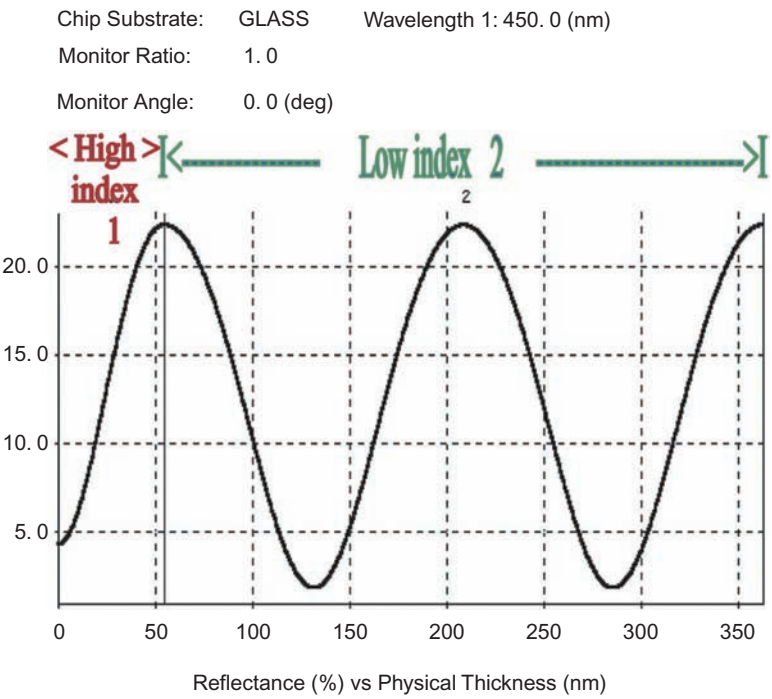

Figure 1.5 An optical monitor's change in $\%R$ as the film is applied (for a 450-nm wavelength).

maximum is two quarterwaves; three quarterwaves is at the next minimum; finally, the layer is stopped at the third maximum or the four-quarterwave point.

This simple technique provides a very consistent product as long as the materials have transparency at one-third the desired wavelength (using this indirect monitoring technique). I used this technique for a back-surface coat for wavelength-division-multiplexer (WDM) filters that work in air.

1.6 High-Reflection Coatings

For very high reflectances, many more layers are necessary in all-dielectric designs (I will not consider metallic films in this section). The films discussed here are transparent (the absorption coefficient $k = 0$), and the thickness of each layer will be a quarterwave at the design wavelength, which is the maximum effect for a film at this point. The ensemble can be considered as a multilayer stack. For a multilayer stack, this book will utilize the practical materials for today's technology. Tantalum pentoxide is selected as a high-index ($n = 2.06$) material, and quartz is selected, which deposits at $n = 1.46$. These are the preferred materials for high- and low-index films, respectively, used at the wavelengths for WDM filters.

Coatings that use only a few layers are called partial reflectors and are useful for beam splitting. Fewer layers than nine do not give a very high reflection. The stacks shown below (Fig. 1.6) contain an odd number of layers that start and end with a high index. Using HLHL (high, low, high, low) or LHLHL structures produces less reflection on glass substrates. The L layer on the end reduces the possible reflection, and an L layer for a first layer increases the reflection by a very small amount. When the layer count is high, the design is described symbolically as

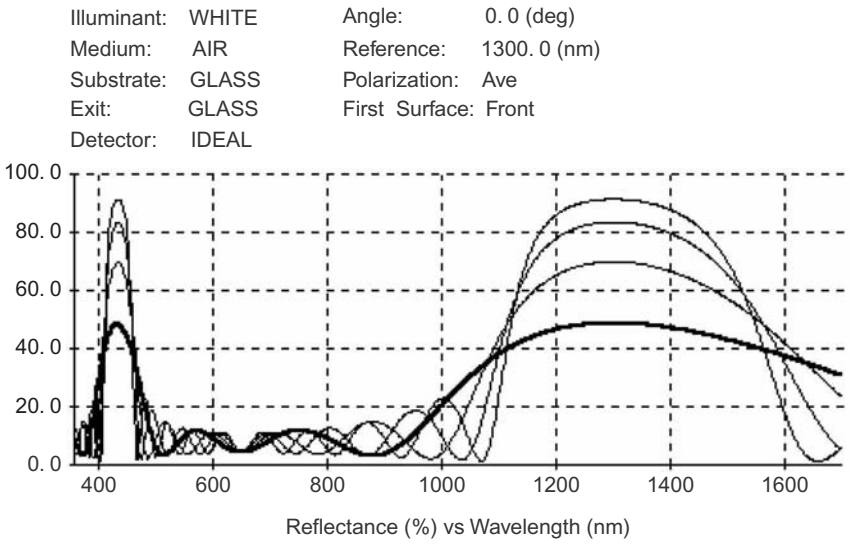

Figure 1.6 Partial reflectors. Various multilayer combinations: 3, 5, 7, and 9 layers. Reflection at 425 and 1300 nm increases with the number of layers.

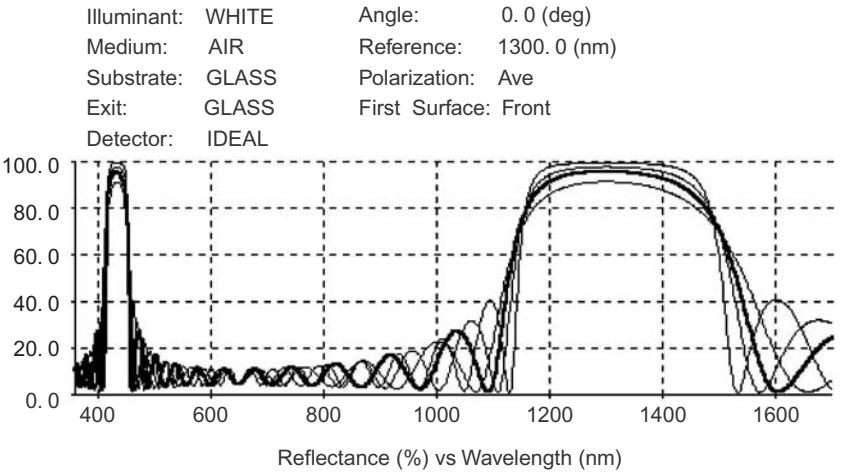

Figure 1.7 Various multilayer combinations. More layers: 9, 11, 13, and 17. Reflection at 400 and 1300 nm increases with the number of layers.

$(HL)^3$ for HLHLHL, where the superscript number is the number of repeats for the formula inside the parentheses. If the quarterwave position is altered from the reference wavelength, a multiplier can be positioned in front of the parenthesis, that is, $1.27(HL)^2$ represents 1.27H 1.27L 1.27H 1.27L. These formulas can be copied into most thin-film programs directly, and then the spectral response can be calculated. Consult your program manual for details.

The graph in Fig. 1.7 shows layer counts of 9-, 11-, 13-, and 17-layer quarterwave designs at 1300 nm. The 15-layer design is left out only for clarity. Changes in the reflection peak value become small. The halfwave position occurs at 650 nm, and the reflection for this wavelength is identical to that of glass alone. At the wavelength ~ one-third of 1300 nm, the curves go through the same reflection values as at 1300 nm. This spectral feature is called the third order. Higher orders are defined similarly. There are no large reflection peaks on the high-wavelength side.

1.7 Comments

The reflection band of the films moves to lower wavelengths if the light strikes the substrate at an angle. This effect is caused by differential phase shifting that alters the effective index of each material. For large angles, polarization may become an important consideration. The width of the 55-deg response is smaller for the *average* polarization of high reflection (Fig. 1.8). This film consists of three materials. The outer films are (ALA) where A has an index of 1.7. Thelen[4] wrote an article about notch filters and suggested using this approach to reduce reflection near the reflection zone. The technique is used to clarify how the shift of center wavelength with an angle for the high-reflection zone works in the graph.

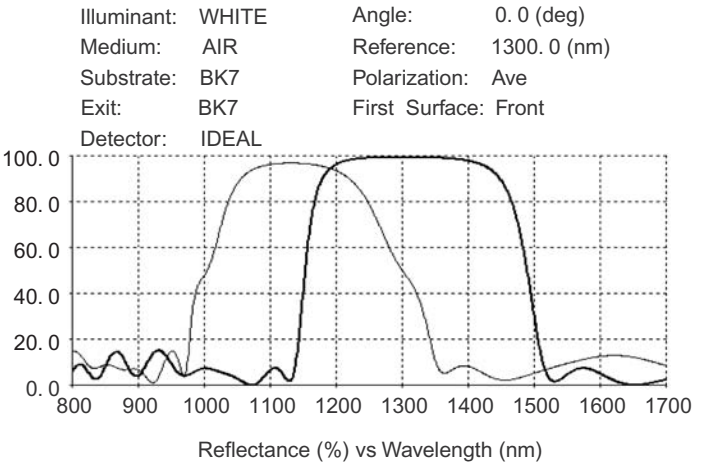

Figure 1.8 A 21-layer film at 55 deg and *normal incidence*. The thick line is the reflection at the 0-deg angle; the thin line is reflection at the 55-deg angle.

The crude design is (ALA) $(LH)^7$ L (ALA). H and L are still 2.06 and 1.46, respectively. All interference filters display this angle-shift property to some degree, and some metal dielectric filters are less angle sensitive.

References

1. P. W. Baumeister, *Optical Coating Technology*, SPIE Press, Bellingham, Washington (2004) [doi:10.1117/3.548071].
2. H. A. Macleod, *Thin Film Optical Filters*, 3rd ed., McGraw-Hill, New York (2001).
3. A. J. Thelen, *Design of Optical Interference Coatings*, McGraw-Hill, New York (1989).
4. A. J. Thelen, "Non-polarizing edge filters," *J. Opt. Soc. Am.* **71**, 309–314 (1981).

Chapter 2
Methods of Deposition and Materials Used

Films can be created by a variety of methods. In this chapter I will describe the ones that are familiar to me, in order of complexity. For all methods of vapor deposition, wavelength stability over time is important; it may be achieved with the careful selection of a starting material and, possibly, some processing before adding the chemicals to the coater.

2.1 Vapor Deposition Methods

2.1.1 Thermal deposit

For many years I have been making filters that have remarkable wavelength stability. The use of zinc sulphide or zinc selenide for high-index films and mixed fluorides or thorium fluoride for low-index films will produce stable bandpass filters when the substrate has been heated to approximately 110 °C. The chemicals are heated to deposit in stainless steel crucibles after pressing the materials into the crucible to improve density. A tungsten spiral filament is positioned over the crucible, and a few amperes at 115 V transformed to 5–20 V will heat the surface to evaporation. The sulphides sublime, and the fluorides melt. Other methods of heating the chemicals can work just as well. After a filter has been deposited, the stability can be guaranteed by heating the filter to approximately 250 °C for a few hours. If the conditions for a stable film have been met, the wavelength should not have shifted more than 1–2 nm. This baking provides a densification of the films. For filters manufactured with cryolite and other mixed fluorides, the best condition for use and storage is in an epoxy medium. Films will survive in air, but they are easy to scratch. Also, if the substrate was not perfectly clean before deposition, there will be a possible pinhole problem over time. If a surface has mobility, there is an opportunity for trouble.

The thermal coefficient of expansion for thermally deposited films cannot be reduced to zero, and this limits their use even though the films are simple to deposit compared to other methods of deposition. The advantage of these films is lack of stress for certain combinations of materials. I have found that the reflective metals are best deposited by the resistance sources; the films are the coldest and the smoothest in a normal deposition sequence.

2.1.2 Electron beam

For more durable coatings and filters, the chemicals are deposited from crucibles in an electron-beam (e-beam) gun. Refractory oxides may be deposited for AR coatings and ultraviolet filters, which are very durable when the substrate is heated. Some chemicals require the addition of oxygen to the chamber in order to achieve low absorption (TiO_2, in particular), and temperatures up to 300 °C may be needed to raise the refractive index to a high value. The resulting films are porous and have a columnar structure, and the wavelength of the film arrays can increase by as much as 5% when the film is kept in room-temperature air. Water fills the voids, and there are both permanent and transitory refractive-index changes in the films. Heating the filters causes a temporary *negative* shift in wavelength as some of the water leaves the surface. A variety of chemicals may be deposited with e-beam technology, including many metals.

2.1.3 Ion-aided deposition

In order to make the films high density, the substrate can be bombarded with a gas that is ionized during deposition. An ion source of the end-hall type has energy in the proper electron volt range to peen the film so that there is no room for voids. The oxides and metals harden with this process. Fluorides absorb light through film breakdown when more than a small electron flow is used. After venting the chamber, there is generally a very small change in wavelength for all of the film types. The film is created at a temperature of about 125 °C; stress alters the wavelength when the substrate returns to room temperature. The deposition conditions will most likely not be perfect throughout the whole filter deposition, and the film also undergoes minor changes in stress over a short period of time. Afterward, the films are quite stable as long as the filter is not heated above some temperature threshold—typically 250–400 °C. Permanent small wavelength changes may occur after the high-temperature heating due to densification of the films through stress relief. Manufacturers adjust the wavelength of filters by controlled baking of the filters after they are cut to the final dimension. Changes in crystallization may occur at even higher temperatures that alter the index of refraction of the films, resulting in a changed recipe. Each material has its own rate of index change, and for high-precision filters the transmission profile suffers.

Another variation of the e-beam deposition process is ion plating. Oerlikon Balzers made a unit for oxide film deposition. The unit has not been manufactured for a while but may become available again. The densest smooth films with the most stress are made with this approach.

2.1.4 Oerlikon Leybold advanced plasma source

Oerlikon Leybold manufactures a large box coater that densifies e-beam-deposited films with their advanced plasma source (APS). Oxygen and argon are ionized and energized in a plasma that fills the chamber. Large areas of substrates can be coated with multilayers; the uniformity is controlled with masks.

2.1.5 Sputtered films

The sputtering process utilizes either a metallic or conducting ceramic target with gas added to the chamber to establish a plasma. Oxides are produced by reactive evaporation to create a stoichiometric film. Each material requires its own source. High-quality films with hundreds of layers can be deposited; this process requires fine tuning to obtain good results.

2.1.6 Ion-beam sputtering

If the energy to melt the chemicals is supplied by an ion source—and possibly densified with another ion source—smooth films are created. This process can be used with a high degree of thickness precision; very complex filters are routinely manufactured with this technique. Masking is needed to achieve uniform films for conventional filters. There are newer processes available.

2.2 Stable Films for Wavelength-Division-Multiplexer-Type Applications

One area in which I did a lot of work was manufacturing filters for WDM fiber-optic applications. Films can be made with complete wavelength stability over time from all methods of vapor deposition, and the difference between methods can yield other useful properties. The thermal coefficient of expansion for *thermally* deposited films cannot be reduced to zero; this limits their use even though the films are simple to deposit in comparison to other methods of deposition. The advantage of these films is the lack of stress for certain combinations of materials.

2.2.1 Thermal deposit

Visible filters composed of zinc sulphide or zinc selenide for high-index films and mixed fluorides for low-index films produce stable bandpass filters when the substrate has been heated to about 80 °C. After a filter has been deposited, the stability can be guaranteed by heating the filter to about 120 °C for a few hours. If the conditions for a stable film have been met, the wavelength should not have shifted more than 0.1–0.2 nm. For filters manufactured with cryolite, the film should be cemented with epoxy. As indicated in the introductory section, WDM filters can be assembled with low-index films that are composed of mixtures of various fluorides. The films for WDMs were made using this approach with thorium fluoride for the low index at the 125 °C temperature point. After a filter has been deposited, the stability can be guaranteed by heating the filter to about 250 °C for a few hours. If the conditions for a stable film have been met, the wavelength should not have shifted more than 1–2 nm. Filters made with resistance sources have a large positive thermal coefficient due to the nature of the film structure.

2.2.2 Electron beam

In order to make films with zero change in wavelength for any temperature change, I investigated alternative deposition methods. Oxide materials can be stabilized by

adding energy to the substrate during the deposition process. In 1994 I purchased filters made with ion-assisted deposition (IAD), but the films were not as stable as I wanted.

Filters were then developed with a Balzer ion plater (IP), which consisted of layers of tantalum pentoxide (see Table 2.2 and Fig. 2.1) and quartz and could be heated to 450 °C before permanent changes occurred. The crystal structure was modified at this point; however, this IP process was expensive to maintain, and another problem with the filter was very high stress. The substrates bend badly when they are thin.

I then investigated the use of a Leybold APS to produce filters made with titanium oxide and quartz. Wideband filters with 40–60 layers were deposited on 6-in square substrates with reasonable results. The films still had stress, but not quite as much as those made with IP. Good filters were fabricated that had a small loss. Establishing truly stable conditions is a long process. The films need to be analyzed frequently over at least a two-month period to verify their stability (see Table 2.3, Fig. 2.2). To improve on the final filter transmission, niobium oxide was substituted as a high index. Loss was better overall, and the film had a good, consistent, high index. Leybold sells their APS systems for WDM applications with tantalum oxide used as the high-index material. The index is lower than that of niobium oxide, but loss is almost zero at the design wavelengths. Many APS systems have been sold that will make filters with bandwidths as narrow as 50 GHz; these filters contain about 150 layers. The plasma source is expensive to maintain both in cost and time. The yield is about a 15-mm diameter for 100-GHz filters.

The end-hall ion sources have been improved, and a few companies sell them. Commonwealth Scientific presented a paper comparing the results of a round robin test for depositing a high-index coating. The agency reports that their Mark II source gave the best results, but I cannot confirm this. I have used one of their sources with a Kaufman power supply and obtained good TiO_2 films but not as good as the reported results.

2.2.3 Sputtered films

In 1997 it became necessary to develop a coater for high production of WDM filters. JDS Uniphase selected pulsed magnetron sputtering with IAD as the technology of choice. Film properties can be determined with high certainty, and the deposition conditions are predictable. An annulus about 1-in wide on a 16-in diameter can be coated to produce a filter with a center-wavelength variation of about +/−0.1 nm. Better results are possible with careful coater preparation and precise control of source position. Filters for coarse wavelength-division multiplexing (CWDM) do not require as close a tolerance on wavelength. The useful area for filters will be larger; 2–4-in annuluses are possible. Filters with an excess of 200 layers have been deposited by sputtering, but continuous operation for 40 hours was required; the resulting films have some loss.

If no loss in the filter were a true necessity, the film would have to be deposited from an oxide mode rather than a metallic mode or with a ceramic target. However,

oxide-mode films might take about five times longer to deposit. Reports on ceramic targets to make an oxide conductive are encouraging.

2.2.4 Ion-beam sputtering

At this point the best technology for providing low-loss films would be ion-beam sputtering (IBS). Control of both the film thickness and the uniformity are more difficult because of the nature of ion-beam optics and targets. Most WDM filter manufacturers have purchased these machines for research but do not obtain many square inches of quality films. If I had to make the narrow filters, I would use pulsed magnetrons and fully oxidized films.

Many filter manufacturers use the IBS coaters to make high-quality filters for other applications. Tolerances for edge filters can be demanding, but the uniformity can apparently be controlled. There are a few companies that sell these films.

2.3 Materials

The chemicals with which I am familiar are discussed alphabetically. They include metals, dielectrics, and semiconductors.

Aluminum. (Table 2.7) This is the most-used metal for mirrors and is also the only choice for use in UV filters. Aluminum is fairly easy to evaporate with resistance coils. I use four-strand Tungsten wire. Standard coils are only three-strand and offer less surface area for the metal to wet when the charge is melted. Five or six coils can hold four ~3/4-in lengths of 1-mm-diameter aluminum wire. If the distance to the substrate is about 18 in, an opaque layer can be formed. The technique for performing a deposition is examined in Chapter 6.

Aluminum fluoride. This is a useful low-index material, especially for the low-UV region. When mixed with other fluorides, stable films are possible.

Aluminum oxide. I use Al_2O_3 as an intermediate index in AR coatings that are coated at 300 °C and as a high index for UV filters and coatings in the 185–220 nm range. It is easily evaporated with an e-beam gun and can also be utilized in simple silver filters as a spacer layer. The index is ~1.6–1.75 depending on wavelength and temperature.

Cerium fluoride. This is an intermediate-index material for the low-UV region and can be used as Al_2O_3 is used.

Chromium. This metal sublimes from the crucible of an e-beam gun. Small quantities of the metal may be resistance heated from a plated tungsten rod. Chromium (Cr) is useful as a sticking layer for silver and gold mirrors. It is also used as a sticking layer for plastic substrates before applying dielectric layers.

Cryolite. This is the low-index material used for soft-coating technology. The index is about 1.3, and the films are transparent from below 200 nm to beyond 2500 nm. Thick films will stress crack, so equivalent-layer multilayers must be used as an infrared quarterwave layer. This compound is only available as a synthetic chemical and must be baked at about 900–1200 °C for a few hours to remove

moisture. The compound reacts with quartz and cheap ceramic crucibles, so if these materials are used they must be discarded frequently. The films are water soluble and require protection from direct contact with moisture. Do not breathe on these films.

Germanium. This is a very high-index material that is transparent from ~1800 nm to the far infrared. It may be resistance heated from a tungsten boat or from a crucible in an e-beam hearth. This is the major film material for infrared filters and is combined with SiO, SiO_2, and ZnS for multilayers.

Gold. Gold can be used for stable but soft mirrors for the infrared. Chromium is used as the sticking layer most of time. A protective layer made of a variety of fluorides is recommended. The film will still be soft because for reflectivity reasons only thin overcoats are used.

Hafnium oxide (see Table 2.5, Fig. 2.4). For the 220–400-nm region, this is the high-index material of choice. The index is about 2.0, and the film may be applied with an e-beam gun; the index varies with the temperature of the substrate and the method of deposition. Filters with more than 100 layers are deposited with ion-beam deposition, but I have not performed this method.

Inconel®. This is an alloy that is easy to e-beam evaporate. It is useful as a sticking layer and a neutral-density layer or component (see Table 2.6).

Indium tin oxide. Indium tin oxide is a transparent conductive film with an index of about 2.0; it can be e-beam coated or sputtered. Replacements for this compound are sought because indium is expensive and difficult to obtain.

Lanthanum fluoride. This is an intermediate but higher-index material for the low UV. Use in the same manner as Al_2O_3.

Lead fluoride. Lead fluoride is used with cryolite for UV filters. A platinum liner in a resistance source with something to tie the material in place is very effective for evaporation. Filters made with this material lose some transmission immediately on venting the chamber, and the filter then stabilizes. One of the workhorses at filter companies, the index is ~1.75. Lead fluoride is toxic.

Magnesium fluoride (see Table 2.1). This has been the most-used substance for coated optics since the 1940s. The index is ~1.38 when applied to a heated substrate. I use it extensively as the spacer for UV metal filters and as a component in multilayer AR coatings. It is easily evaporated with resistance sources and by e-beam. Ion assist will allow room-temperature coating with reasonable stability and hardness. More information on AR coating for nonpolarizing filters can be found in Chapter 3.

Nickel. This metal can be used as an e-beam evaporate or sputter.

Niobium oxide. A high-index coating material that has been evaporated by e-beam with IAD or by reactive sputtering from the metal. The index is about 2.3, and the material is useful at ~400–2000 nm. I used niobium oxide to make WDM filters and AR coats because the absorption is low and the layers are easy to control.

Silicon. High-index films with an index >3 can be sputtered or e-beam evaporated. Films are fully transparent above 1000 nm. Vacuum must be ~6–10 Torr to stop or retard oxide formation.

Silicon dioxide. This is quartz (SiO_2). The index is ~1.45–1.49 depending on the density and IAD conditions. Easily evaporated with e-beam, reactive-sputtered Si is easy to control and makes stable films when combined with a number of high-index oxides.

Silicon monoxide. SiO is used to make a film with an index of ~1.8 in the infrared. It sublimes, uses resistance or e-beam sources, and works well in combination with Ge for infrared filters.

Silver. (Table 2.8) Silver is a useful metal for visible and infrared applications. It requires both a sticking layer and a protective layer; the bare film is reactive to atmospheric elements. Silver produces the highest reflection for metals and is extensively used in solar applications. The best films are formed with a molybdenum boat that has been resistance heated.

Tantalum pentoxide. Films formed by reactive sputtering or IAD e-beam provide an index of ~2.06 for use at the 1550-nm range. Many WDM filters are made by combining Ta_2O_5 with SiO_2. The films made with IBS are useful at ~320 nm and above.

Zinc sulphide. ZnS is used extensively for visible and infrared filters and easily evaporates (sublimes) by a variety of resistance sources. The index is 2.2–2.5 depending on temperature and wavelength. The film will not stick if the temperature of the substrate is above 150 °C. I used zinc sulphide to make filters that flew on the Voyager and Galileo spacecraft missions.

Zirconium oxide. This material is useful for filters for the 250–400-nm range. The index is between 1.8 and 2.1. An e-beam evaporates at some elevated substrate temperature ~80–200 °C. It is not easy to control uniformity for multilayers because it sublimes. Dobrolowsky recommends e-beam evaporating Zircaloy™ reactively to achieve a higher index with good control of the process.

2.4 Dispersive Index Values

Table 2.1 lists the values used throughout this book. The low-index chemicals generally have low dispersion; the exact index is dependent on process parameters. Graphs of dispersion (and data) for selected high-index materials are displayed in Figs. 2.1–2.4 and Tables 2.2–2.8. The deposition process used is indicated in Section 2.2.1. Use of this data is appropriate for the designs shown in the remainder of the book.

Table 2.1 Optical Constants of MgF_2 and SiO_2.

MgF_2		SiO_2	
Wavelength	Index	Wavelength	Index
180.0	1.44	190.0	1.55
190.0	1.43	250.0	1.5
200.0	1.422	300.0	1.485
225.0	1.408	400.0	1.465
250.0	1.401	530.0	1.455
275.0	1.397	1000.0	1.435
300.0	1.393	1600.0	1.425
350.0	1.387	2000.0	1.42
400.0	1.382	2500.0	1.415
450.0	1.381		
600.0	1.38		
1000.0	1.375		
1600.0	1.37		
2000.0	1.367		
2100.0	1.367		

Table 2.2 Optical constants of Ta_2O_5 (IBS).

Wavelength	*n*	*k*
200	2.5	0.4
225	2.5	0.37
250	2.5	0.3
260	2.6	0.24
270	2.65	0.12
280	2.6	0.05
290	2.55	0.013
300	2.48	0.004
320	2.38	0.002
350	2.29	0.000700
400	2.22	0.000400
450	2.17	0
500	2.145	0
600	2.11	0
700	2.09	0
1000	2.06	0
1550	2.04	0
2000	2.03	0

Table 2.3 Nb_2O_5 (sputtered).

Wavelength	*n*	*k*
190	2.5	0.2
250	2.5	0.15
270	2.5	0.11
300	3.2	0.05
330	3	0.02
350	2.7	0.009
360	2.6	0.005
365	2.55	0.00330
370	2.515	0.00220
380	2.47	0.000900
390	2.433	0.000300
410	2.4	0.0000400
450	2.365	0.000025
520	2.308	0.000022
600	2.265	0.00002
750	2.213	0.00002
980	2.18	0.000013
1500	2.166	0.000001
2000	2.16	0.000001

Table 2.4 Optical constants of Ti_2O_3 (ion assisted).

Wavelength	*n*	*k*
190	3	0.37
250	3	0.37
320	3.03	0.25
340	2.73	0.06
360	2.63	0.012
380	2.55	0.0027
405	2.465	0.000600
415	2.44	0.000450
435	2.41	0.000330
480	2.35	0.000250
580	2.28	0.000210
800	2.23	0.000160
1060	2.21	0.000130

Table 2.5 Optical constants of HfO_2 (e-beam with low heat).

Wavelength	*n*	*k*
180	2.337	0.5
200	2.27	0.07
210	2.24	0.02
220	2.216	0.00650
230	2.195	0.00230
240	2.177	0.00120
250	2.16	0.000700
300	2.097	0.000110
350	2.059	0.0000810
400	2.033	0.0000100
600	1.986	0.0000100
800	1.97	0.0000100
1000	1.962	0.0000100
4000	1.95	0.0000100

Table 2.6 Optical constants of Iconel.

Wavelength	*n*	*k*
200	1.05	2.4
250	1.1	2.3
300	1.9	1.86
350	1.75	2.1
400	1.8	2.25
450	1.9	2.4
500	2.05	2.47
550	2.15	2.54
600	2.25	2.57
650	2.4	2.56
700	2.5	2.51
1000	2.9	2.15
1500	3.3	2.25
2000	3.7	2.3
3000	4.1	2.4
10000	6	2.4

Table 2.7 Optical constants of aluminium.

Wavelength	*n*	*k*
170	0.095	1.763
190	0.115	2.031
220	0.14	2.35
240	0.16	2.6
260	0.19	2.85
280	0.22	3.13
300	0.25	3.33
320	0.28	3.56
340	0.31	3.8
360	0.34	4.01
380	0.37	4.25
400	0.4	4.45
436	0.47	4.84
450	0.51	5
492	0.64	5.5
546	0.82	5.99
577	0.93	6.33
650	1.3	7.11
700	1.55	7
750	1.8	7.12
800	1.99	7.05
850	2.08	7.15
900	1.96	7.7
950	1.75	8.5
2000	2.3	16.5
4000	6.1	30.4
6000	10.8	42.6
8000	17.9	55.3
10000	26	67.3
12000	33.1	78

Table 2.8 Optical constants of silver.

Wavelength	*n*	*k*
301	1.34	0.971
311	1.13	0.623
320	0.81	0.4
325	0.7	0.41
328	0.6	0.42
331.4	0.26	0.5
342.4	0.155	1.14
354.1	0.115	1.426
367.8	0.09	1.664
381.4	0.08	1.871
397.3	0.075	2.077
413.2	0.071	2.282
430.4	0.0665	2.469
450.7	0.0635	2.664
471.3	0.063	2.876
495.8	0.0625	3.1
520.8	0.064	3.331
548.5	0.065	3.593
581.9	0.066	3.865
616.7	0.069	4.159
659.3	0.074	4.49
704.3	0.081	4.845
755.8	0.09	5.249
820.9	0.1	5.734
891.7	0.12	6.319
983.7	0.14	7
1087.3	0.17	7.8

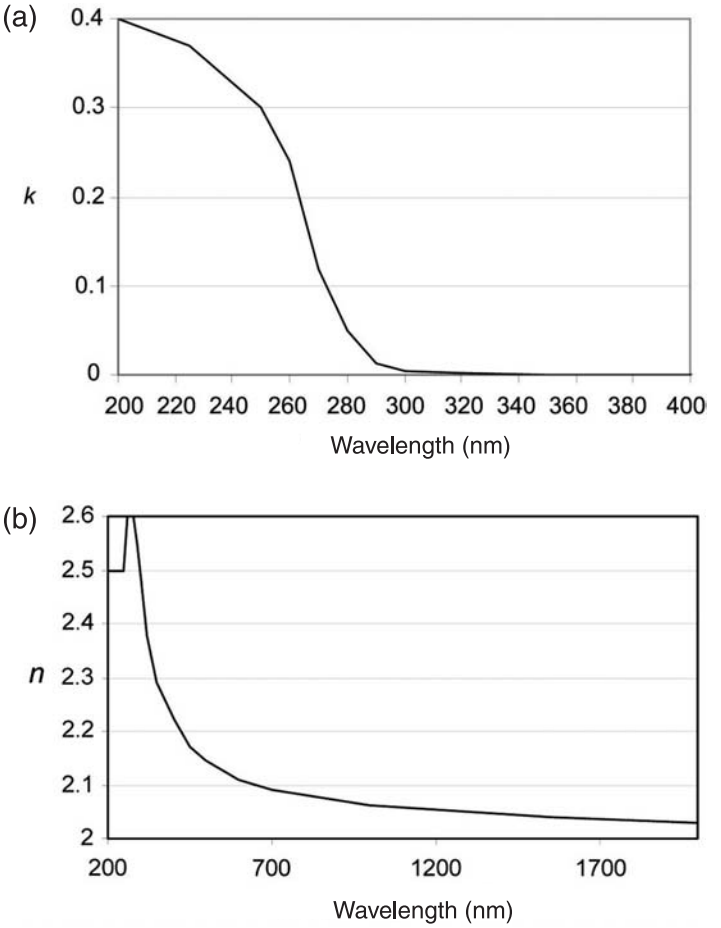

Figure 2.1 (a) k vs wavelength in Ta_2O_5 (IBS). (b) n vs wavelength in Ta_2O_5 (IBS).

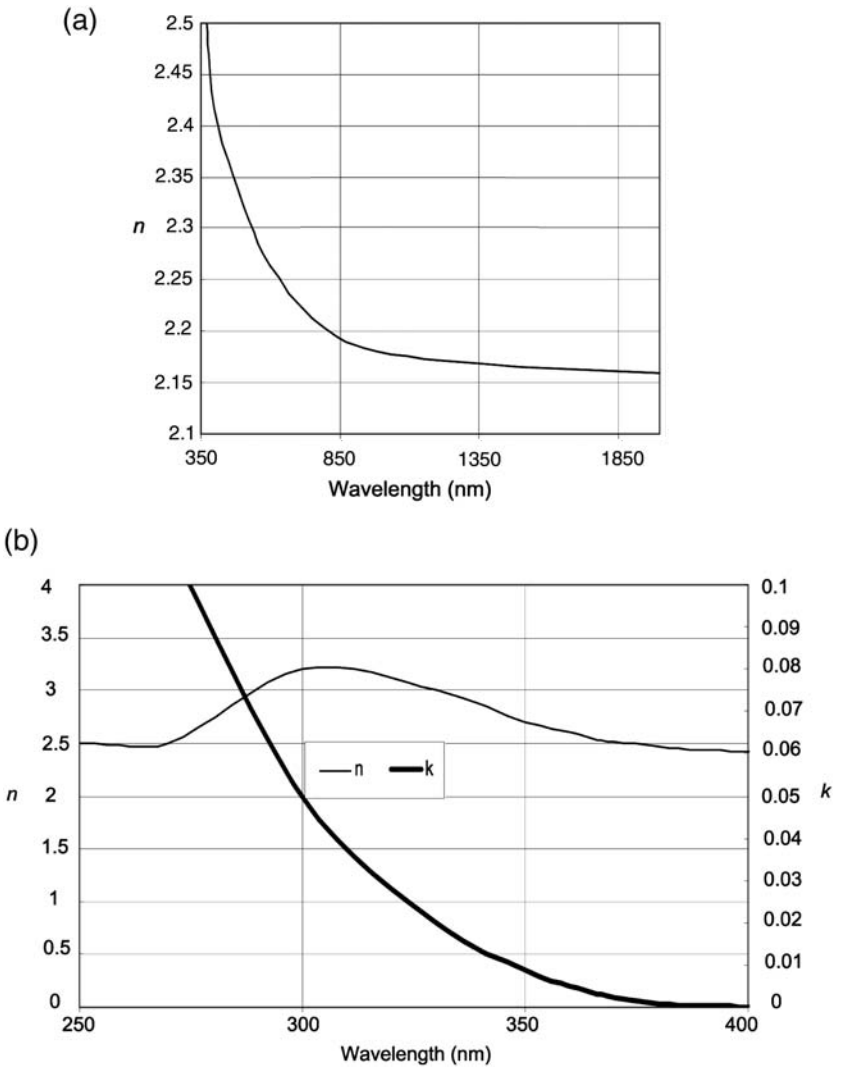

Figure 2.2 (a) n vs wavelength in Nb_2O_5. (b) n and k vs wavelength in Nb_2O_5.

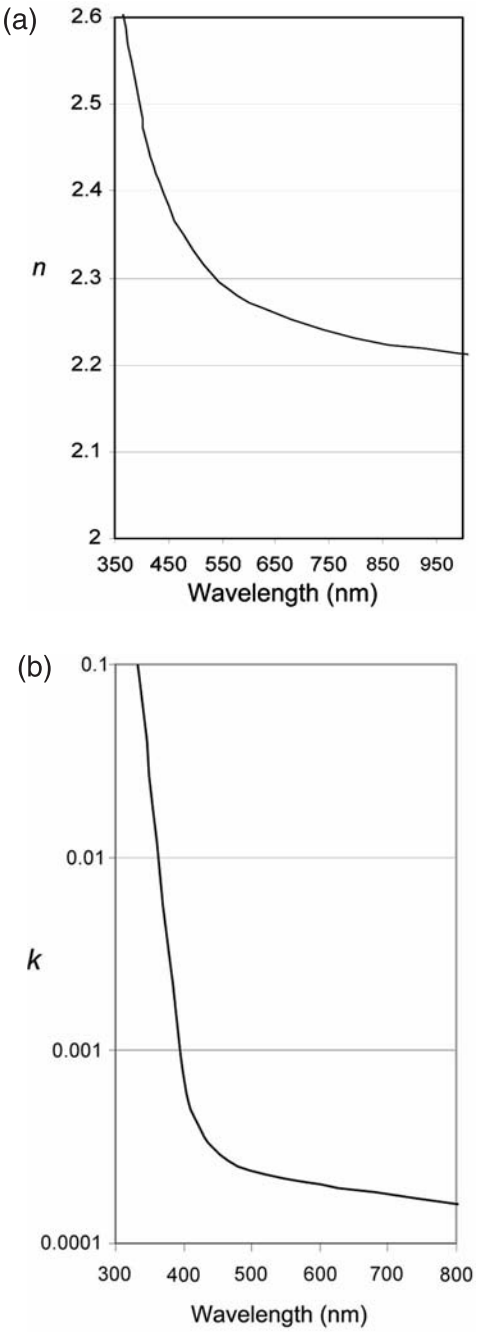

Figure 2.3 (a) n vs wavelength in Ti_2O_3. (b) k vs wavelength in Ti_2O_3.

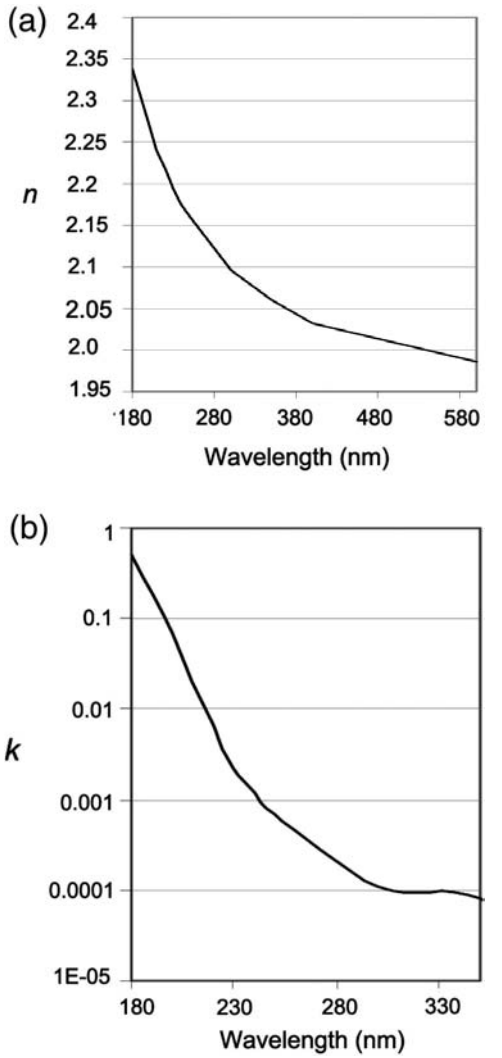

Figure 2.4 (a) n vs wavelength in HfO_2. (b) k vs wavelength in HfO_2.

Chapter 3
Antireflection Coatings

3.1 Introduction

The purpose of AR coatings is twofold: improvement in transmitted energy and a simultaneous reduction of reflected light, typically for the widest possible spectral region. If there are many optical elements in a system, the energy lost through reflection can be substantial. Laser systems need to be loss free and generally at discrete wavelengths; I do not examine those systems. The main property of optical materials is the index of refraction. The production lenses have index values between 1.4 and 1.95; the designs shown are mostly for crown glass (BK7) with a nominal index of 1.52. In this chapter, I examine the visible (light) spectrum for most of the coatings. The eye is not very sensitive to light below 425 nm or above 625 nm, so AR coatings for people are designed to function well only within this range. If the coatings are to be used with cameras or CCDs, the effective range may need adjustment. To judge the surface treatment quality, the amount of light that is reflected or transmitted is calculated for the spectral area of interest, and then comparisons can be made.

3.2 Single-Layer Coatings

The simplest durable coating to reduce reflection consists of a single quarterwave-thickness layer of material that has an index of refraction that approaches the square root of the index of the (glass or plastic) element. For common (BK7) glass, the index is 1.52 (in the middle of the spectrum), and the coating that removes reflection has an index of 1.23. This index is not possible for any durable material, so there will always be some reflection from this type of coating on lower-index elements. Porous coatings are not considered here. The thick line in Fig. 3.1 shows the performance of this quarterwave coating for the visible spectrum (for which AR coatings are typically designed). These reflectance curves are shown only for one coated side, and the quarterwave thickness for designs refer to the reference wavelength in the graph. The glass type BK7 reflects ~4.25%, as indicated by the thick line in Fig. 3.1. The lower line would be the ultimate coating that cannot be attained with a durable coating material. The material of choice from the point of view of durability is SiO_2. However, the reflection from this substance on glass is too high, about 2.5–3%, which is unacceptable. The coating material that is used extensively is magnesium fluoride (MgF_2), which has an index of 1.38

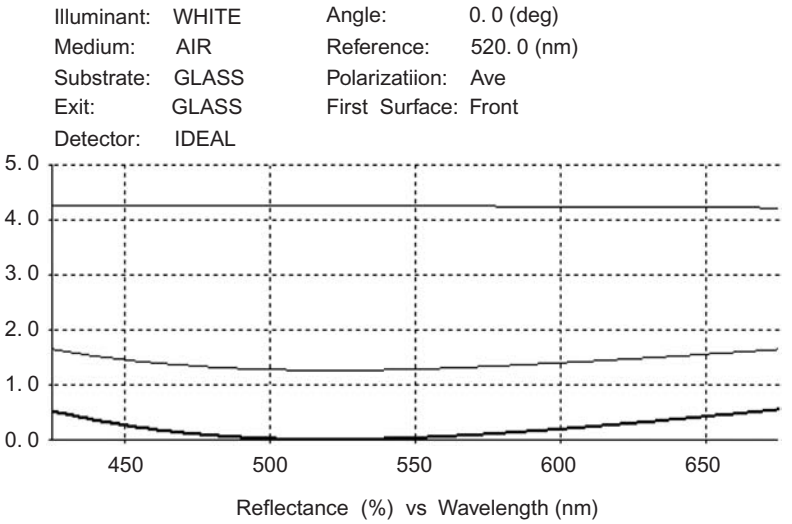

Figure 3.1 AR coats and %R of BK7 glass.

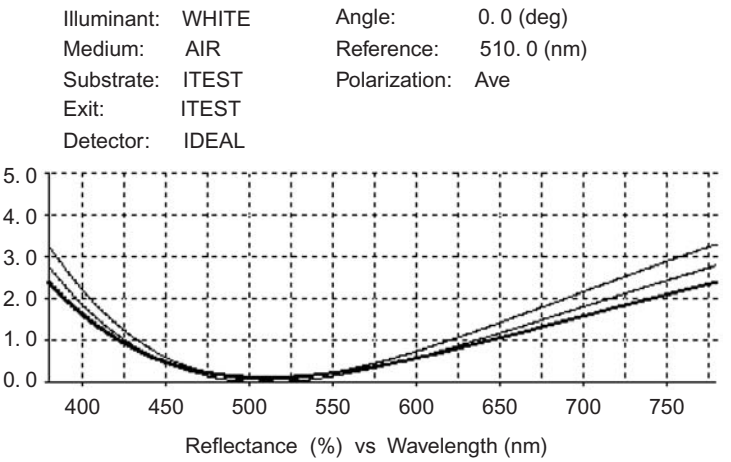

Figure 3.2 MgF_2 quarterwaves on varying-index glasses: 1.8; 1.9; and 2.0 (top to bottom). The reflection values between 425 and 650 nm are reasonable.

and a reasonable hardness compared to other materials in the same index range. Reflection is about 1.5% as shown by the middle curve in Fig. 3.1, which is still too high for the quality demanded by today's industry. For higher-index glasses, a quarterwave of MgF_2 is the best coating available, as shown in Fig. 3.2.

3.3 Two-Layer Coatings

The simplest coatings to understand are multiples of quarterwaves at the monitor wavelength. One design technique is to use a high-index (H) layer that is a halfwave

thick between the low-index quartz (Q) quarterwave outer layer (HQ) and the lens [Fig. 3.3(a)]. This multilayer coating extends to the low-reflection zone. The two-layer coating in Fig. 3.3(b) consists of a halfwave of titanium oxide and a quarterwave of quartz. The effective range is good, but the substrate must have a very high index before the reflection is low enough to be acceptable. A good range is shown in Fig. 3.3(b); the improvement over a single layer is evident from examination of the graphs. These graphs show the flattening and range-increasing power of the halfwave addition. If the substrate has an index less than 1.85, I recommend using different materials and/or another type of design. Substituting zirconium oxide for the first layer ($n = 2.05$) and magnesium fluoride for the final layer provides an improvement for most of the lower-index glasses (Fig. 3.4). The range of the T/Q coating is better than that of the Z/M coating for

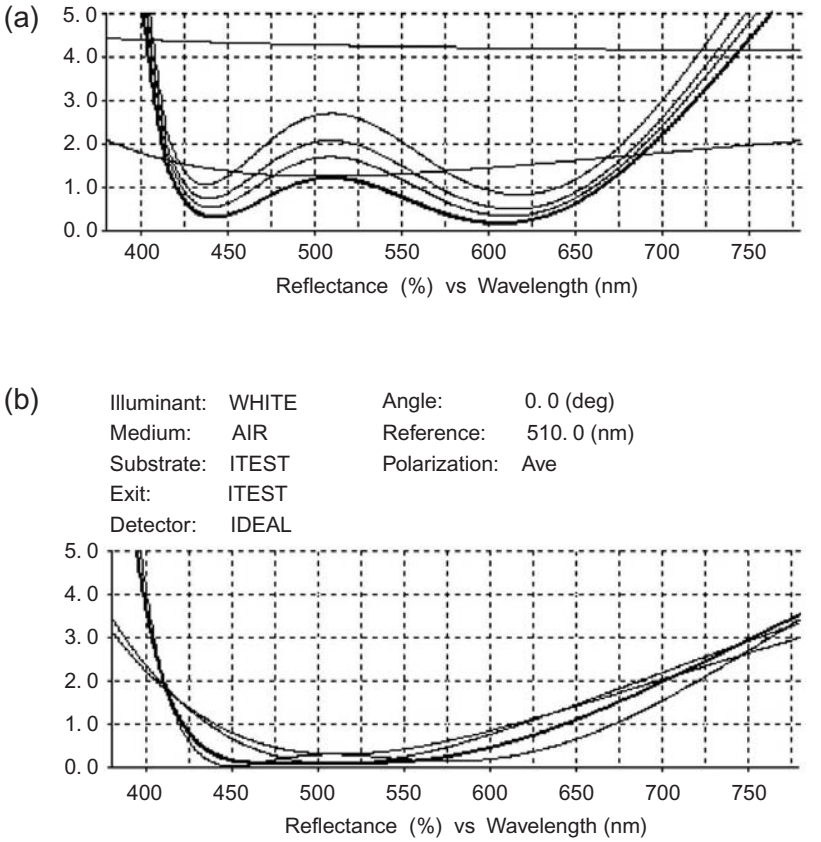

Figure 3.3 (a) Two-layer HQ coatings on various substrates: 1.52; 1.585; 1.63; and 1.7 index. %R glass (higher flat line) and MgF_2 (on glass) (lower straight line) are shown for reference. (b) The same two-layer coating on higher-index glasses (1.9 and 2.0 index from bottom to top with two lower lines at 450 nm), as compared to a quarterwave of SiO_2 for each glass (1.9 and 2.0 index with two higher lines from bottom to top at 450 nm).

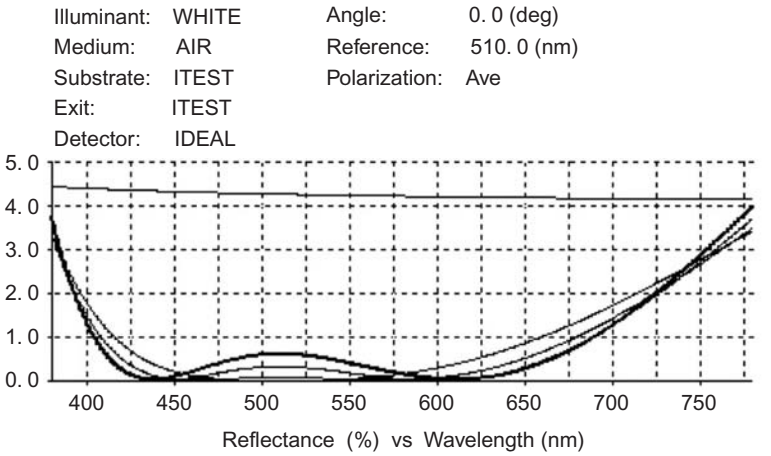

Figure 3.4 A two-layer HQ coating on various glasses: 1.63–2.0 index (top to bottom at 500 nm); ZrO_2 and MgF_2 materials. The flat line is $\%R$ of glass for reference.

higher indices where T is titanium oxide, Q is quartz, Z is zirconium oxide, and M is magnesium fluoride.

3.4 Three-Layer Designs

Lower-index glasses need an additional quarterwave layer next to the substrate (Fig. 3.5). Quarterwave will be abbreviated as qw and halfwave as hw in the following designs and throughout the rest of the book.

Design: Layer 1: qw Al_2O_3 ($n \sim 1.63$); Layer 2: hwZ ($n \sim 2.02$); Layer 3: qwM ($n \sim 1.38$).

For an all-oxide coating, quartz is the final layer; for the first layer, higher-index materials are required to keep the reflection low in the middle of the graph

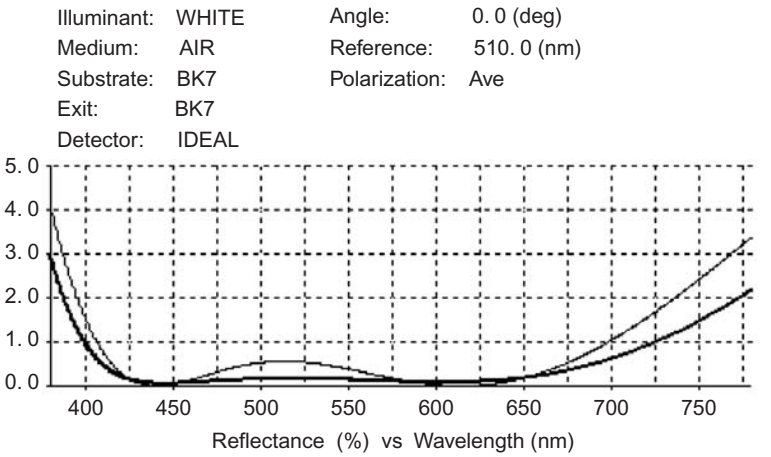

Figure 3.5 Three-layer QHQ coating for $n = 1.52$ (thin line) and $n = 1.63$ (thick line).

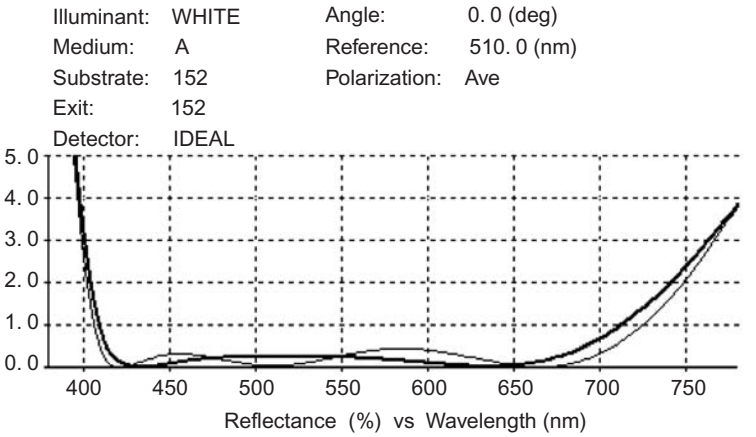

Figure 3.6 QQHQ all-oxide coating; BK7 (thick line) and 1.63 (thin line) are the substrates.

(520 nm). This produces a narrower spectral zone (Fig. 3.6). An alternative is to add one more layer of quartz next to the substrate (QQHQ).

Design: Layer 1: Q; Layer 2: Al_2O_3; Layer 3: T hw; Layer 4: Q (all dispersive).

3.5 Alternate Designs

If the premise of *quarterwave only* is done away with (Fig. 3.7), then two material designs utilizing titanium dioxide and quartz can be substituted for the above four-layer design.

Design: Layer 1: 12nmT; Layer 2: 34nmQ; Layer 3: 114nmT; Layer 4: 87.5nmqwQ.

I took the reflection coefficients from the Fig. 3.6 design and saved them as targets for the Fig. 3.7 design. I assembled the layer type in the order shown—TQTQ—

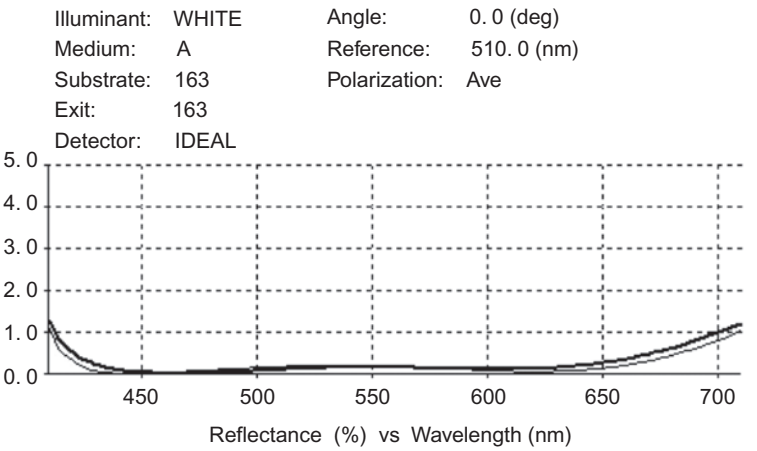

Figure 3.7 Four-layer TiO_2/quartz nonquarterwave design for $n = 1.63$ (thin line) and BK7 (thick line).

and allowed the program to find the proper thickness of the three inner layers that match the Fig. 3.6 results. This is the current technology used for coatings for lower-index lenses at a number of facilities.

3.6 Camera-Type Coatings

Coatings for high-quality cameras typically have at least six layers to expand the wavelength range of the low-reflection band. Nonquarterwave layers of TiO_2 and SiO_2 provide the best index ratio for the desired results (Fig. 3.8). This six-layer coating consists of TiO_2 and SiO_2 deposited with a cold process reactively evaporated with oxygen from e-beam guns with an ion-aided plasma generated by an end-hall-type ion source. Designs are listed in quarterwaves at the wavelength of 524 nm.

Design: 0.27T 0.34Q 1.091T 0.11Q 0.75T 1.08Q.

To reduce the reflectance further, a layer of MgF_2 can be inserted before the final layer (Fig. 3.9).

Design: 0.16T 0.33Q 1.43T 0.11Q 0.55T 0.81M 0.222Q.

A lower-index final layer reduces the reflectance compared to a layer of quartz. MgF_2 is my material of choice, but it is not as durable when deposited by the process described above. The final layer of SiO_2 is only 20 nm thick and is added to protect the MgF_2 layer from abrasion (Fig. 3.10). Adding more layers can extend the low-reflection range.

Design: 2Q 0.27T 0.355Q 1.26T 0.11Q 0.58T 0.78M 0.222Q.

The reflection across the visible spectrum is less than 0.1% average (Fig. 3.11).

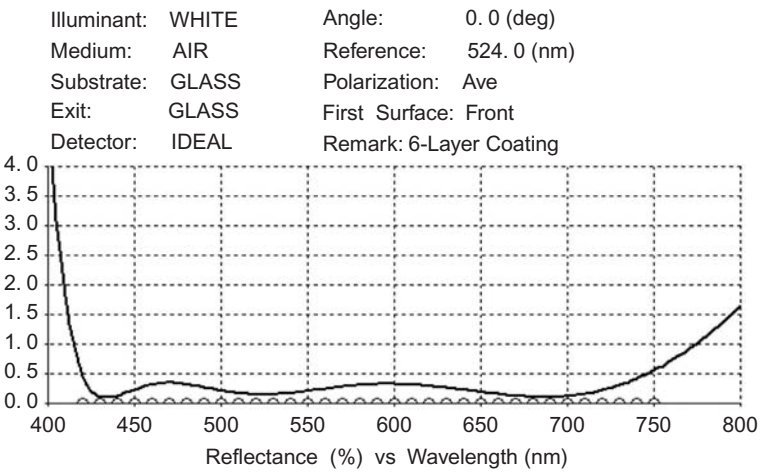

Figure 3.8 A six-layer coating design with targets. The wavy line at the bottom represents the ideal target data.

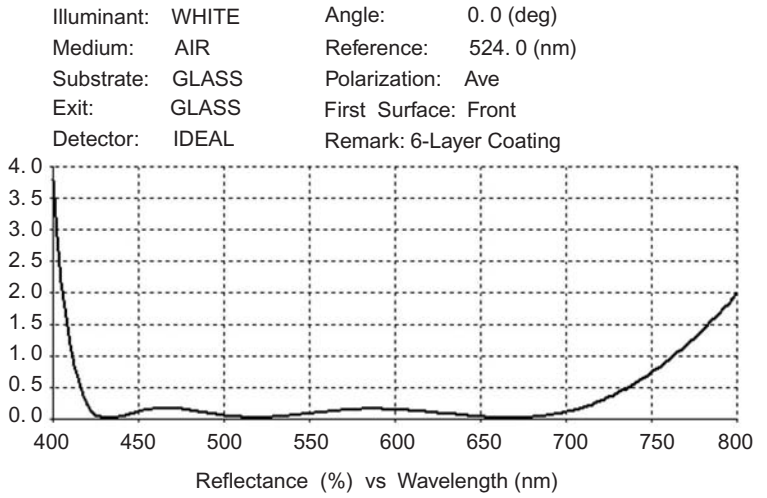

Figure 3.9 A seven-layer coating.

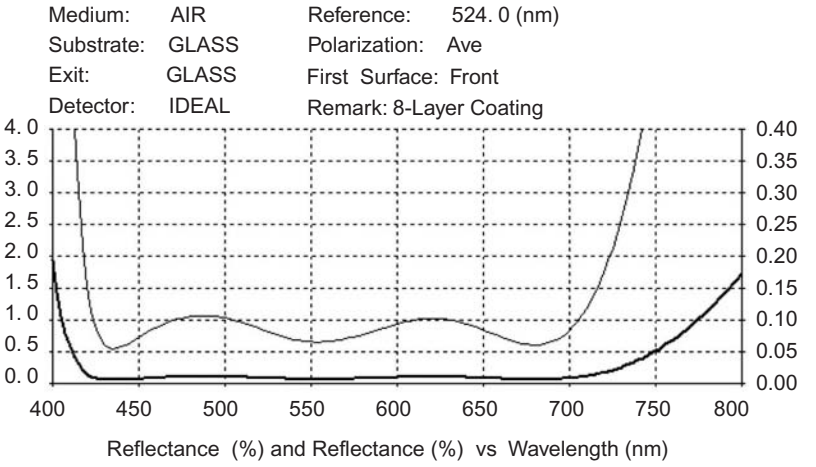

Figure 3.10 An eight-layer coating. The upper line is provided to show a more detailed view below 0.40%.

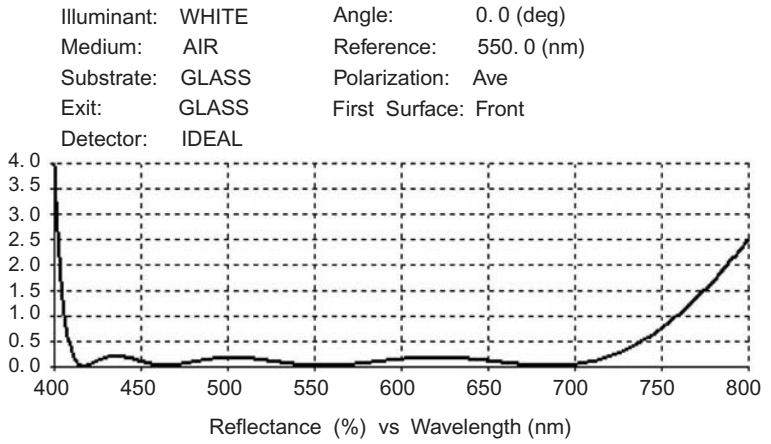

Figure 3.11 An 11-layer antireflection coating.

Design: 0.17T 0.67Q 0.29T 0.74Q 0.41T 0.37Q 1.37T 0.10Q 0.55T 0.76M 0.21Q.

There are two ways in which this AR coating can be improved: the filter can be effective over a broader spectrum, or the filter can have a reduced reflection in the band. Adding a halfwave of quartz at the start of the design and altering the targets for the band can optimize either method (Fig. 3.12). Alternatively, see Figs. 3.14 and 3.15. And finally, Fig. 3.16 shows a very wide-range coating.

Design: 2.31Q 0.17T 0.74Q 0.2T 2.41Q 0.36T 0.27Q 1.41T 0.17Q 0.45T 0.805M 0.22Q.

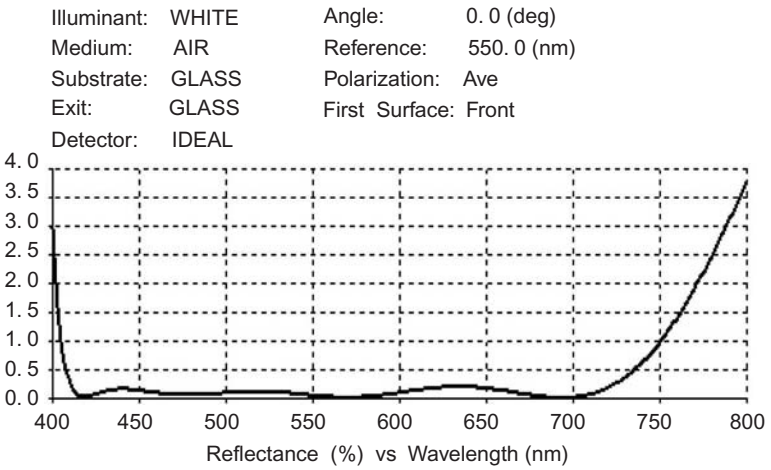

Figure 3.12 A 12-layer coating starting with a halfwave of quartz and optimized for the same reflection targets (0%R at 420–720 nm) as the previous examples. A wider range is shown in Fig. 3.13.

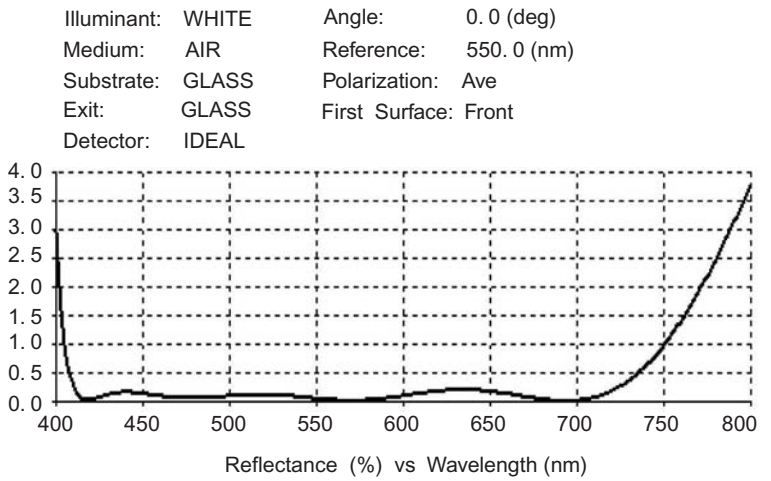

Figure 3.13 The targets have been changed to 410–800 nm. The in-band reflection is marginally increased, and the filter is effective for a wide range.

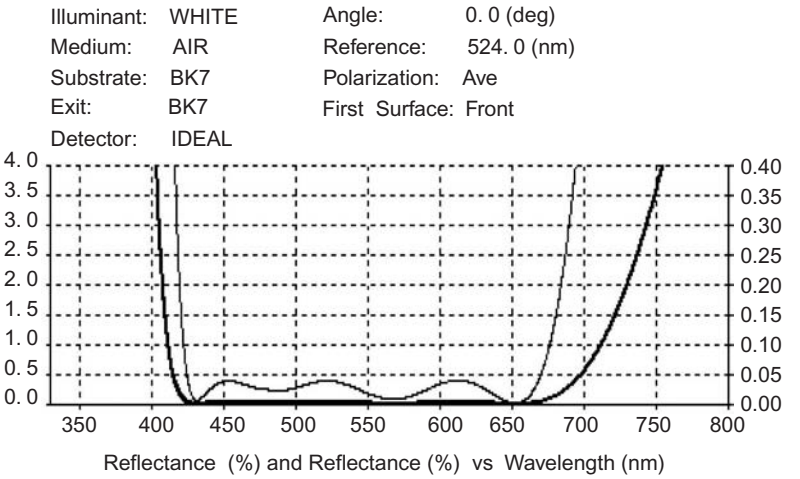

Figure 3.14 A lower-reflection variation with approximately 0.25$\%R$ average in band.

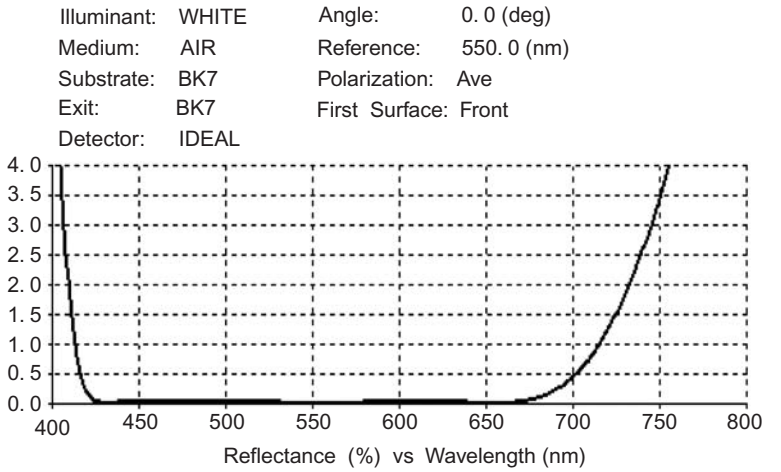

Figure 3.15 An even lower reflection (0.01%) for a wide but constricted range when compared to the other designs.

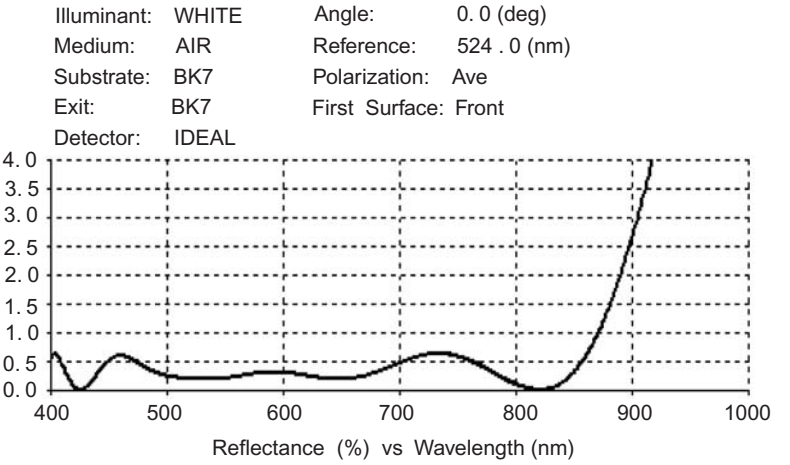

Figure 3.16 A very wide-range coating. Twelve layers provide even wider band coverage.

3.7 Ultraviolet AR Coatings

Coating materials are restricted due to the absorption in high-index chemicals. Tantala can be used from 300 nm and above (Fig. 3.17).

Design: 0.28T 0.35Q 2.14T 1.01Q for 350-nm wavelength.

For the lower-UV range, hafnium oxide is required for a high-index material. Most high-index materials are not transparent in the 250 nm area of the spectrum. The same approach to layer formation and general design is used (Fig. 3.18).

Design: 0.39H 0.32Q 1.24H 1.08Q.

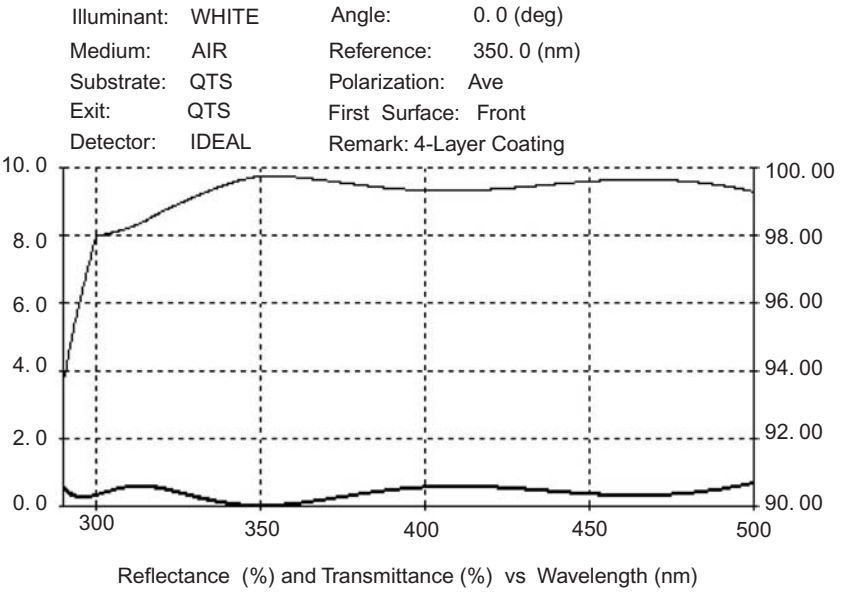

Figure 3.17 A four-layer AR coating with Ta_2O_5 and SiO_2.

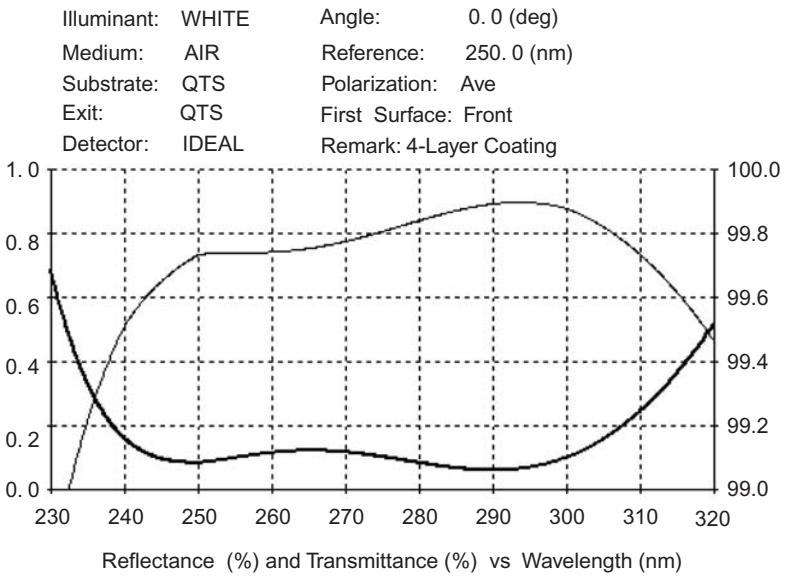

Figure 3.18 A four-layer design for the lower UV.

Adding a few layers can extend the effective range considerably (Fig. 3.19). The filter is deposited on a glass substrate and a quartz layer is added first. For a quartz substrate, that layer is not necessary; design would be slightly changed.

Design: 0.74Q 0.14H 0.67Q 0.6H 0.2Q 1.1H 1.04Q.

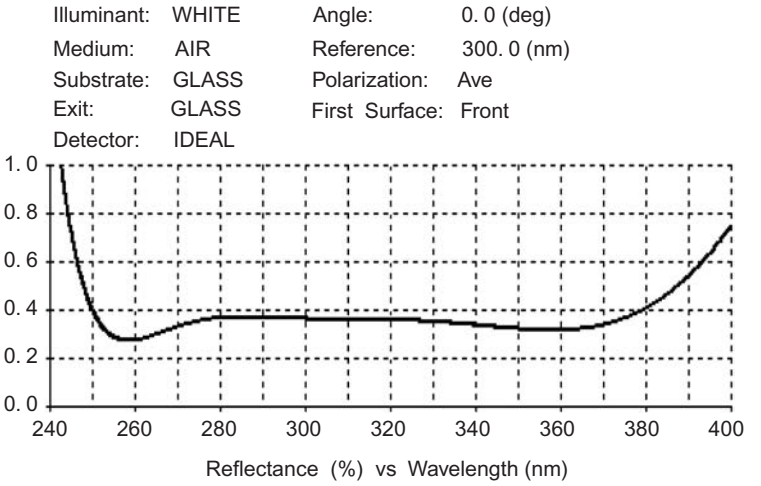

Figure 3.19 A seven-layer coating.

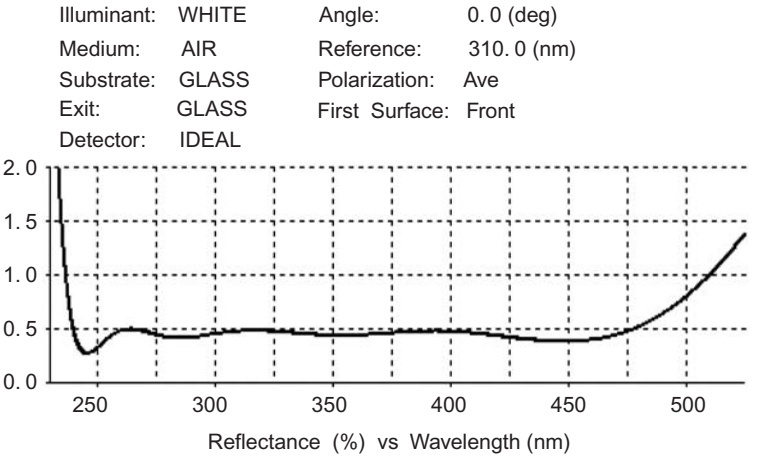

Figure 3.20 A broadband UV 10-layer coating.

Wider bands require many layers. The design shown in Fig. 3.20 is similar to that of Fig. 3.16, but it contains two MgF_2 layers. The coating is referenced to a quarter-wave thickness at 310 nm: 0.5Q 0.14H 0.76Q 0.46H 0.3M 1.22H 0.19Q 0.63H 0.795M 0.28Q

The thin layers can be easily controlled with ion-beam-sputtering technology. The magnesium fluoride layer is best deposited with e-beam or resistance heating using an ion-aided process.

Chapter 4
Multilayer Films

4.1 Extending a Reflection Zone

If the object of a coating was simply to reflect a small-wavelength band, this book would have ended after Chapter 1. Most coating applications require passing the light of one spectral area and reflecting at least one spectral zone, and in many instances there is a requirement to extend the reflection zone. If the requirement is a small stretch of the single-stack zone, the addition of a few pairs of films and an optimization of the thickness of some of the layers provides the most economical use of the coater. For more demanding requirements the width is increased by adding a similar stack at an adjacent band point. A layer added between these stacks is necessary to keep the proper interference relationships in place.[1] The thickness of the layer is a median value of the thickness of the reflectors. Figure 4.1 helps explain the terminology.

The 29-layer design: $1.2375(\mathrm{H\ L})^7\ 1.2375\mathrm{H}\ (\mathrm{H\ L})^7\ \mathrm{H}$.

H indicates a quarterwave of high-index material; L indicates a quarterwave of low-index material; $1.2375(\ )^7$ indicates seven pairs of whatever material is in the

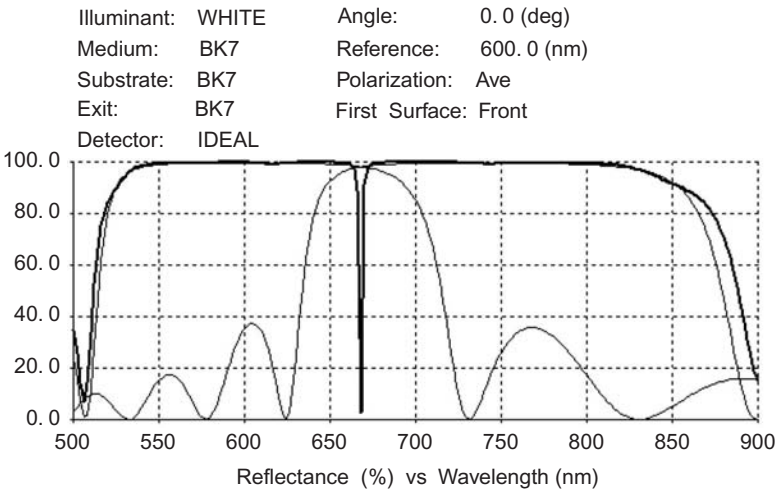

Figure 4.1 A reflector with two stacks. The thick line is the reflection for the assembly of the two stacks indicated by the thin lines.

parentheses; and each layer is a quarterwave thick at the multiplier's wavelength. 1.2375H means 123.75% of the reference wavelength is where the "H" layer is a quarterwave.

One stack is centered at ~750 nm and the other at 600 nm. Although 30 layers are indicated, the center H layers combine for a thickness of 2.2375 quarterwaves. To remove the spike leak at ~670 nm, the thickness of the layer is adjusted to a median value of ~1.12. With dispersion, the thickness is changed to 1.19 quarterwaves to give >99%R for a large span of the spectrum. Note that the reflection is now at a peak for the wavelength of the spike (Fig. 4.2). Reflectors with similar properties can be designed with other techniques, but the film thickness for every layer is different and the methods of design can become complicated. Furthermore, no insight into how reflectors interact with each other is gained.

Adding another stack to extend the range is the next logical step if a much wider reflection zone is needed. Figure 4.3 is a starting design for a hot-mirror-type blocking filter that can eventually be used by a camera with a silicon detector. Removing the infrared corrects the image on the CCD. The design is 57 layers long after the joining layers are combined:

$$(\mathrm{HLLH})^{10}\ (1.2\mathrm{H}\ 2.4\mathrm{L}\ 1.2\mathrm{H})^{9}\ (1.365\mathrm{H}\ 2.73\mathrm{L}\ 1.365\mathrm{H})^{9}.$$

The thicknesses of the layers are referred to quarterwaves at 400 nm, and some layers would have the thickness altered to remove transmission and reflection ripple as the specifications are developed.

The process of adding stacks can be continued, but eventually there will be an overlap of the third order of the reflectance band for the highest wavelength stack with the band of the lowest stack. An etalon is created, and the blocking is

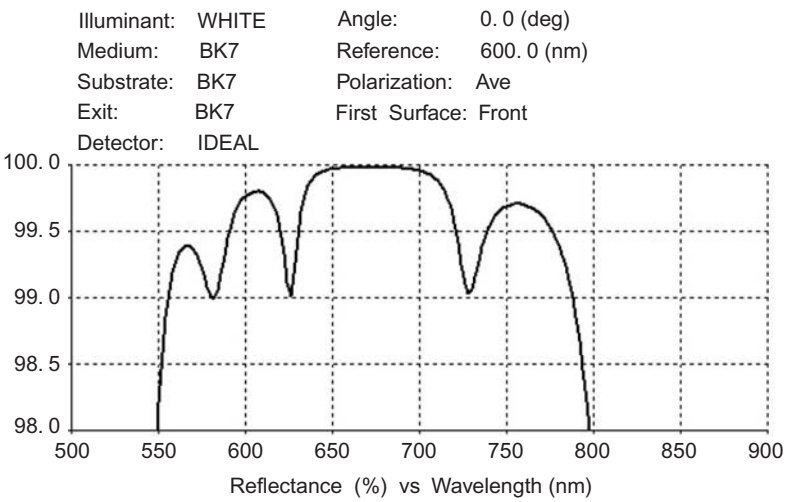

Figure 4.2 A coating with a matching intermediate layer.

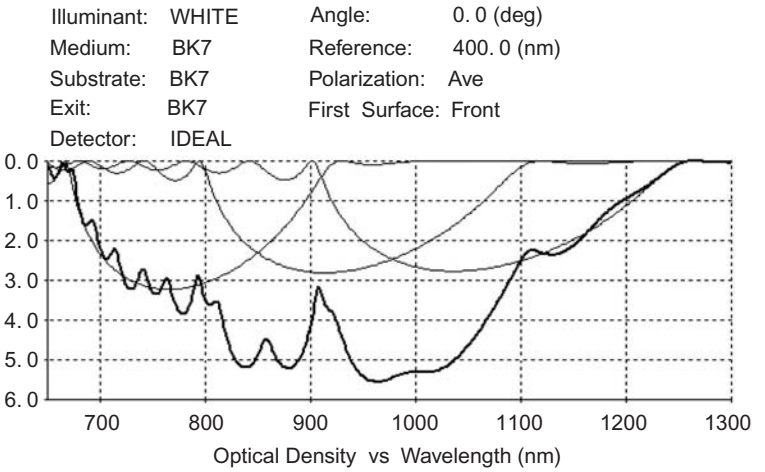

Figure 4.3 A three-stack blocker. The three stacks are shown with thin lines.

frustrated (Fig. 4.4). This design is the basis of either a long- or a short-wavelength pass filter. The design (referenced to quarterwaves at 400 nm) is

$$(0.9\mathrm{H}\ \ 1.8\mathrm{L}\ \ 0.9\mathrm{H})^{17}$$
$$(\mathrm{HLLH})^{6}$$
$$(1.1\mathrm{H}\ 2.2\mathrm{L}\ \ 1.1\mathrm{H})^{12}$$
$$(1.2\mathrm{H}\ 2.4\mathrm{L}\ \ 1.2\mathrm{H})^{12}$$
$$1.375\mathrm{H}\ 2.75\mathrm{L}\ (2.75\mathrm{H}\ 2.75\mathrm{L})^{16}.$$

More layers in each stack and altered spacing can provide a minimum of six densities of blocking at 600–1200 nm. Layer count (>170) can be an issue, and the stress of a film this thick is high.

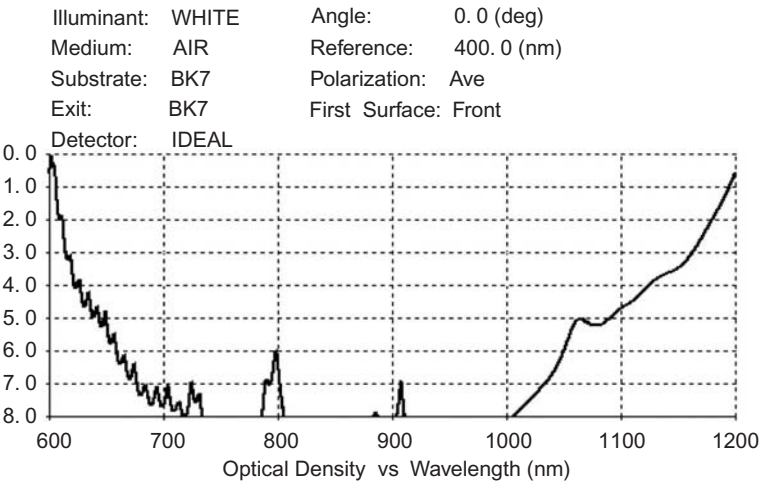

Figure 4.4 A five-stack reflector with 128 layers.

4.2 Beam Splitters

A beam splitter is another type of filter that maintains fairly constant transmittance and reflectance across the widest possible spectral range. Nonquarterwave layers are optimized to match the specified value; the most popular ratio is 50–50 for the visible spectrum. The design for normal incidence using TiO_2 and SiO_2 for materials has a neutral response (Fig. 4.5).

Design: 1.92T 1.15Q 1.11T 1.17Q 0.76T 0.47Q 2.2T 1.11Q referenced to 520 nm.

The light is polarized when the filter is used at 45 deg; wideband designs are not as spectrally flat (Fig. 4.6).

Design: 0.74T 1.27Q 0.17T 1.2Q 2.2T 1.57Q 1.16T 2.49Q referenced to 700 nm.

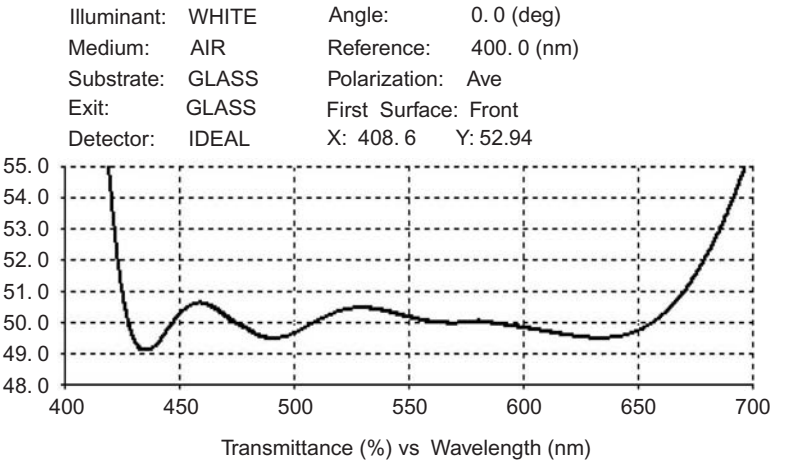

Figure 4.5 An eight-layer beam splitter for normal incidence used in air.

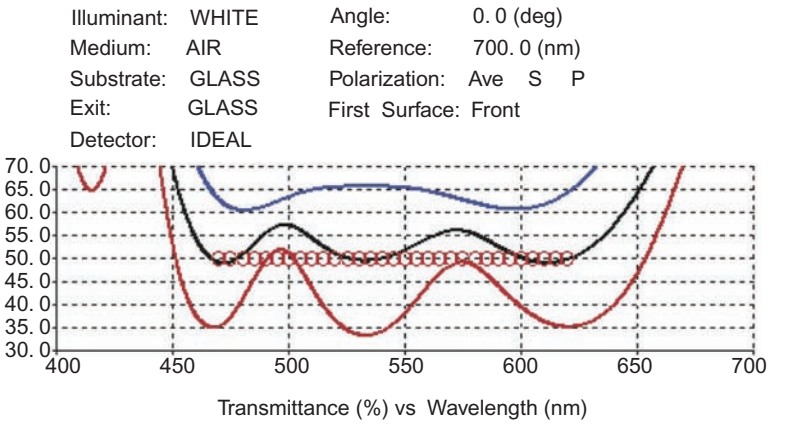

Figure 4.6 An eight-layer design for 45-deg incidence in air and targets. The highest line is the P-polarized transmittance; the middle line is the average transmittance; the lowest line is the S-polarized transmittance. The circles indicate the ideal values for the program design.

For flatter results, the wavelengths considered must be restricted. A filter with 12 layers may be bound by 40 and 60% for each polarization from 500–600 nm. An alternate solution for flat designs includes a layer of silver. Some absorption must be allowed for; the transmission for equal beams is ~48% instead of 50%. A design for the same conditions of wavelength coverage with 10 layers is

5nmT 24.5nmAg 0.59T 1.05Q 0.28T 0.7Q 0.28T 0.42Q 1.26T 0.8Q.

This design has a better spectral flatness than the eight-layer design. The first layer is a binder for the silver layer (Fig. 4.7). The reflectance has slightly different characteristics for each side facing the incident radiation; the substrate side has a higher reflectance than the film side. The film side reflectance is approximately equal to 95% minus the transmittance. An AR coat was added with ~ 2%R average (Fig. 4.8).

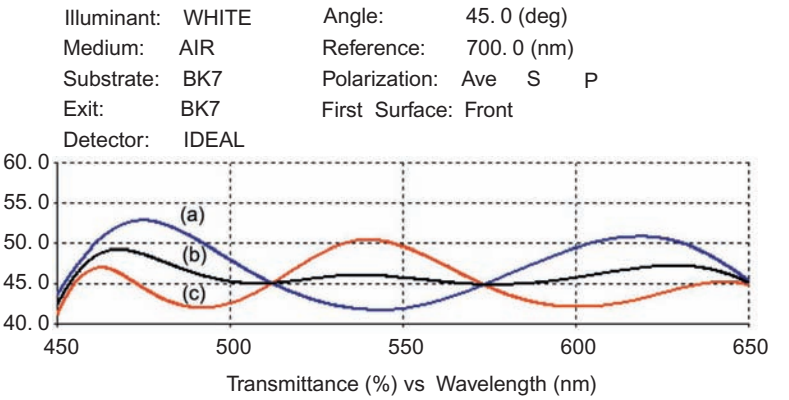

Figure 4.7 Transmission of a 10-layer coating. (a) The highest line at 600 nm is the P-polarized transmittance; (b) the middle line at 600 nm is the average transmittance; (c) the lowest line at 600 nm is the S-polarized transmittance.

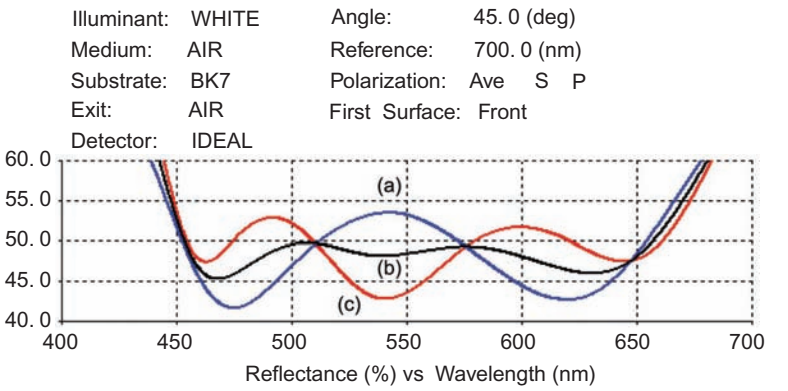

Figure 4.8 The %R from a coated slab at 45 deg with an AR coat on the exit side. (a) The highest line at 550 nm is the P-polarized transmittance. (b) The middle line at 550 nm is the average transmittance. (c) The lowest line at 550 nm is the S-polarized transmittance.

Some optical systems require a sample of the light beam to control an optical component, and femtosecond lasers need output mirrors with exacting spectral outputs. The design of Fig. 4.9 was optimized to provide 99%R with low ripple; it consists of 28 nonquarterwave layers. Virtually any specification can be designed for and probably built when nonquarterwave layers are used. Two applications are discussed further.

A linear reflector is one that follows a straight-line equation for a discrete portion of the spectrum. The example shown in Fig. 4.10 is linear in transmission; the linearity can also be specified for a density plot. The filter is linear only for a short wavelength range. The signal from an optical tap can be used to control the wavelength of a tunable filter when the filter is in the circuit.

Design: H 4L HLH 8L $(HL)^5$ 3H 2L HLHL 1.3H 1.3L for a 1572-nm wavelength.

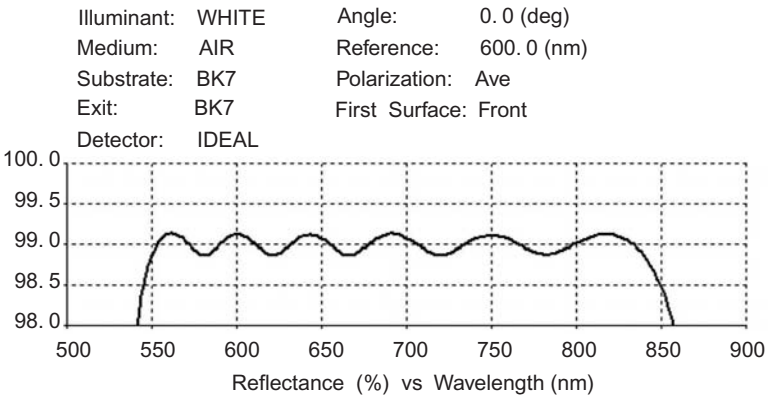

Figure 4.9 A reflector with 99%R.

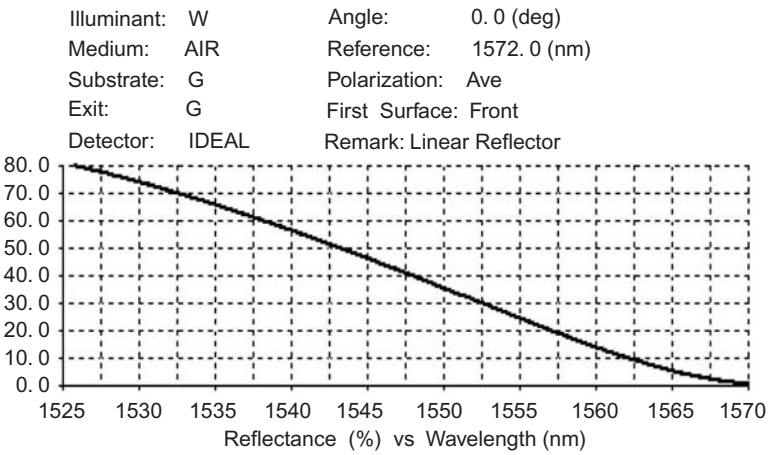

Figure 4.10 A 24-layer filter designed for a straight-line response.

4.3 Profile Filters or Gain-Flattening Filters

Profile filters, as described by Dobroloski, function over large segments of the spectrum.[2] They were a curiosity film that demonstrated computing power. I manufactured gain-flattening filters (GFFs) for JDS Uniphase Corporation customers to their specification. The filters were to have a "transmittance" at the opposite of the intensity of the spectrum that the erbium amplifiers emitted. Each customer had different requirements; the amplifiers are quite sensitive to the doping level and length of fiber used. When I was first asked if I could design and build a filter, I said no. At the time, I did not have a program that optimized layers, but then I figured out a way to do it. In reflection, a filter with controlled losses is fairly simple to design if the curve is not complex (Fig. 4.11). The filter will have no losses in the blocking zone (100%R), and if some layers are left off of a bandpass filter, a predictable reflection loss at the peak is possible. The profile of the filter can be further altered with additional filters in series to mimic complex shapes.

The methodology of filter designs is discussed in Chapter 3. A quarterwave design approach is used here; optical monitoring is the best way to make bandpass filters, and the monitors easily adapt themselves to quarterwave layers. The design consists of building up three filters on the substrate:

$$(HL)4\ (LH)4\ L\ (HL)5\ (LH)5\ L\ (HL)5\ (LH)4\ 0.42H.$$

The filter bandwidth and slope are controlled by the number of filter segments and filter designs. Targets are entered into the program, and the filter is modified until an acceptable match is established. With practice, this is a reasonably fast design technique. Minor changes to the slope are effected by adding halfwaves to some of the layers.

For complex shapes, two or more separate filters may be used in series; when the filters are assembled, there will be some minor loss in signal. An alternate approach uses nonquarterwaves for a single component to follow the contour needed (Fig. 4.12); however, the layer count may increase substantially.

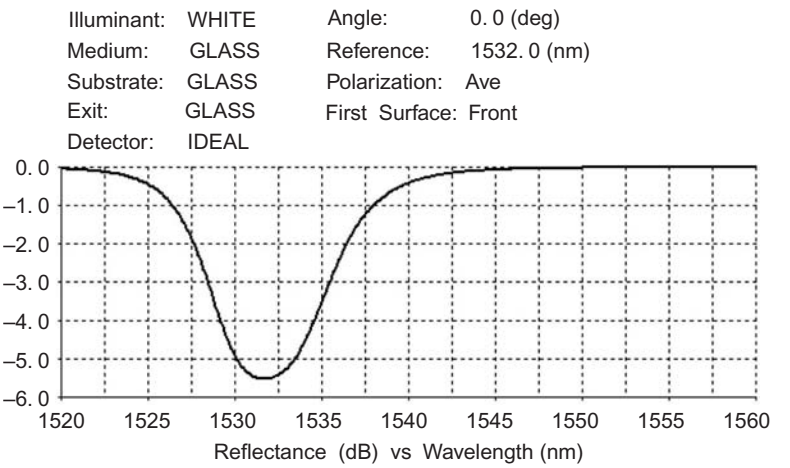

Figure 4.11 A GFF component.

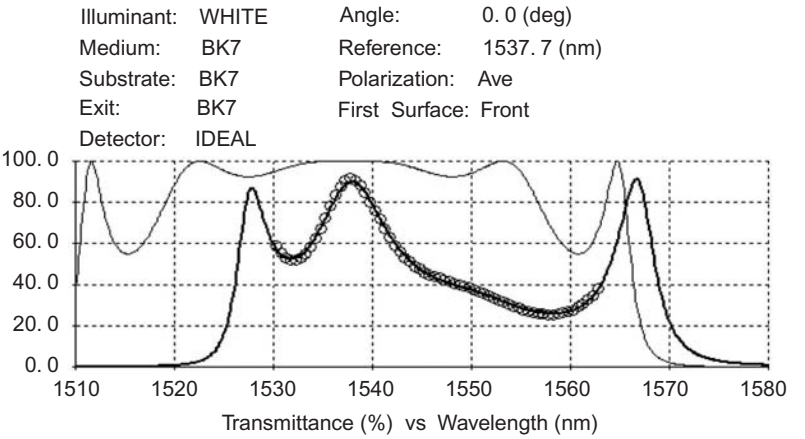

Figure 4.12 Nonquarterwave transmissive GFF (thick line); starting design (thin line); targets (circles).

Nonquarterwave GFF: Another approach for complex curves involves many nonquarterwaves. The initial transmission filter design uses a 48-layer multicavity wideband filter: (HLH 8L HLHL)^6. The optimization program alters the layer thickness to match the targets; the first four layers of this particular filter are not allowed to be changed, providing a calibration for the thickness monitor. The final filter has 46 layers.

4.4 Reflection Type

It does not matter whether the filter is reflective or transmissive from a design point of view; the results are roughly equal for complexity and layer count (Fig. 4.13). Nonquarterwave GFF: The GFF is designed to have no losses near

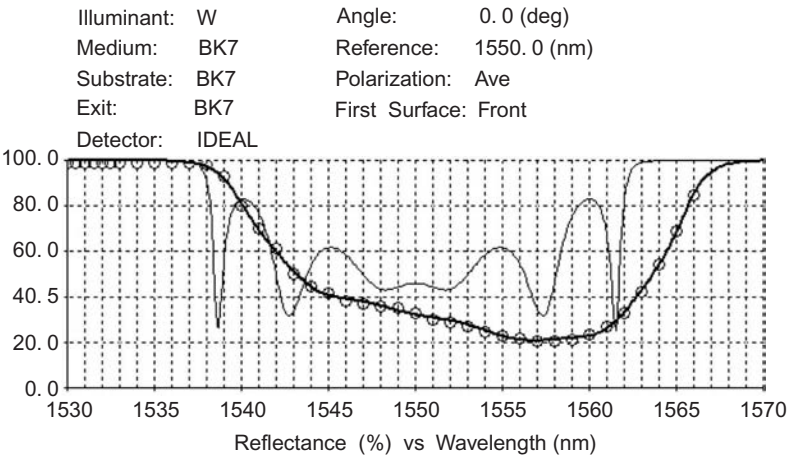

Figure 4.13 A 75-layer reflection GFF (thick line); starting design (thin line); targets (circles).

1530 nm and controlled losses to 1566 nm. The film is cemented to a fiber optic collimator stub used strictly in reflection. The six-cavity starting design is $[(HL)^2\ H\ 8L\ H\ (LH)^2\ L]^6\ HLH$. The last three layers are added to increase the minimum reflectance from ~0% to a range that approaches the desired target. Fewer cavities will give results fairly close to the chosen reflection values, but this design has very low deviation from the perfect answer.

References

1. A. F. Turner and P. W. Baumeister, "Mulitlayer mirrors with high reflectance over an extended region," *Appl. Opt.* **5**, 69–76 (1966).
2. J. A. Dobrowolski, "Completely automatic synthesis of optical thin film systems," *Appl. Opt.* **4**, 937–946 (1965).

Chapter 5
Dichroics

5.1 Introduction

Dichroic means "two color." Any film combination that has to perform to a specification at more than one wavelength zone is dichroic. The films may even have similar specifications, that is, high reflection at 450–650 nm and also high reflection at 1060 +/−10 nm. Generally, dichroic refers to high reflection for a certain distance and then low reflection for another distance. Examples: *cold mirrors* reflect 400–700 nm and pass 760–2000 nm; *hot mirrors* pass 400–700 nm and reflect 800–1200 nm. The definitions become complicated if the design is also used at a 45-deg angle.

High-quality coatings can be very difficult to manufacture, although designing is easier now with the use of computers and good software. However, errors in achieving the prescribed thickness of the layers can alter the spectral performance of the coating. A number of stacks and partial quarterwave layers are needed to smooth out *ripple* in the transmission zones.

By altering a few layers in the reflector, the performance of the coating can be profoundly improved. The stack $(HL)^9$ L will become a yellow filter when the first four and last five layers are changed by the TFCalc program (Fig. 5.1). This is a *long-pass filter*. All of the wavelengths above the reflection zone are passed (transmitted).

Design: 0.4H 1.18L 0.82H 0.97L $(H\ L)^4$ H 0.94L 1.18H 0.8L 85H 2.08L utilizing Ta_2O_5 (H) and quartz (L).

After selecting the position of the quarterwave stack by running the software and moving the wavelength, I instructed the computer program to find the best thickness for low reflection at 563–1300 nm (at 10 nm intervals) and high reflection at 440–510 nm. I then selected the layers that allow their thickness to be changed. It took approximately 5 sec of optimization to select these thicknesses. A *short-pass filter* has the opposite properties. The exact same starting design of the long-pass filter was used as the starting design for this filter. Targets of low reflection from 400–550 nm and high reflection from 590–690 nm were selected; the same layers were selected for modification. After 5 seconds of optimization (~125 steps), the design in Fig. 5.2 appeared.

Design: 0.15H 1.14L 1.15H 0.96L $(HL)^4$ H 0.8L 1.13H 0.97L 1.14H 1.96L.

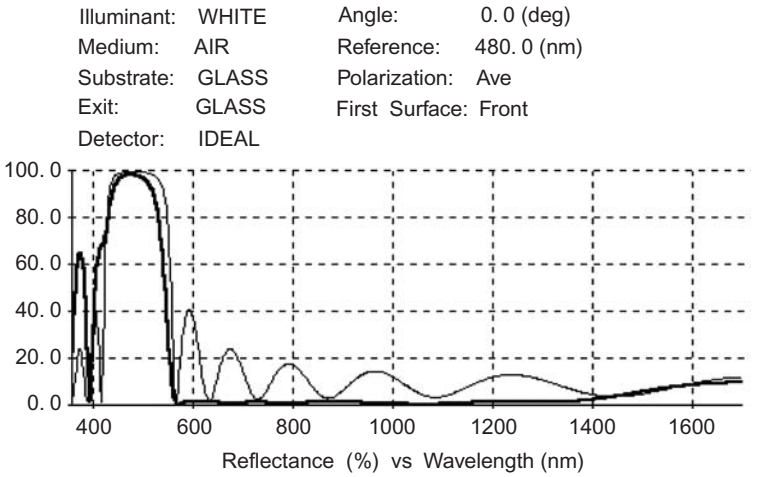

Figure 5.1 Yellow transmitting filter. The thin line shows the reflection of the basic stack; the thick line is the reflection after optimization.

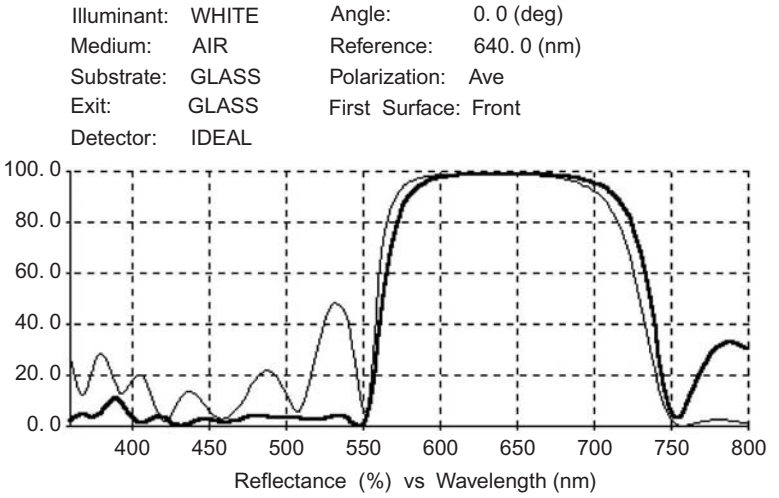

Figure 5.2 Blue transmitting filter and starting design. Thin line: $(HL)^9$ L before optimization.

To smooth the transmission zone, by simply altering the reflection zone to correspond to a normal reflection envelope, the optimization routine will find a smoother design. The circles are the new targets to aim for; the scales are expanded by a factor of 10 (Fig. 5.3).

Design: 1.24H 1.08L 1.08H 0.99L $(HL)^4$ H 1.02L 1.02H 1.08L 0.98H 0.56L.

If more layers are altered, the filter achieves even higher transmission. The blocking level reduces as layer thicknesses are changed. More quarterwave layer pairs increase the blocking and the ripple. Decide the acceptable value for the

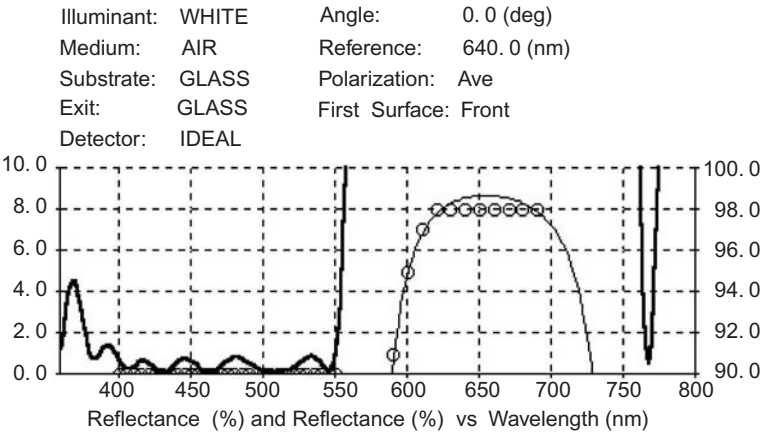

Figure 5.3 Detailed properties after changing targets to correspond to reality.

transmission, and select the number of layers you are willing to alter to reach that point. If the resulting filter is not close enough, alter more layers.

A specification usually requires a compromise somewhere in the spectrum. Frequently, the objectives called for are unreasonable for simple designs. For instance, in the blue filter example, if the blocking range were extended into the infrared, more stacks (at least more pairs of layers) would be needed. The design can become very complicated and may not be easily achieved in practice. Unfortunately, this translates to expensive!

The slope for a long- or short-pass filter improves as the number of layer pairs increases. An example of a long-pass filter for isolation of 980 nm illustrates how the layer structure changes to achieve low ripple for various densities. The designs for 52–66-layer filters are shown after the curves in Fig. 5.4. Each filter was specified to have >99.5%T at 1012–1100 nm and various blocking levels at 980 nm (Fig. 5.5). See Table 5.1.

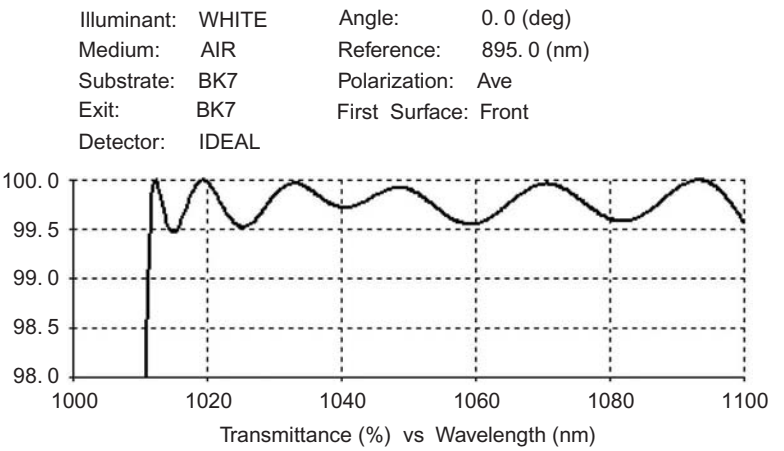

Figure 5.4 Detail of transmission for a typical filter as described below.

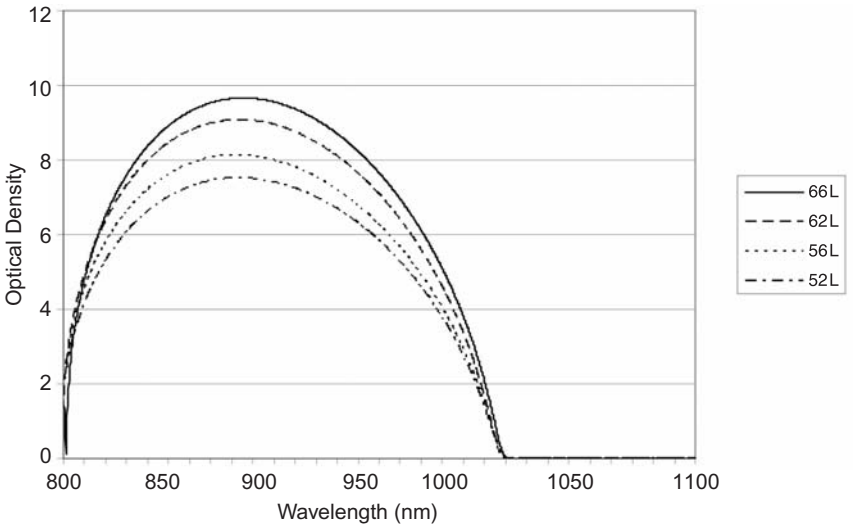

Figure 5.5 Blocking of the various designs.

Table 5.1 Quarterwave thickness for the designs (referenced to 887 nm).

Layer number	Material	Quarterwave 52	Quarterwave 56	Quarterwave 62	Quarterwave 66
1	TAMACL	1.05	1.08	1.05	1.03
2	SiO_2	0.72	0.95	0.91	0.92
3	TAMACL	0.66	0.66	0.68	0.72
4	SiO_2	1.03	0.85	0.88	0.84
5	TAMACL	1.11	1.03	1.01	1.04
6	SiO_2	1.09	1.07	1.06	1.04
7	TAMACL	1.03	1.08	1.06	1.05
8	SiO_2	0.90	1.06	1.03	1.03
9	TAMACL	0.77	0.99	0.98	0.97
10	SiO_2	0.97	0.89	0.90	0.95
11	TAMACL	1.10	0.86	0.91	0.92
12	SiO_2	1.14	0.97	0.99	0.96
13	TAMACL	1.15	1.07	1.01	1.02
14	SiO_2	0.76	1.09	1.07	1.02
15	TAMACL	1.00	1.14	1.09	1.06
16	SiO_2	1.00	0.84	0.88	1.00
17	TAMACL	1.00	1.00	1.00	0.97
18	SiO_2	1.00	1.00	1.00	0.97
19	TAMACL	1.00	1.00	1.00	1.00
20	SiO_2	1.00	1.00	1.00	1.00
21	TAMACL	1.00	1.00	1.00	1.00
22	SiO_2	1.00	1.00	1.00	1.00
23	TAMACL	1.00	1.00	1.00	1.00
24	SiO_2	1.00	1.00	1.00	1.00
25	TAMACL	1.00	1.00	1.00	1.00
26	SiO_2	1.00	1.00	1.00	1.00
27	TAMACL	1.00	1.00	1.00	1.00
28	SiO_2	1.00	1.00	1.00	1.00

(*continued on next page*)

Table 5.1 (*continued*)

Layer number	Material	Quarterwave 52	Quarterwave 56	Quarterwave 62	Quarterwave 66
29	TAMACL	1.00	1.00	1.00	1.00
30	SiO_2	1.00	1.00	1.00	1.00
31	TAMACL	1.00	1.00	1.00	1.00
32	SiO_2	1.00	1.00	1.00	1.00
33	TAMACL	1.00	1.00	1.00	1.00
34	SiO_2	1.00	1.00	1.00	1.00
35	TAMACL	1.00	1.00	1.00	1.00
36	SiO_2	1.00	1.00	1.00	1.00
37	TAMACL	0.73	1.00	1.00	1.00
38	SiO_2	1.16	1.00	1.00	1.00
39	TAMACL	1.15	1.00	1.00	1.00
40	SiO_2	1.13	1.00	1.00	1.00
41	TAMACL	1.08	0.83	1.00	1.00
42	SiO_2	0.91	1.12	1.00	1.00
43	TAMACL	0.71	1.12	1.00	1.00
44	SiO_2	0.94	1.05	1.00	1.00
45	TAMACL	1.06	0.99	1.00	1.00
46	SiO_2	1.11	0.88	1.00	1.00
47	TAMACL	1.11	0.88	0.89	1.00
48	SiO_2	1.10	0.97	1.08	1.00
49	TAMACL	0.89	1.05	1.04	1.00
50	SiO_2	0.57	1.06	1.05	1.00
51	TAMACL	0.90	1.07	0.99	0.90
52	SiO_2	2.27	1.03	0.92	1.03
53	TAMACL		0.87	0.93	1.09
54	SiO_2		0.68	0.96	1.01
55	TAMACL		0.93	1.00	1.00
56	SiO_2		2.17	1.05	0.94
57	TAMACL			1.04	0.91
58	SiO_2			1.03	0.98
59	TAMACL			0.93	1.00
60	SiO_2			0.69	1.03
61	TAMACL			0.87	1.05
62	SiO_2			2.14	1.00
63	TAMACL				0.91
64	SiO_2				0.77
65	TAMACL				0.85
66	SiO_2				2.13

TAMACL is the name used for the dispersive index in Macleod's program for Ta_2O_5. SiO_2 is ~1.45. Over half of the layers have been altered in each design to obtain the extremely low reflectance in the pass zone. If the $\%T$ requirement was not as demanding, the filter could use more unaltered quarterwaves and possibly fewer layers to produce blocking. For the Ta_2O_5 values there are minor thickness changes for each filter.

5.2 Short-Pass Filters

A short-pass filter is one with a pass zone on the low-wavelength side of the blocking zone. The starting design is a quarterwave stack with a sufficient

number of layers to block to a given specification—e.g., 10^{-5} transmission—using Macleod's Ta_2O_5 for a high-index material. Enough transmission targets are selected so that the ripple will be accounted for when the optimization routine is invoked. Select the number of layers to alter on each side of the stack; the transmission of the filter will not be as high as that of the long-pass filter. A 50-layer filter is designed to pass 400–700 nm and block ~730–870 nm; the first 15 layers and the last 16 layers are optimized to gain the high transmission shown in Fig. 5.6. For errors of 0.5% the transmission remains above 94% for the design; if the error is 1%, the $\%T_{\min}$ becomes ~85%. TFCalc uses a different routine to minimize the worst-case scenario; the design may be altered to achieve a $T_{\min}$ of 94% with errors of 1%. The design transmittance is not as high, but it is acceptable. After the best design has been found, adding two thin layers adjacent to the substrate helps smooth the rippling (Fig. 5.7).

Extended blocking of the filters: a similar filter with fewer layers is applied to the substrate at $1.18 \times \lambda$ to extend the blocking zone. The filter in Fig. 5.7 is then appended to it. After reoptimizing, the filter contains 100 layers with excellent

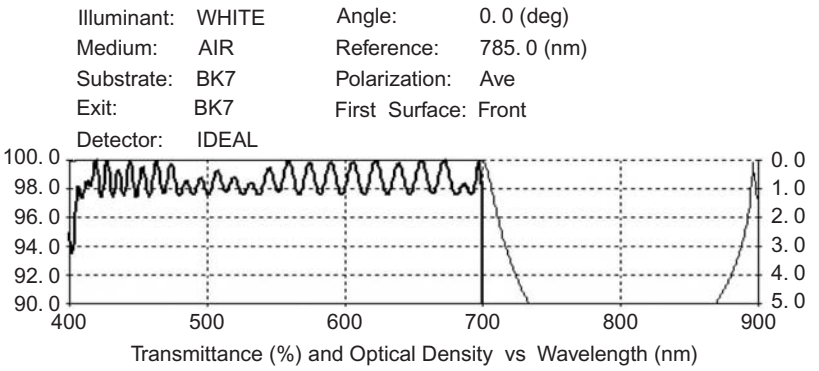

Figure 5.6 A 50-layer short-pass filter.

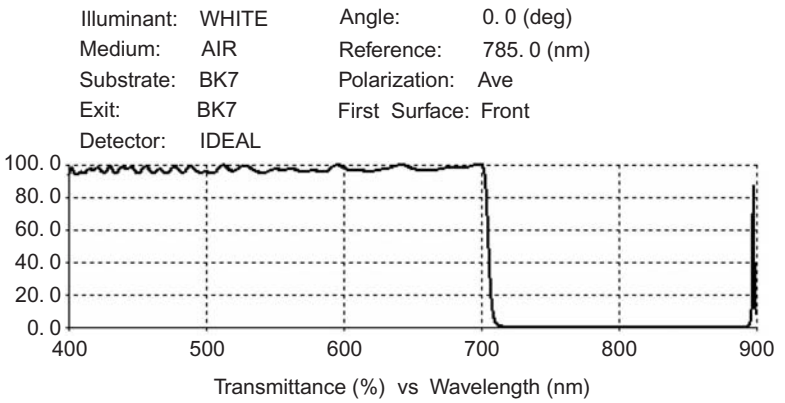

Figure 5.7 Short-pass filter with 50 layers that transmits >94% with random 1% errors.

blocking and high transmission (Fig. 5.8). The long-pass filter is handled similarly. First a stack with 18 layers is deposited at 79% of the wavelength of the clean long-pass filter. The filter of Fig. 5.2 is shifted to a 530-nm wavelength design. First an 18-layer blocker, $(HL)^9$, is applied at 0.79 thickness, and then the long-pass filter designed for 530 nm is appended to the blocker (Fig. 5.9).

TFCalc allows the designer to move a set of layers spectrally with a group factor subroutine. The value of 0.79 was selected by examining the transmission at the crossover point near 480 nm, as the value was altered for the position of the blocker. Figure 5.9 shows that the selected crossover is at about $8\%T$. Targets ($<2\%T$) are then selected to maximize the blocking zone, and a slope is defined;

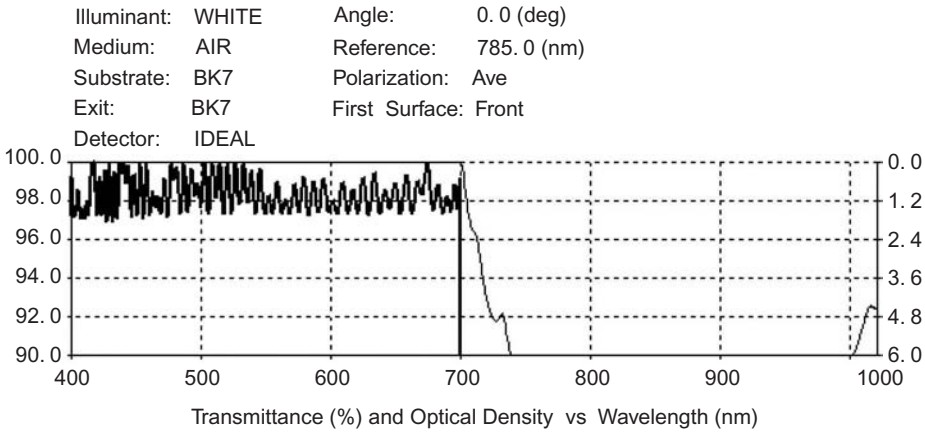

Figure 5.8 Extended blocking of a short-pass filter.

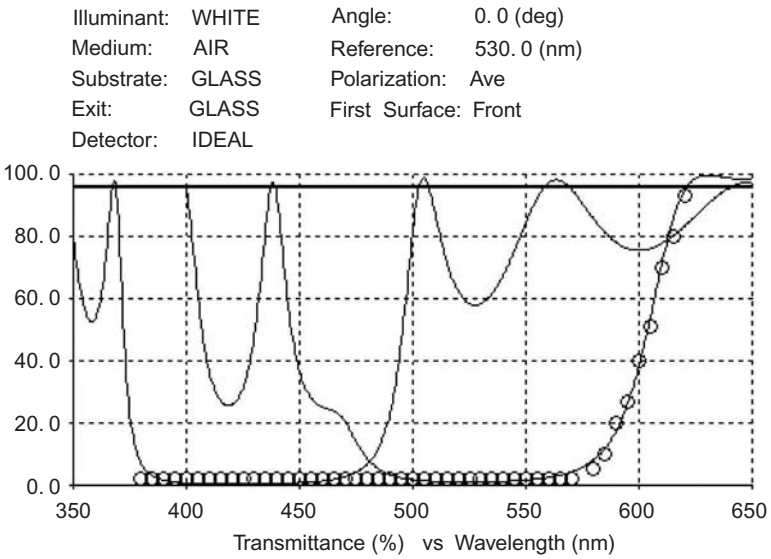

Figure 5.9 Components of the blocked long-pass filter and targets (circles).

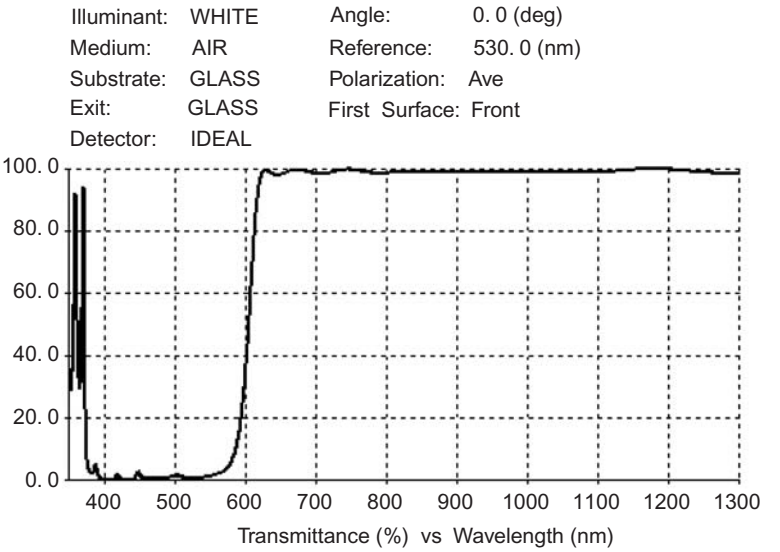

Figure 5.10 Blocked 38-layer long-pass filter.

the reflection in the pass zone is also defined (<1.0%R). Only the first four layers of the blocker are allowed to have nonquarterwave thicknesses in addition to those altered in the long-pass portion. Optimization yields a clean filter with blocking to 380 nm (Fig. 5.10).

I have made many filters similar to those described by utilizing TiO_2 and quartz materials with crystal monitoring for thickness control. The spectral performance is always in agreement with the design once the tooling factors are established for the controller.

5.3 Notch Filters

Two concepts that Thelen developed are used to design reflection filters that have low ripple in the pass zones on both sides of the reflecting notch.[1,2] Thelen's idea of examining the *equivalent index* of a basic filter type and finding another index-ratio filter of the same type that antireflects the former works well. If quarterwave stacks (QWSs) are used, the filter will consist of ALBLCL $(HL)^x$ CLBLA, where A, B, and C have differing index values. The starting design must have matching substrate and entrance mediums. Optimizing one pass zone is all that is necessary for a QWS; index values are quickly found with the optimization routine. Once the index values are selected, the layers can be *converted to equivalent layers* of the material H and L. The matching medium is then changed to air, and an L layer is added. More optimization targets are now needed to include the high-side %T zone; the odd thickness layers are reoptimized. If the ripple is more than you want, then increase the number of layers altered (Fig. 5.11). The final design in air is illustrated in Fig. 5.12. Filters with clean performance result from using this process. The bandwidth of the filters is a function of the ratio of the indices used to

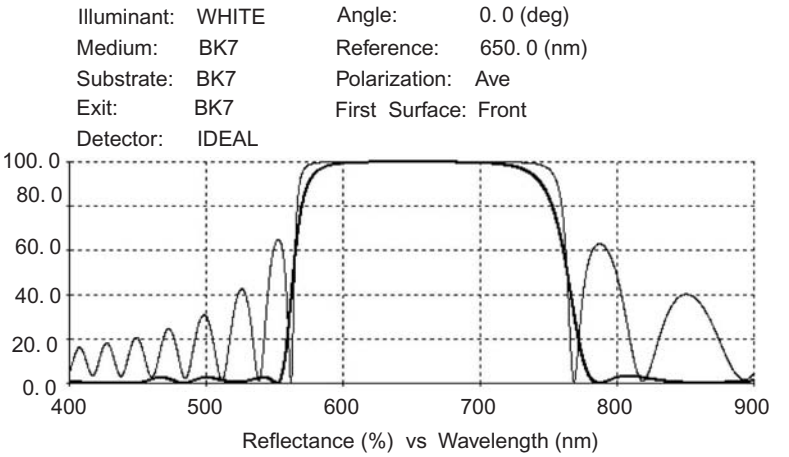

Figure 5.11 A notch design for five materials (thick line) and the QWS (thin line) starting design, matching to glass on both sides.

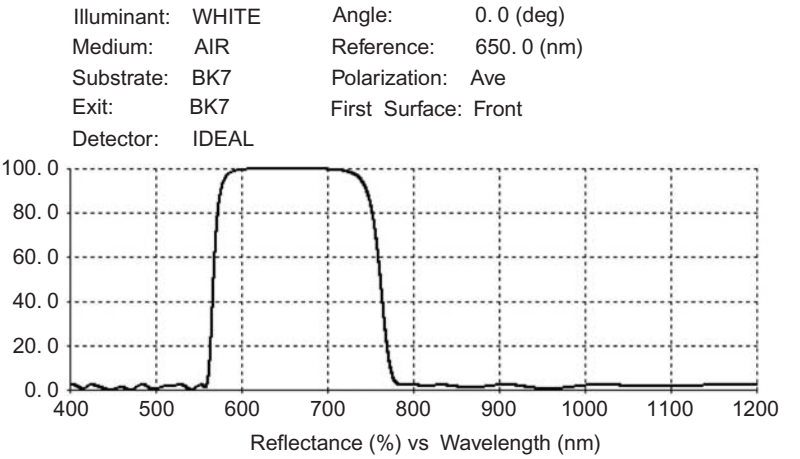

Figure 5.12 The final design in air.

make the QWS. Based on the materials that are available, only a limited variety of filters are feasible. Third-order filters make narrower notches with a series of other reflection bands added. Another type of reflection filter, that is, metal, is discussed in the next chapter.

References

1. A. J. Thelen, "Design of optical minus filters," *J. Opt. Soc. Am.* **61**, 365–369 (1971).
2. A. J. Thelen, "Equivalent layers in multilayer filters," *J. Opt. Soc. Am.* **56**, 1533–1538 (1966).

Chapter 6
Metal Films and Filters

6.1 Mirrors

The first films produced by vacuum deposition—as we know it—were aluminum films for mirrors made by John Strong in the 1930s; he coated mirrors for astronomical use. This chapter discusses the reflective qualities of mirrors, not the optical qualities. The films can be applied to virtually any material as long as the shape of the blank does not bend too far because the coatings lose their reflection at severe angles. Also, the surface needs to be polished or smooth drawn.

The metals used for most reflectors are gold, silver, or aluminum. There are advantages for each (Fig. 6.1). If a mirror is to be used only from 700 nm to the far-infrared spectrum, then gold is a good choice. For the visible and most of the infrared spectrum, the highest reflection is achieved with silver. Aluminum is a good choice if durability is a concern; it is also the only choice for the ultraviolet spectrum (Fig. 6.2).

6.2 Overcoats

Protection of a mirror surface is a necessity for most applications. Adding one layer of *any* index of refraction to a metal surface reduces the reflectance for the whole spectrum except at one wavelength. If the overcoat is thin (in comparison to the wavelength), the loss may be neglected. For instance, a gold mirror used

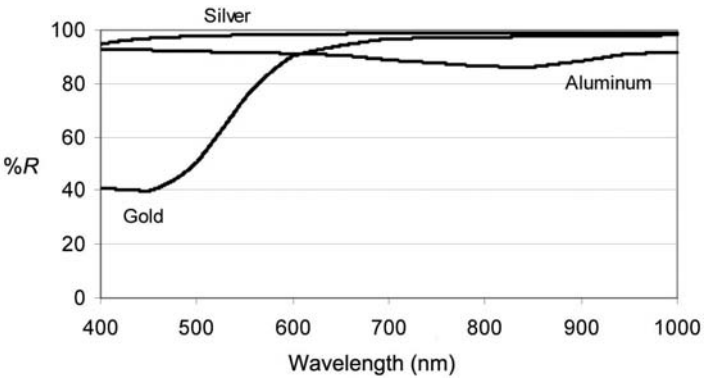

Figure 6.1 The reflectance of bare metals.

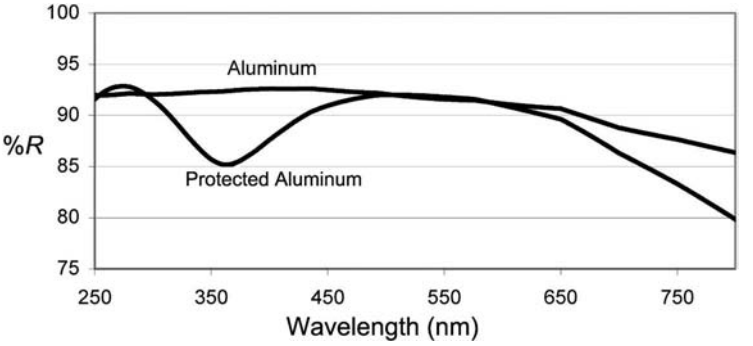

Figure 6.2 Protected aluminum.

at 10 μm can have a covering of hafnium oxide and still have practically full reflection.

Millions of protected aluminum mirrors have been made. The metal layer is covered with silicon dioxide (quartz) to preserve the reflectance at about 550 nm. The thickness of the quartz overcoat is an effective halfwave; the surrounding wavelengths suffer some minor loss of performance. Figure 6.2 shows the reduction for a visible mirror. To preserve the reflection, another higher-index layer is added, and the thickness of the quartz overcoat is reduced to an effective quarterwave; the high-index layer is a quarterwave thick. This structure is an enhanced mirror, and the reflection can be substantially increased with the proper choice of materials (Fig. 6.3). Refractory oxides such as TiO_2, Nb_2O_5, Ta_2O_5, ZrO_2, HfO_2, and Al_2O_3 with SiO_2 are used in various areas of the spectrum to advantage (Fig. 6.4).

Same-layer structures with transparent high-index materials give good performance for the ultraviolet spectrum. The improved spectral zone can be shifted to make a desired area higher in reflection; the mirrors can be optimized for use at 45 deg (Fig. 6.5); however, polarization of the light needs to be considered.

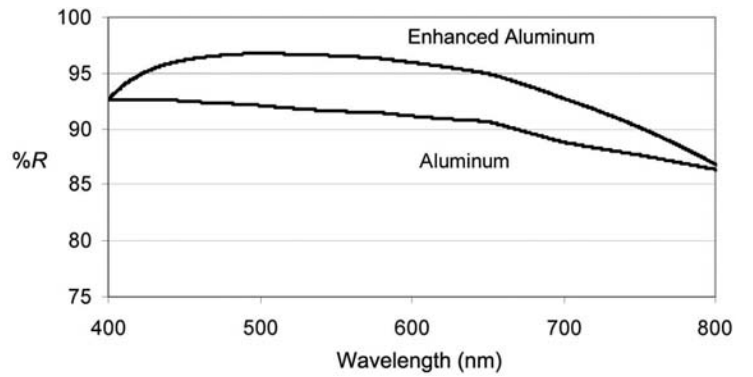

Figure 6.3 Enhanced aluminum for the visible spectrum using Nb_2O_5.

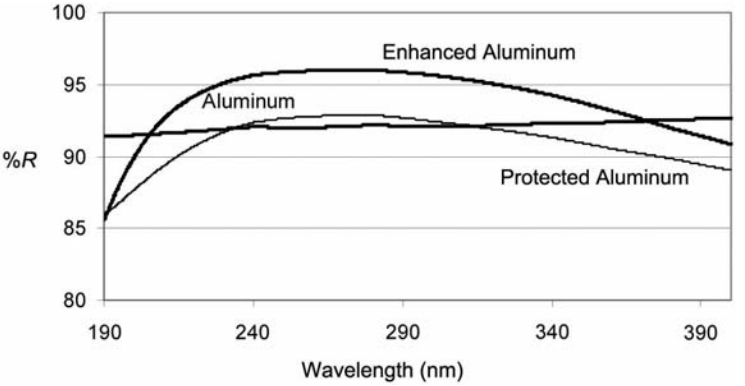

Figure 6.4 A comparison of aluminum, protected aluminum, and enhanced aluminum using HfO_2 with low absorption for the ultraviolet spectrum.

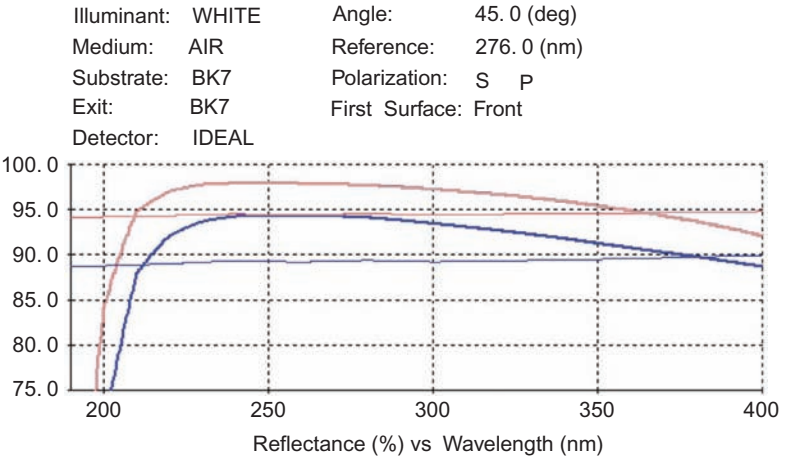

Figure 6.5 S- and P-polarized reflectance of aluminum and a two-layer-enhanced aluminum design at 45 deg using absorbing HfO_2 for the ultraviolet spectrum. The thick lines are for two-layer-enhanced aluminum; the thin lines are for aluminum. The highest reflection curve (in each pair) is the S-polarized reflectance; the lowest reflection curve (in each pair) is the P-polarized reflectance.

The wavelength zone for maximum performance is restricted for the two-layer overcoating and is quite narrow for a four-layer type, as shown in Fig. 6.6.

To increase the reflection of the wavelengths below 220 nm, either fluorides or Al_2O_3 must be used. I used MgF_2 combined with Al_2O_3 instead of SiO_2 for the low-index layer (Fig. 6.7). To achieve this type of performance, during the metal deposition the vacuum must be in the low 10^5 Torr range and the deposit should take less than 5 seconds. A 5-nm layer of MgF_2 is quickly added to the Al film to seal it from oxidation, the substrate is heated to ~100 °C, and the remainder of the films is then added. The design is 60-nm Al 0.58 qw L plus quarterwaves of

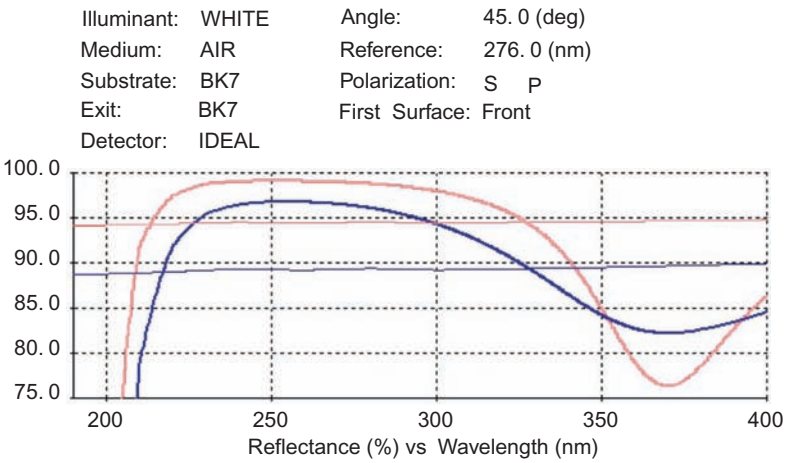

Figure 6.6 S- and P-polarized reflectance of aluminum and a four-layer-enhanced aluminum design at 45 deg using absorbing HfO_2 for the ultraviolet spectrum. Thick lines are for four-layer-enhanced aluminum; thin lines are for aluminum. The highest reflection curve (in pairs) is the S-polarized reflectance; the lowest reflection curve (in pairs) is the P-polarized reflectance.

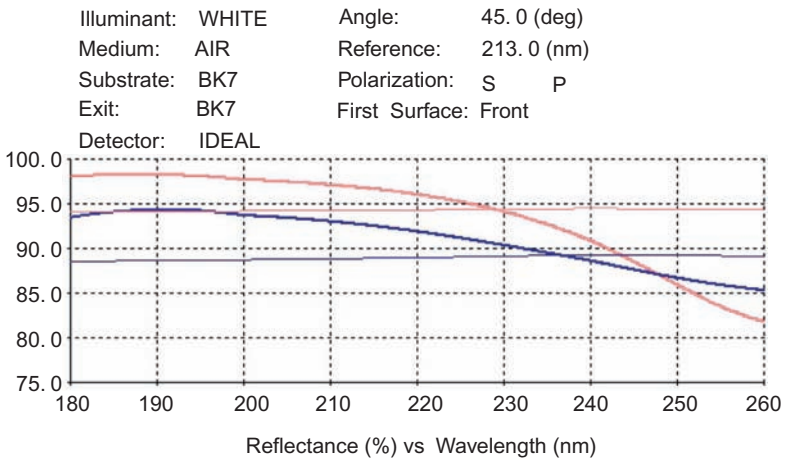

Figure 6.7 S- and P-polarized reflectance of aluminum and a four-layer-enhanced aluminum design at 45 deg using Al_2O_3 and MgF_2 at 193 nm. Thick lines are for four-layer-enhanced aluminum; the thin lines are for aluminum. The highest reflection curve (in pairs) is the S-polarized reflectance; the lowest reflection curve (in pairs) is the P- polarized reflectance.

HLH at 213 nm. The layers are quarterwave for normal incidence. I have not used an ion source with these films, but the density of the layers improves when IAD is incorporated; low power is recommended.

6.3 Silver Mirrors

Silver mirrors yield the highest reflection for the visible and infrared regions. The silver layer tarnishes easily, so it requires a durable protective overcoat. Further, the silver layer has a tendency to lose adhesion to a very necessary sticking layer, and finding the optimal sticking layer is difficult because it could take a month or longer for the loss of adhesion to become apparent. Many times I thought I had the answer, only to face problems a few months later. In the near-ultraviolet region, the silver layers also have a problem of low reflection that is caused by surface plasmons. If the silver layer is deposited from a boat, either with resistance heating or a special technique of heating with an e-beam gun, the loss of reflectance is minimized.

6.4 Protected Silver

For mirrors, the thickness of a sticking layer is not critical. If ambient light is transmitted through the metal, the reflected light from the substrate never completely penetrates the metal layer for any reasonable intensity of ambient light. To seal the silver layer, a small thickness of high-index refractory oxide such as TiO_2 is deposited without an ion source or oxygen; the layer does not have much of an optical effect but does stick quite well to the metal. The dielectric layers following the seal layer are deposited with IAD. Films made with this technique have survived for at least a few years and still pass the tape test and mil-spec cheesecloth rubbing. Theoretical curves for silver, protected silver, and enhanced silver are shown in Fig. 6.8. The lowest reflection curve is the protected type; the middle curve is the metal. The enhanced coating consists of six layers:

5nmT 150nmAg 5nmT 0.7qwQ 0.97qwT 1.15qwQ.

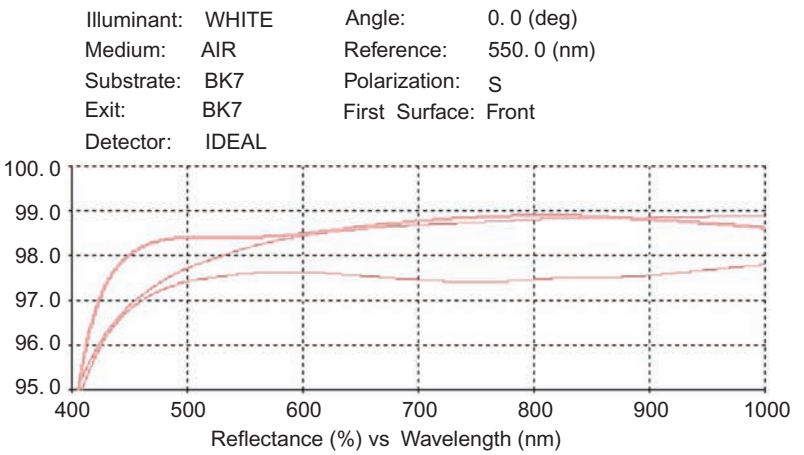

Figure 6.8 A comparison of silver, protected silver, and enhanced silver (from top to bottom at 500 nm).

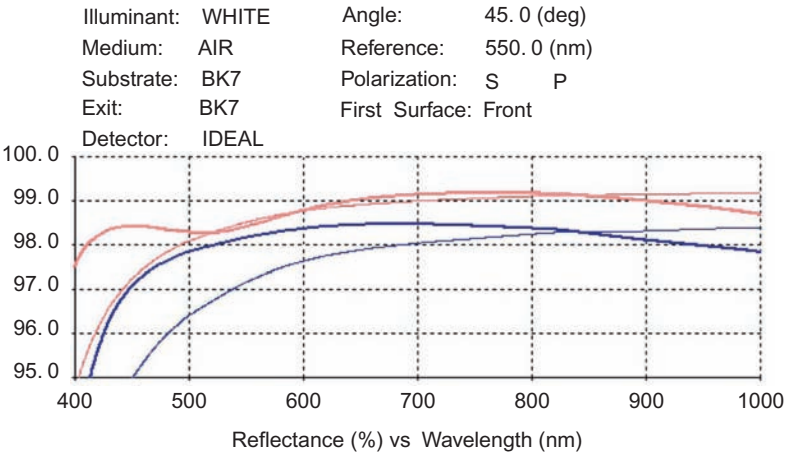

Figure 6.9 The same enhanced silver and silver at a 45-deg angle. Thick lines are for enhanced silver; thin lines are for silver. The highest reflection curve (at 500 nm) in pairs is for the S-polarized reflectance; the lowest reflection curve (in pairs) is the P-polarized reflectance.

Reflectance in the blue–green region is improved with no loss of reflection to beyond 900 nm (Fig. 6.9). The performance at 45-deg is excellent with no further optimization for the enhanced mirror.

6.5 Gold Mirror

The enhanced gold coating should provide excellent results for the near-infrared spectrum to ~4 μm (Fig. 6.10). For 12 μm a simple overcoat of yttrium oxide deposited with IAD will render greater than 98%*R*, even at a 45-deg angle (Fig. 6.11).

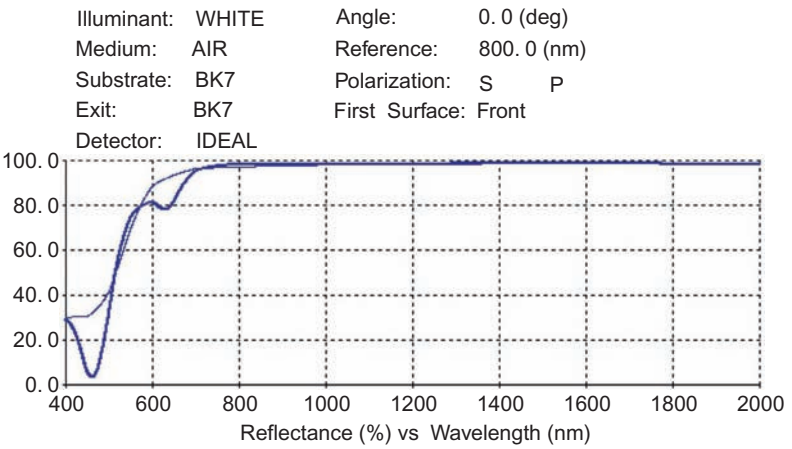

Figure 6.10 P-polarized reflectance for gold (thick line) and enhanced gold (thin line) for 400–2000 nm.

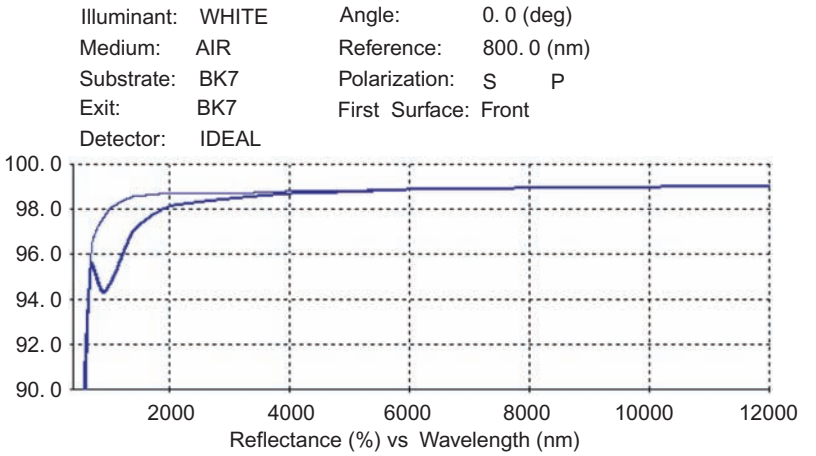

Figure 6.11 P-polarized reflectance for protected gold (thick line) and gold (thin line) for the 2–12 μm region. The advantage of gold over silver is gold's lack of sensitivity to pollution, acids, and bases in the air; gold is quite inert.

6.6 Beam Splitters

As mentioned in Chapter 4, the inclusion of a silver layer improves the performance of thin-film beam splitters. The designs for this section are used in air at a 45-deg angle. Polarization is a major problem for filters used at an angle and must be examined for the film arrays. These filters are not loss free; the metal absorbs about 4% of the energy. The spectral flatness for the relatively low number of films makes thin-film beam splitters preferred over all-dielectric ones (Fig. 6.12).

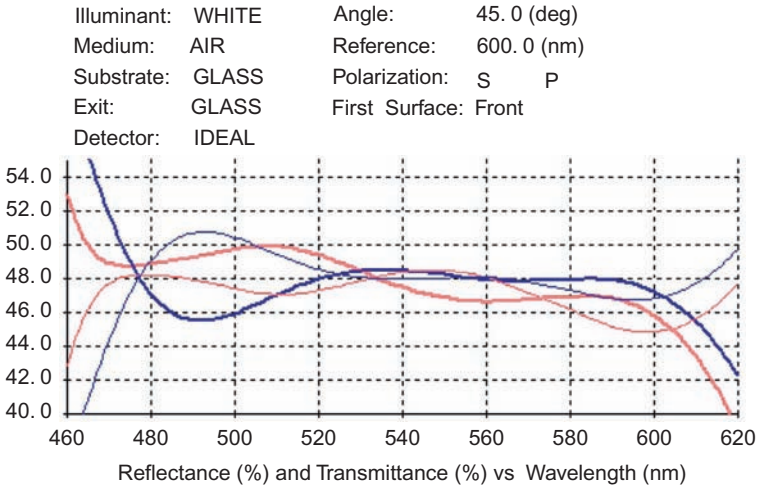

Figure 6.12 A 50–50 beam splitter. The thick lines are reflectance; the thin lines are transmittance. The highest thick curve at 460 nm is P-polarized reflectance; the lowest thick curve at 460 nm is S-polarized reflectance. The highest thin curve at 460 nm is S-polarized transmittance; the lowest thin curve at 460 nm is P-polarized transmittance.

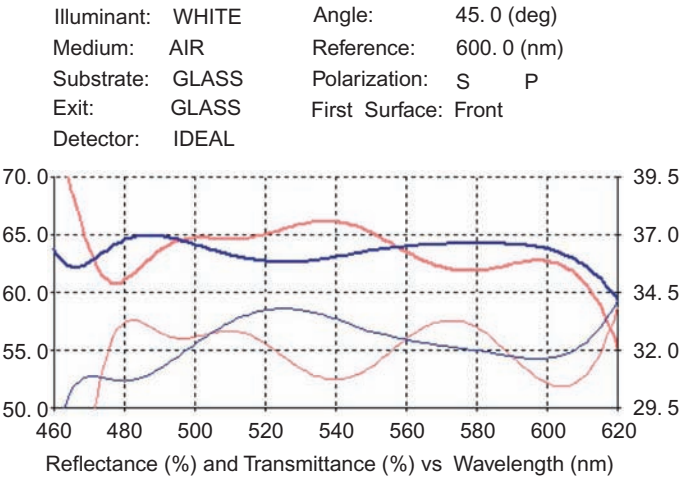

Figure 6.13 A 33T–67R beam splitter. Thick lines are reflectance; thin lines are transmittance. The highest thick curve at 480 nm is P-polarized reflectance; the lowest thick curve at 480 nm is S-polarized reflectance. The highest thin curve at 480 nm is S-polarized transmittance; the lowest thin curve at 480 nm is P-polarized transmittance.

A design utilizing TiO_2 and SiO_2 for the 14-layer slab filter is

0.32qwT 0.65qwQ 0.37qwT 0.81qwQ 1.13qwT 1.68qwQ 5nmT 26nmAg 0.57qwT 1.34qwQ 1.2qwT 1.46qwQ 1.27qwT 0.96qwQ

with quarterwave reference thickness at 600 nm. Equal-intensity beams for the average transmitted and reflected light beams occur at ~470–610 nm. The polarized beams are within ±2.5%; wider spectral zones require more ripple. All-dielectric beam splitters require more layers and work over smaller spectral ranges. A similar filter for reflecting twice as much light as the light transmitted is shown in Fig. 6.13. A 16-layer design utilizing TiO_2 and SiO_2 is

0.55qwT 0.5qwQ 0.52qwT 0.9qwQ 0.95qwT 1.85qwQ 5nmT 31.2nmAg 0.6qwT 1.25qwQ 1.7qwT 0.67qwQ 1.15qwT 1.68qwQ 1.27qwT 0.77qwQ

with quarterwave reference thickness at 600 nm. The reflection is ~64%, and the transmission is ~32% in Fig. 6.14. An eight-layer design utilizing TiO_2 and SiO_2 is

0.3qwT 13.4nmAg 0.52qwT 0.57qwQ 0.4qwT 0.88qwQ 0.83qwT 1.21qwQ

with quarterwave reference thickness at 600 nm. The reflection is ~32.5%, and the transmission is ~65%.

6.7 Etalon Coating

Historically, coatings for wideband etalons have been strictly a silver layer. The reflection of a layer with ~80% reflection varies from 40 to 90% and from 400 to 700 nm. The finesse of a filter made from assembling two of these layers can

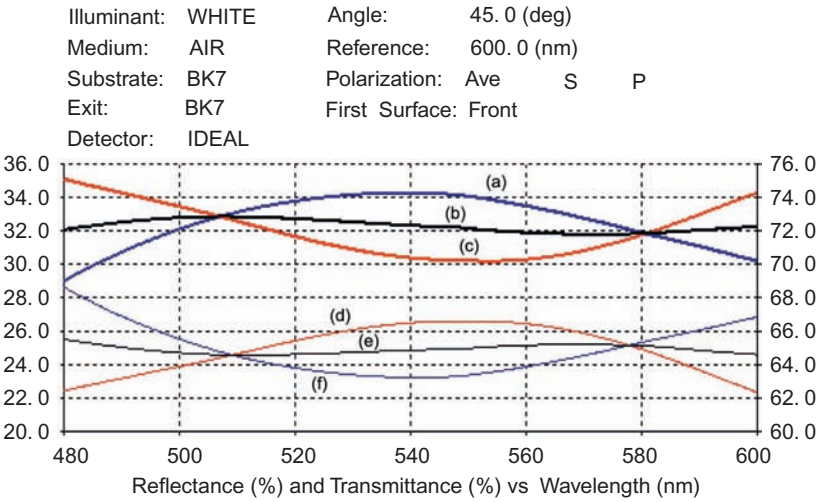

Figure 6.14 A $67T$–$33R$ beam splitter. Thick lines are reflectance; thin lines are transmittance. (a) The highest thick curve at 540 nm is P-polarized reflectance; (b) the middle thick line at 540 nm is average reflectance; (c) the lowest thick curve at 540 nm is S-polarized reflectance. (d) The highest thin curve at 540 nm is S-polarized transmittance; (e) the middle thin line at 540 nm is average transmittance; (f) the lowest thin curve at 540 nm is P-polarized transmittance.

vary too far to be useful. I sold a coating similar to the design in Fig. 6.15 to a manufacturer of a wavelength meter instrument. The flatness of the reflectance is outstanding for any reflectance value selected. The design has six layers: 0.8qwT 29.5nmAg 5nmT 0.31qwQ 0.59qwT 0.76qwQ.

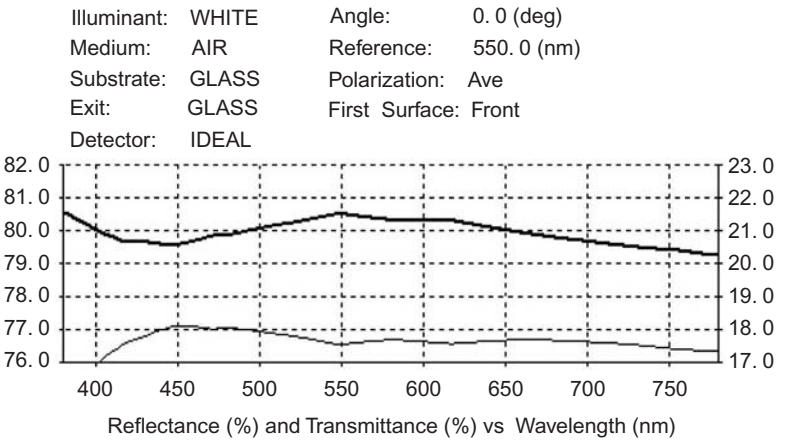

Figure 6.15 Normal-incidence etalon coating. The thick curve is reflectance; the thin curve is transmittance.

6.8 Neutral-Density Filters

The mainstay of the industry has been a single-layer coating of Inconel® (abbreviated as I in the designs that follow). For high-transmission neutral-density (ND) filters there is only a small slope for the visible–near-infrared spectrum. High-density (low-transmission) films have a brown tint. The transmission near 400 nm is much less than that near 700 nm; over- and undercoats can be applied to alleviate this. I have a patent (probably not active) for low-reflection ultraviolet ND filters in which the density is achieved by using a number of metal layers with oxide films between the layers. The reflection is quite low over a 1.5–1 μm span with flat transmission for the same range. The same general technique works for the visible–near-infrared spectrum. The low reflection can be one-sided (simpler) or two-sided (Fig. 6.16). Similar designs for the visible and near-infrared spectrum are shown in Figs. 6.17 and 6.18.

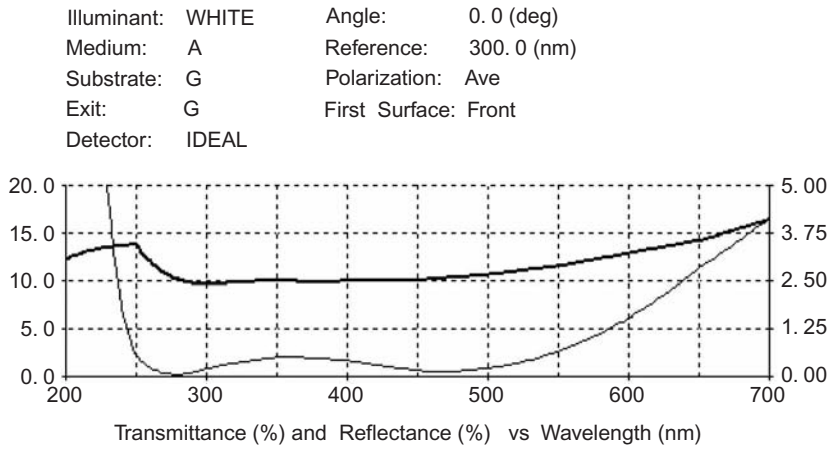

Figure 6.16 A UV ND filter with 11 layers. The thick curve is reflectance; the thin curve is transmittance.

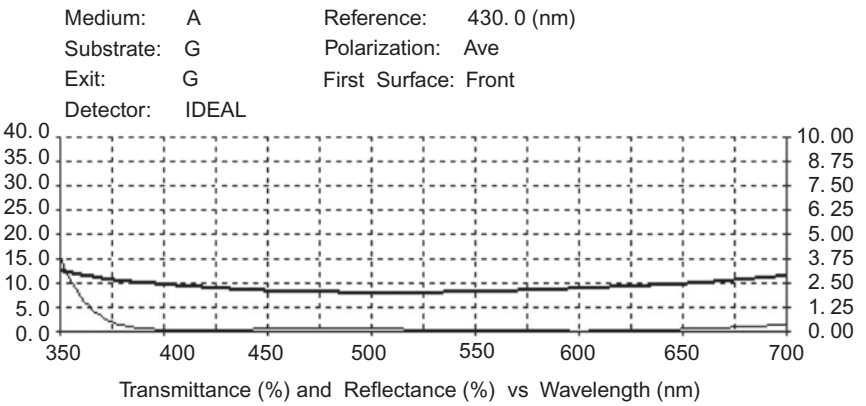

Figure 6.17 A nine-layer ND filter for the visible spectrum. The thick curve is reflectance; the thin curve is transmittance.

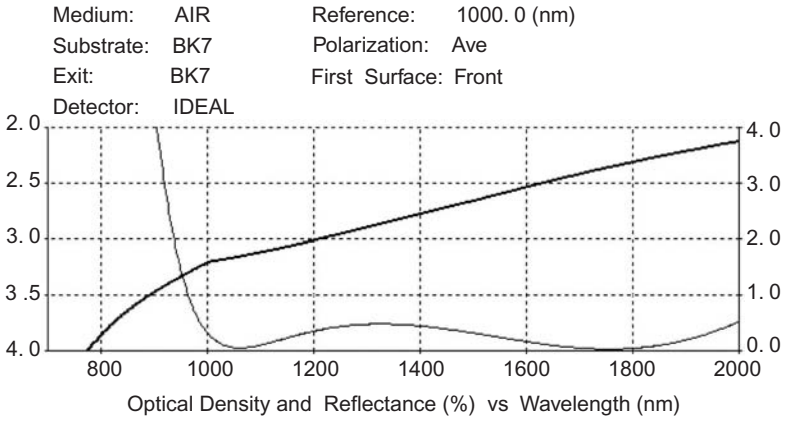

Figure 6.18 A ND filter for the near-infrared spectrum. The thick curve is reflectance; the thin curve is transmittance.

Design: 0.66qwAl_2O_3 0.38qwHfO_2 4.5nmI 0.77qwHfO_2 8nmI 0.83qwHfO_2 12nmI 0.89qwHfO_2 6.5nmI 0.28qwHfO_2 1.01qwQ referenced to 300 nm qw.

Design: 0.83qwHfO_2 4.4nmI 0.26qwHfO_2 5nmI 0.91qwHfO_2 19nmI 0.99qwHfO_2 8nmI 1.01qwQ referenced to 430 nm qw.

This design was optimized for low reflection from both sides of the film. If the density flatness was the most important parameter, the reflection loss would be larger.

Design: 1.38qwAl_2O_3 1.2qwNb_2O_5 27nmI 0.96qwNb_2O_5 80nmI 90nmI 0.61N 50nmI 9nmI 1.28Q referenced to 1000 nm qw.

Low reflection is important because if two or more density filters (or any kind of filter) are used in series, the densities do not add together if they are reflective filters. One low reflective surface is sufficient to allow adding the densities together.

6.9 Solar Coatings

Solar barrier coatings available for high sunlight areas typically have ~5% transmission of visible and infrared light (Fig. 6.19). Typically, light-colored screens with many holes are used because it is difficult to see clearly through them. A barrier film can be applied to glass or plastic, which has superior clarity and much better removal of infrared radiation compared to light color screens.

A choice of materials is available for manufacture: metals with reasonable reflectance in the infrared spectrum, such as nickel and niobium, are sandwiched with a high-index clear—but not necessarily nonabsorbing—oxide material. A high-efficiency design with seven layers works well on a roll coater (Fig. 6.20). The design is set up to run through four magnetron targets with two passes; one in reverse; V2 has a nonabsorbing high index of 2.2.

Seven-layer design: 1qwV2 10nmNi 10nmNb_2O_5 0.93qwV2 10nmNb_2O_5 10nmNi 0.79qwV2.

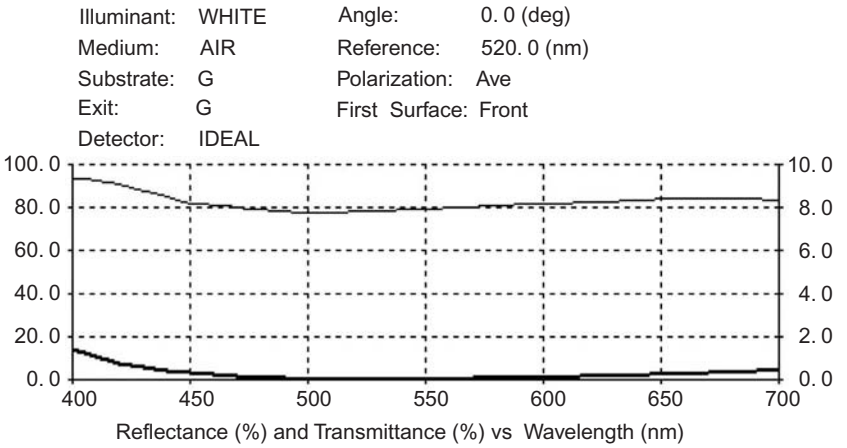

Figure 6.19 Visible performance of solar coating. The thick curve is reflectance; the thin curve is transmittance.

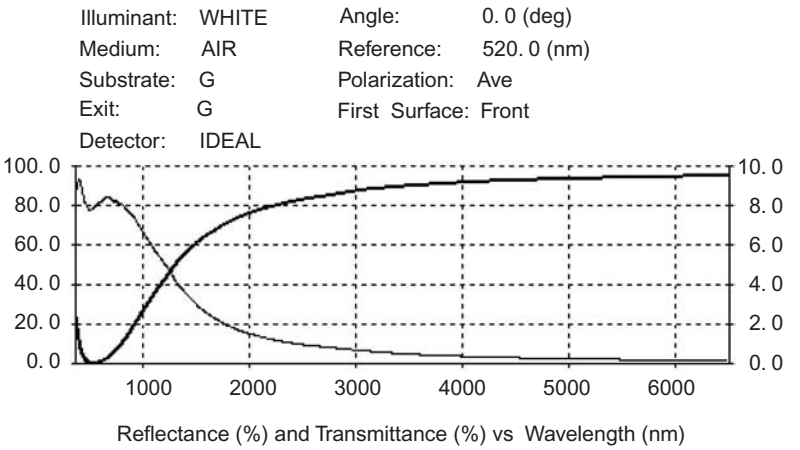

Figure 6.20 Infrared spectral characteristics. The thick curve is reflectance; the thin curve is transmittance.

Errors of 5% do not change the results appreciatively. The dielectric V2 can be any high index between 2 and 2.3 used with slightly different metal thicknesses.

6.10 Absorbers

Coatings that absorb the solar spectrum applied to metal tubes can be used to heat liquids to high temperatures. Baumeister describes a "cold mirror" coating that is deposited on a metal substrate and consists of a long-pass all-dielectric layer applied to a "dark mirror."[1] A design for a dark mirror was given using nearly opaque titanium metal deposited on any surface as the base (Fig. 6.21). Then six layers are applied starting with a quartz film. I prefer using Inconel® as a base metal (Fig. 6.22), as do Dobrowlosky, Ho, and Waldorf.[2]

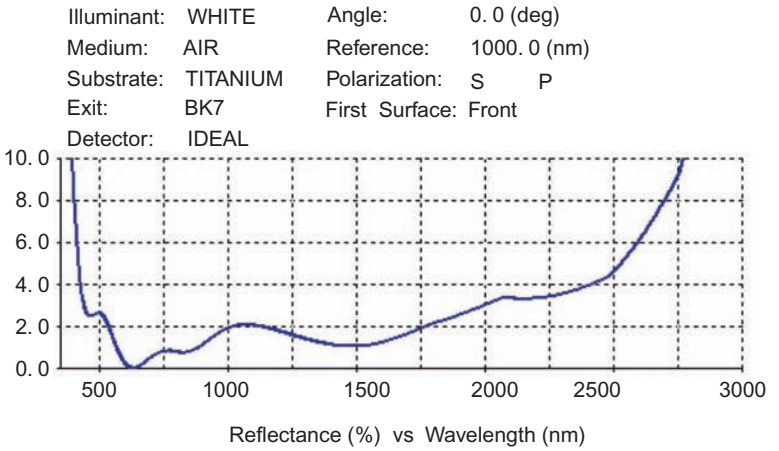

Figure 6.21 P-polarized reflectance of a dark mirror from Baumeister.

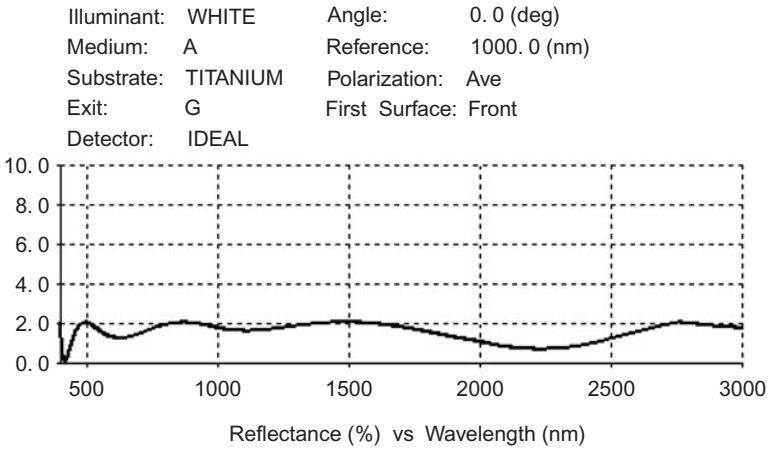

Figure 6.22 A dark mirror featuring Inconel layers on a metal substrate.

Design: 0.36L 12nmT 0.57L 11nmT 0.38H 0.67L with quarterwave layers at 1000 nm.

Design: 0.48qwQ 33nmI 0.23qwNb 0.37qwQ 12nmI 0.4qwQ 12nmI 0.66qwQ referenced to 1000 nm.

Altering the targets can provide lower reflectance for a smaller wavelength range. Figure 6.23 displays a high-efficiency visible absorber.

Design: 60nmI 2.14qwQ 37nmI 0.79qwQ 12nmI 0.74qwQ referenced to 550 nm.

6.11 Dual-Function Film

Liquids flowing through solar absorbers provide steam for megawatts of electricity. A concentrating mirror (for the entire spectrum) with controls to follow the sun

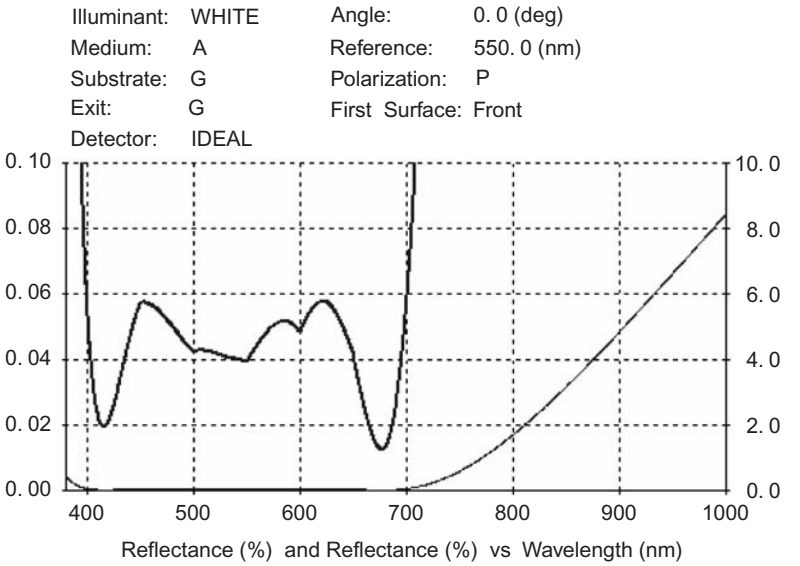

Figure 6.23 Low-reflection visible coating with six layers. The thick line shows a zoomed view.

focuses the sun's radiation on a reflector that is added to a dark mirror. The dark mirror is then refocused on the sensor area of a silicon detector for the visible–near-infrared region. Reflectors are applied to tubes that are shaped to concentrate the visible light; electricity for dark periods can be stored to heat the liquid for solar heating when the temperature falls. The absorbed radiation produces steam. The first coating shown (Fig. 6.24) maximizes the reflection zone for silicon; the other simpler coating provides more absorption of the solar spectrum (Fig. 6.25). The 17-layer coating shown in Fig. 6.24 consists of two metal layers with silicon and quartz dielectric layers selected to reflect the whole spectrum used by a silicon detector. The coating in Fig. 6.25 is a simplified version of the 17-layer filter. The wavelength response can be shifted to suit any cutoff requirement. A metal slab (aluminum in this example) *absorbs* all of the radiation that is *not* reflected.

6.12 Reflective Color Filters

To make a "stained-glass mirror" (instead of a stained-glass window), low-transmission color filters are used. Light coming from the rear surface has little effect on the observed reflection of the front surface; good results do not require many layers. The films can be applied to any surface by increasing the thickness of the Inconel barrier layer with some slight modifications in the designs. Designs for normal incidence perform well for small angles. Long- and short-reflection designs have two metal layers that act as a selective dark mirror; then a dichroic is deposited over the metal–dielectric–metal (MDM) coating (Figs. 6.26–6.30).

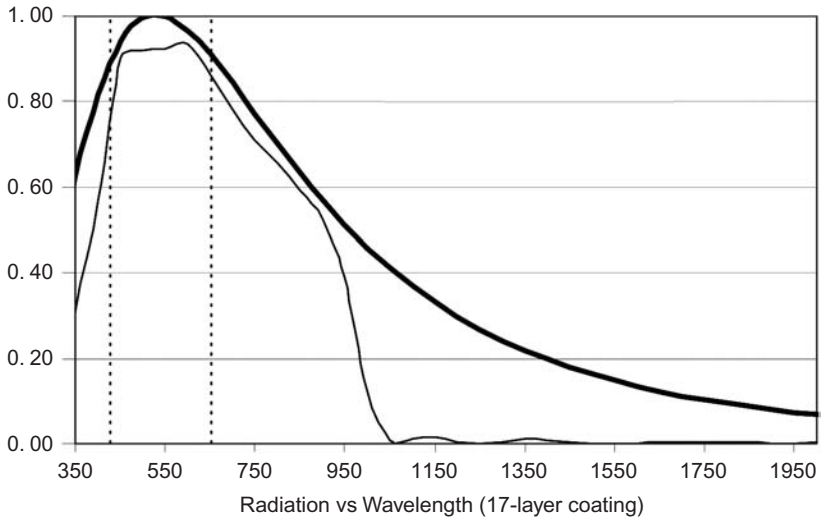

Figure 6.24 A silicon spectrum-reflecting coating. The thick line is radiation for a 5500 K source; the thin line is a 17-layer coating; the visible spectrum is between the straight dashed lines.

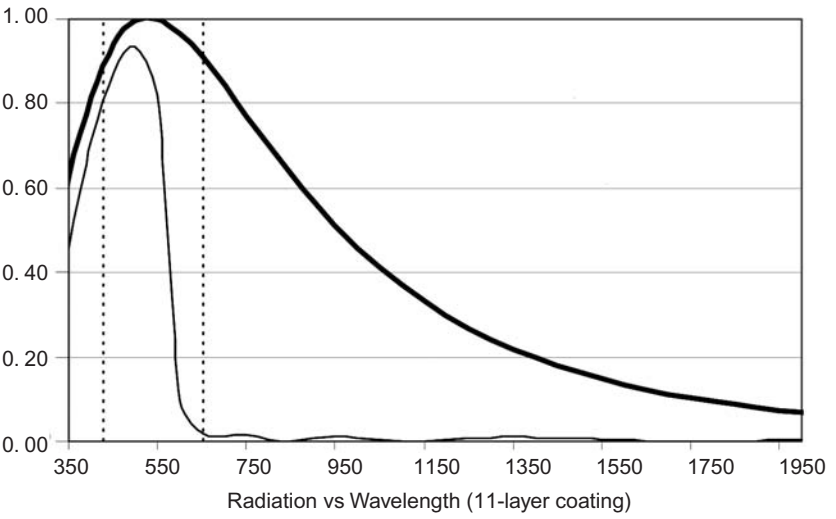

Figure 6.25 An 11-layer variation of the silicon spectrum-reflecting coating. The thick line is radiation for a 5500 K source; the thin line is for an 11-layer coating.

Design: 30nmI 1.42qwQ 0.62qwT 13.3nmI 2.11qwT 0.41qwQ 1.2qwT 1.47qwQ 0.48qwT 2.33qwQ referenced to 600 nm.

Design: 30nmI 2.27qwT 1.07qwQ 0.61qwT 7.1nmI 1.17qwQ 1.53qwT 0.82qwQ 0.79qwT 1.24qwQ 1.49qwT referenced to 630 nm.

Design: 40nmI 0.58qwT 13.6nmI 1.88qwT 1.3qwQ 1.17qwT 1.21qwQ 1.17qwT 1.22qwQ 1.3qwT 2.24qwQ referenced to 600 nm. The slope is moderate.

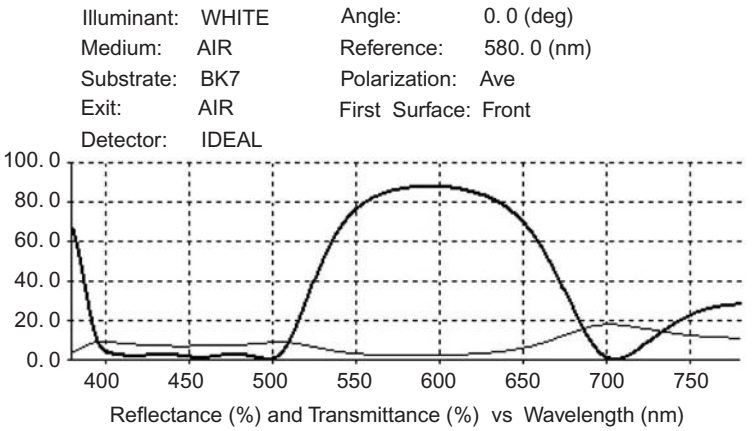

Figure 6.26 A yellow filter with 10 layers. The thin line is $\%T$; the thick line is $\%R$.

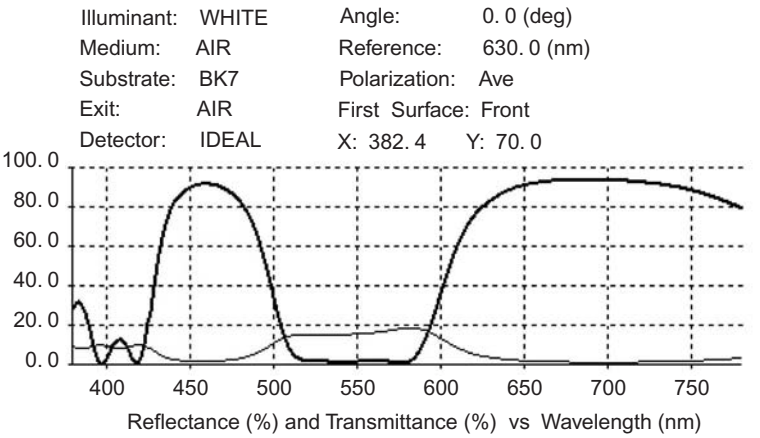

Figure 6.27 Magenta filter (#5) with 11 layers. The thin line is $\%T$; the thick line is $\%R$.

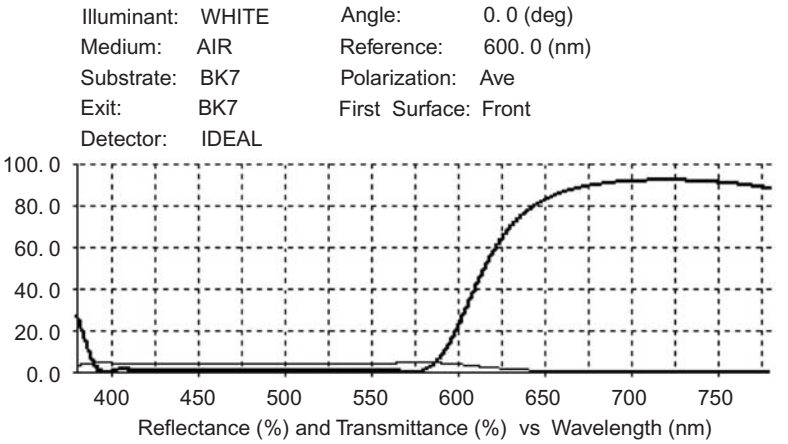

Figure 6.28 An 11-layer red–orange filter. The thin line is $\%T$; the thick line is $\%R$.

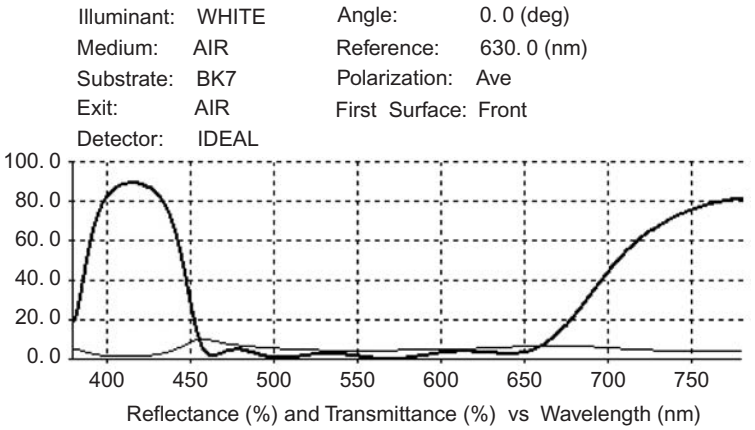

Figure 6.29 A purple filter with nine layers. The thin line is $\%T$; the thick line is $\%R$.

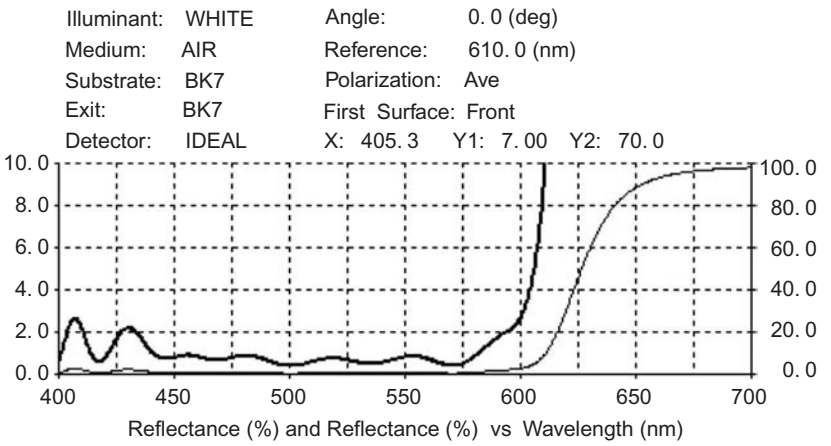

Figure 6.30 A red reflector with 15 layers.

Design: 30nmI 0.93qwQ 1.55qwT 13.6nmI 1.61qwQ 1.04qwT 0.21qwQ 1.97qwT 2.62qwQ referenced to 630 nm.

Blocking visual light is high for the 450–575 nm area. The bandwidth is uncontrolled for the higher wavelengths because the eye does not respond (comparatively) to this region of the spectrum. Having more light increases the red visibility (Fig. 6.31).

Green filters require blocking of both the blue and red areas of the spectrum. Dobrowolski, Ho, and Waldorf[2] describe one filter with three metal layers in their paper on anticounterfeiting. Designs can become complicated with only two metal layers, and wide bands are possible. Select the targets and change the position of the metal layer to find a reasonable design.

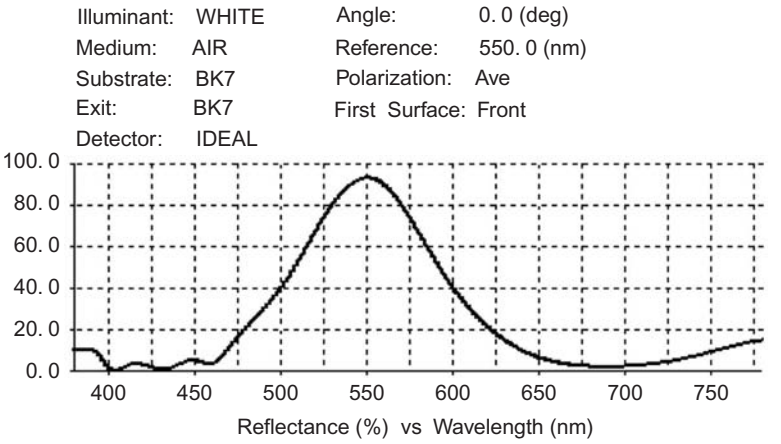

Figure 6.31 A reflective filter with the spectral response of the eye.

Design: 60nmI 1.69qwT 1.08qwQ 1.26qwT 0.8qwQ 1.59qwT 1.43qwQ 23nmI 0.62qwT 0.24qwQ 1.27qwT 0.37qwQ 1.64qwT 0.28qwQ 1.391qwT 2.04qwQ referenced to 550 nm.

Similar performance for most filters can be achieved with a combination of color targets and blocking targets. All of the yellow–red colors can be achieved with high saturation of color using 11–15 layers in a long-pass configuration. The blues and purples are selected with a short-pass filter; blue–green to green–yellow require bandpass-type designs. The bandpass filters can be used for all of the wavelengths with limited luminosity (Fig. 6.32). This filter has 15 layers with 3 Inconel layers; performance was optimized by targeting the color coordinates and a selected luminosity. Using more layers allows for a narrower bandwidth that produces lower luminosity. More information about bandpass filters follows in the next section.

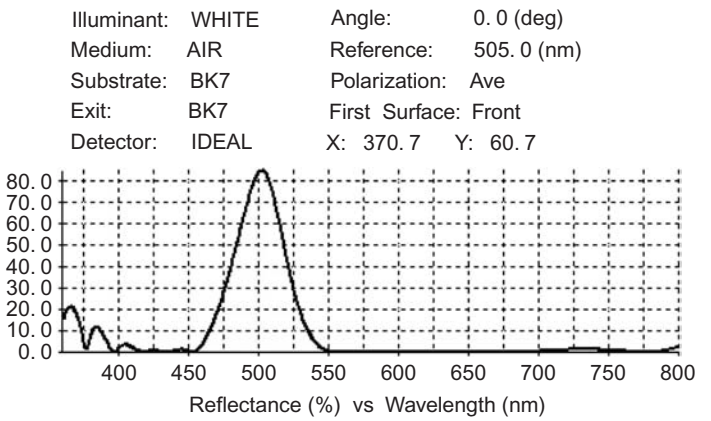

Figure 6.32 Bandpass filter for 500 nm with 40-nm bandwidth.

6.13 Narrower Bands

In addition to the two metal layers near the substrate that initially act as a dark mirror, a third metal layer near the outer surface is required. The filter acts as a solid etalon. Filters for narrower bandpasses require more layers. The filters are designed to *absorb* the radiation that is not reflected as a bandpass; the designs are based on work first described by Gamble and Lissberger,[3] Tan, Lin, Zhao,[4] and others. A series of dielectric layers is inserted between a mirror and a thin metallic layer that acts in the skin-depth region. My filters do not require a mirror; in fact, the substrate can be almost any material. There are at least one to as many as four metal layers. The metal type used is one that has somewhat of a low reflection such as chromium, nickel, and alloys such as Inconel. The ratio of n to k for these metals is close to 1. If the metal layer near the substrate is removed, the filter will still function in reflection; the optical properties are poor, but there is still a peak reflection.

Bandshape cannot be easily improved beyond the performance shown in the designs. Multicavity filters are not allowed. The filters designed for this chapter typically function only in the visible spectrum; further blocking is possible with more layers and less contrast. In Chapter 11 I discuss the use of this structure for a nonpolarizing filter for a 45-deg angle. The low-index material for these filters is SiO_2; the high-index material can be selected from Ta_2O_5, Nb_2O_5, and TiO_2 for the visible spectrum and HfO_2 for the lower-ultraviolet spectrum.

The designs shown were arrived at after much iteration of the optimization program and a great deal of intuitive design sorting and modifications of the structure. The filter in Fig. 6.33 is for the reflection of a mercury line for a black light. The center wavelength is 365 nm, and the filter contains 18 layers.

Design: 20nmI 1.74qwQ 20.5nmI 1.63qwNb_2O_5 1.29qwQ 0.4qwNb_2O_5 1.55qwQ 1.2qwNb_2O_5 0.39qwQ 1.31qwNb_2O_5 0.63qwQ 1.4qwNb_2O_5 0.82qwQ 1.16qwNb_2O_5 1.82qwQ 10.7nmI 0.36qwNb_2O_5 1.28qwQ referenced to 365 nm.

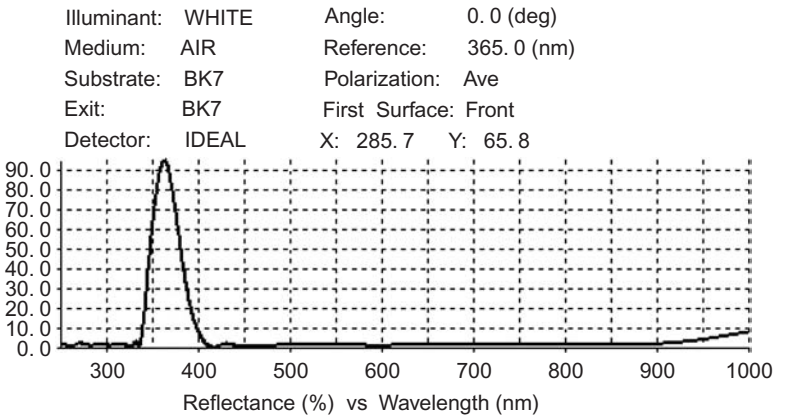

Figure 6.33 An 18-layer filter for 365 nm.

The materials are Inconel, SiO_2, and Nb_2O_5. If the blocking on the high side is optimized to only 800 nm, the out-of-band reflection will be less than 2%. A 488-nm filter with a narrower bandwidth requires more layers (Fig. 6.34). As the center wavelength increases, the low-side blocking becomes more difficult to achieve. A filter for 550 nm has 24 layers with the metal layers in similar positions (Fig. 6.35). The same general layout produced a good filter for 585 nm.

A red filter with 27 layers is shown in Fig. 6.36. The bandwidth is 32 nm, the low-side blocking extends to 400 nm, the high side is blocked to 920 nm, depth of blocking is about 1.5% average, and peak reflection is ~90%. Low-side blocking is more difficult to achieve for bandpass filters, which is why so many layers are required for a narrow-band filter. If the application is in the visual spectrum, the high-side blocking can be relaxed and filters with good contrast can be achieved with fewer and thinner layers. For example, see Fig. 6.32.

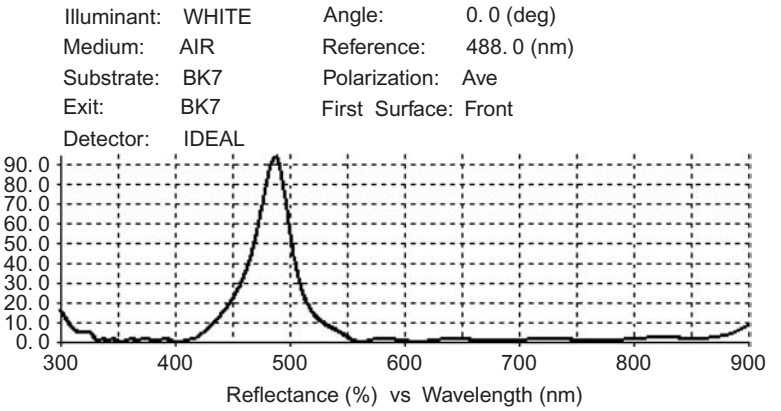

Figure 6.34 A 22-layer filter for 488 nm; TiO_2 and SiO_2 are the dielectrics.

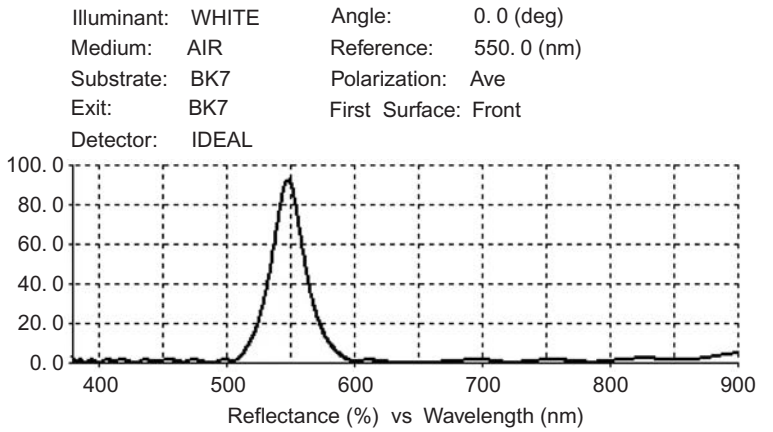

Figure 6.35 A 24-layer filter for 550 nm.

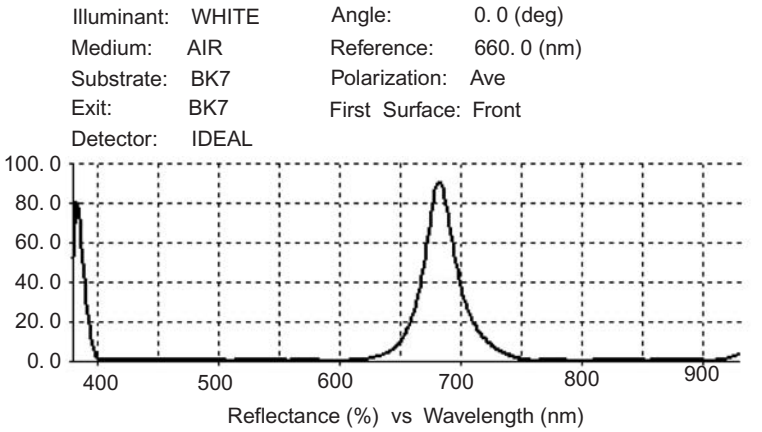

Figure 6.36 A 27-layer filter for 683 nm.

References

1. P. W. Baumeister, *Optical Coating Technology*, SPIE Press, Bellingham, WA (2004) [doi:10.1117/3.548071].
2. J. A. Dobrowolski, F. C. Ho, and A. Waldorf, "Research on thin film anti-counterfeiting coatings at the National Research Council of Canada," *Appl. Opt.* **28**, 2702–2717 (1989).
3. R. Gamble and P. H. Lissberger, "Reflection filter multilayers of metallic and dielectric thin films," *Appl. Opt.* **28**, 2838–2846 (1989).
4. M. Tan, Y. Lin, and D. Zhao, "Reflection filter with high reflectivity and narrow bandwidth," *Appl. Opt.* **36**, 827–830 (1997).

Chapter 7
All-Dielectric Bandpass Filters

Two types of all-dielectric bandpass filters are possible: QWS filters that achieve a bandpass by optimization and Fabry–Perot filters.

7.1 Wide Bandpass Filters

Wideband filters can be designed by combining two reflectors, such as those used in Chapter 5 to make long- and short-pass filters. The 36-layer filter shown in Fig. 7.1 results from shifting the reflection zones of two 18-layer QWSs slightly to the right and left and optimizing to allow the green light to pass. Wideband filters typically will not have the smoothest shapes possible without using huge amounts of layers. Other design techniques are required to remove the wrinkles. A patented approach by Erdogan, Wang, and Clarke[1] utilizes a large number of layers in a QWS that is optimized for a fast cutoff slope; the bandpass can be achieved by target selection (Fig. 7.2). The edges can be selected and improved; all of the layers are nonquarterwave. A long-pass filter can be deposited on the second surface to complete the filter.

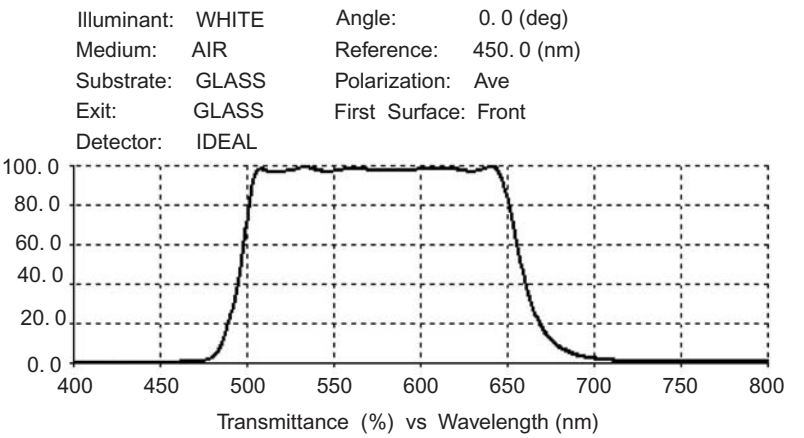

Figure 7.1 A 36-layer, 2-stack green filter.

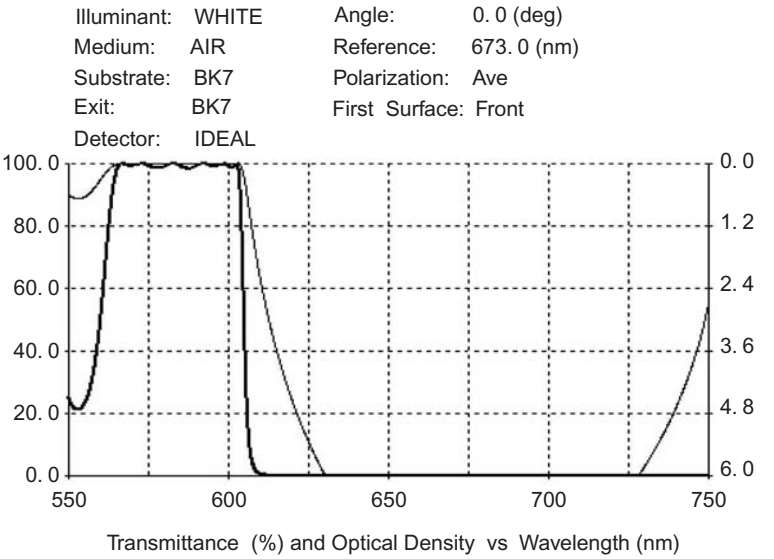

Figure 7.2 Limited-bandpass filter using the Erdogan[1] approach.

7.2 Etalon Filters

Bandpass etalon-type filters are designed with reflectors that are all-dielectric stacks. The simplest filters are made with quarterwave-thickness reflectors only. Perfect matching for an etalon filter (from microwave theory) requires partial quarterwaves; monitoring these layers is difficult. This is not considered in this introduction.

I believe that the earliest etalon filters were designed for the microwave region. The distance between reflectors was machined, and a cavity was left between walls. The simplest explanation of how a bandpass works is that two equal partial reflectors are separated with an air space. The result is an etalon for the parallel surfaces. An illustration of a simple etalon is shown in Fig. 7.3. Each substrate has three layers: HLH.

When the thickness of the air between the reflectors is an even number of halfwaves, the transmitted light is reinforced. When the air's thickness is an odd number, the reflection is reinforced. The number of halfwaves of separation divided by two is defined as the order number. Bandwidth is narrow when the spacing is large. These assembly types are used commercially to observe solar prominences; variations of this structure are used to make tunable filters for communications applications. Although the spectral performance shown in the graphs may not look promising, this filtering technique is the basis for high-quality filters.

The simple expedient of adding more cavities in series improved the bandshape, which is not easy to do with air spacers because of alignment issues and spacing difficulties. Solid etalons are needed, preferably with halfwaves of low-order-number spacers. Thick films tend to crack and many thin-film combinations have high stress; as a result, substrates can bend. Once these factors are considered, the

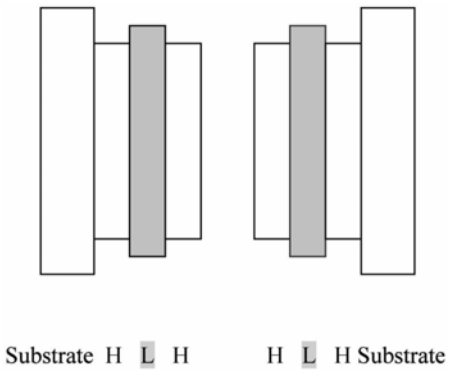

Figure 7.3 Etalon filter layout.

outcome is the fabrication of multicavity Fabry–Perot filters [Fig. 7.4(a) and (b)]. Using the same materials and the same reflector format as in the Fabry–Perot, the structure of a high-transmission film layer set is HLH LL HLH. Then, an identical filter is added on the substrate with a coupling layer between filters (Fig. 7.5). Figures 7.6 and 7.7 illustrate the plots with different numbers of cavities. The transmission is shown for the total filter as each cavity is added. With the few layers used in the reflectors, the blocking level is unsatisfactory for a filter with two or less cavities. For four or more identical cavities, the transmission at the top level of the bandpass has too much ripple. Commercial filters with two, three, and four cavities are the usual catalog types available from manufacturers and have been sold for over 50 years.

Many techniques have been used to reduce the undulations in the transmission zone[2], and only a few methods lead to filters that have superior performance in

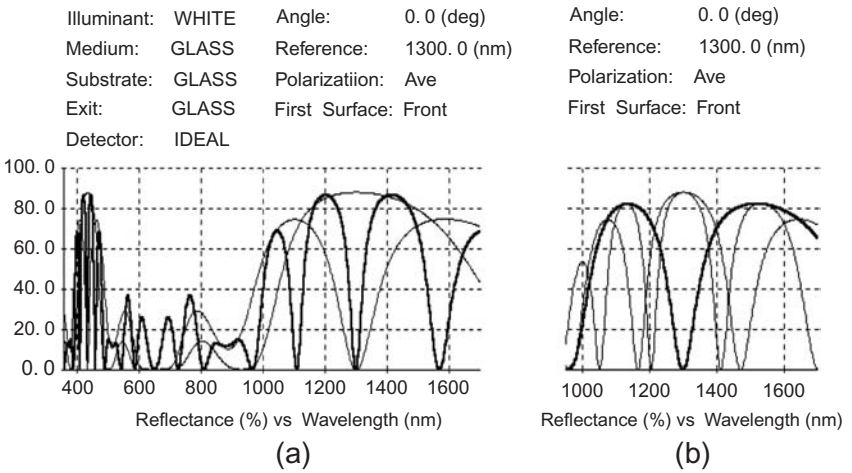

Figure 7.4 (a) Fabry–Perot etalon. HLH reflectors are separated by 1, 2 (thin lines), and 10 (thick line) quarterwaves of air. (b) HLH reflectors are separated by 7, 11 (thin lines), and 4 (thick line) quarterwaves; quarterwaves at 1300 nm.

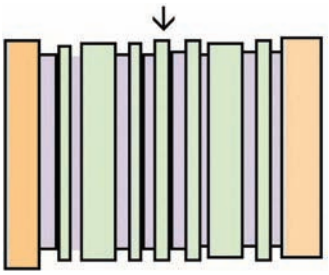

Figure 7.5 Fabry–Perot filter with two cavities (HLH LL HLH) shown for clarity. The arrow indicates the position of the coupling layer between the filters.

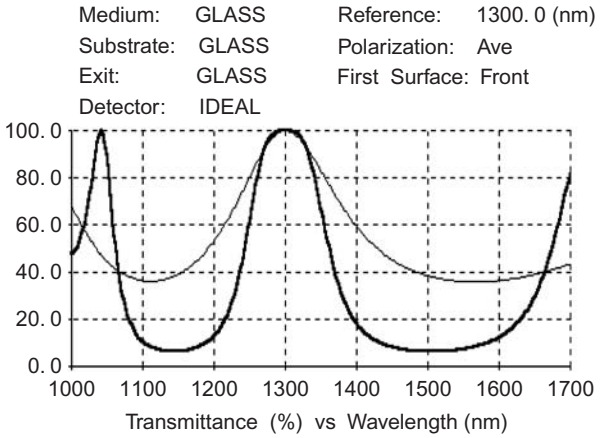

Figure 7.6 One (thin line) and two (thick line) cavities: HLH LL HLH.

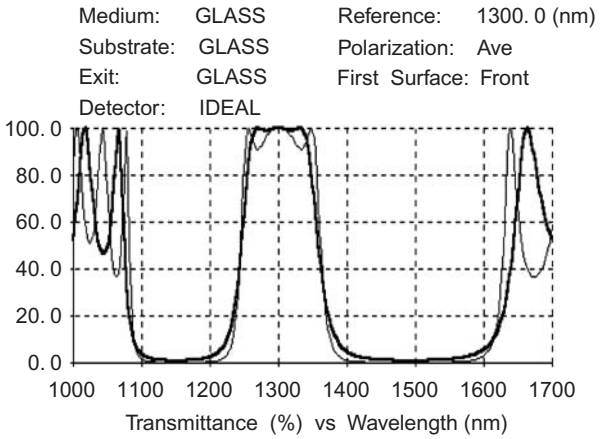

Figure 7.7 Three (thick line) and four (thin line) cavities.

the real world. One way to smooth the transmission is to use fewer layers in the outer cavities than in the inner ones.[3,4] A useful design procedure is to begin by making the outer filters with four fewer layers than the number of filters in the inner cavities. By doing so, the index of the spacer is consistent throughout the filter. This is important because of angular considerations, and it reduces sensitivity to uniformity variations while improving manufacturability. A further refinement is to add three quarterwaves to some of the cavities to reduce the ripple even more. Though I have been issued a patent for this approach, no one seems to pay attention to it. At the OSA's Optical Interference Coatings (OIC) meeting in Banff in 2001, there was a design contest for a WDM filter. Thelen[5,6] remarked that he noted use of the three quarterwave technique in his book to make the filter; however, I do not agree with him because there is nothing obvious to demonstrate that filter ripple for two material filters is improved with the use of three-quarterwaves. His designs were for three materials with indices of 4.3, 1.45, and 1.95; he found a particular equivalent index. For example, Thelen's design #10–16 has a *diverse* structure of the form:

$$(\mathrm{LLLMH})^2\ (\mathrm{LHMHL})^2\ (\mathrm{MHHLH})^2\ (\mathrm{LHMHL})^2\ (\mathrm{LLLMH})^2.$$

M indicates metal in this design. This arrangement includes halfwaves utilizing two different materials and a number of layers that have no optical changes during deposition. A five-cavity filter designed for the same bandwidth using my technique can be compared (I adjusted the value of the high index until the bandwidth of my design matched Thelen's).

My design for Ta_2O_5 and SiO_2 materials in a glass medium is

$$(\mathrm{LH})^2\ \mathrm{LL}\ (\mathrm{HL})^2$$
$$(\mathrm{HL})^2\ \mathrm{H}\ \mathrm{LL}\ (\mathrm{HL})^2\ \mathrm{HL}$$
$$\mathrm{HLHLH}\ \mathrm{LL}\ (\mathrm{HL})^2\ \mathrm{HL}$$
$$(\mathrm{HL})^2\ \mathrm{H}\ \mathrm{LL}\ (\mathrm{HL})^2\ \mathrm{H}$$
$$(\mathrm{LH})^2\ \mathrm{LL}\ (\mathrm{HL})^2.$$

The bandshapes are similar, but my design has a better reflection profile, although I could improve Thelen's filter with a little effort. When you know what to do, it is easy: the major advantage is illustrated in Fig. 7.8.

Virtually all filters are used in some cone angle, or they may be angle tuned. Diverse cavities have terrible performance at angles. If the cavities are all similar (as in the halfwave type), the transmission profile will not distort badly for moderate angles. For solving angle problems, read on and also examine my published papers for more detail.[2–4] The spectral response for a 20-deg angle for the filters is illustrative (Fig. 7.9). This is an extreme example, but filters are sensitive to angle; even at small angles the transmission is badly distorted for the diverse filter.

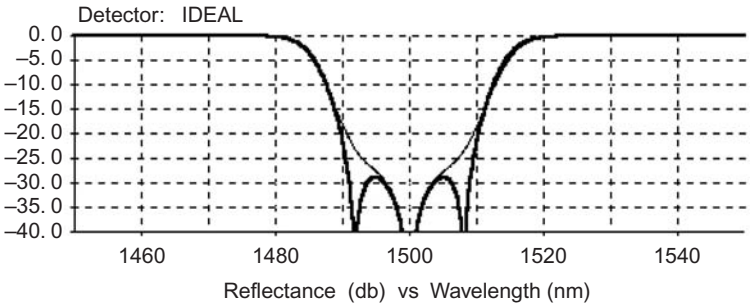

Figure 7.8 Bandpass filters at normal incidence; my design (thick line) vs Thelen's (thin line): −40 dB is 0.01%R.

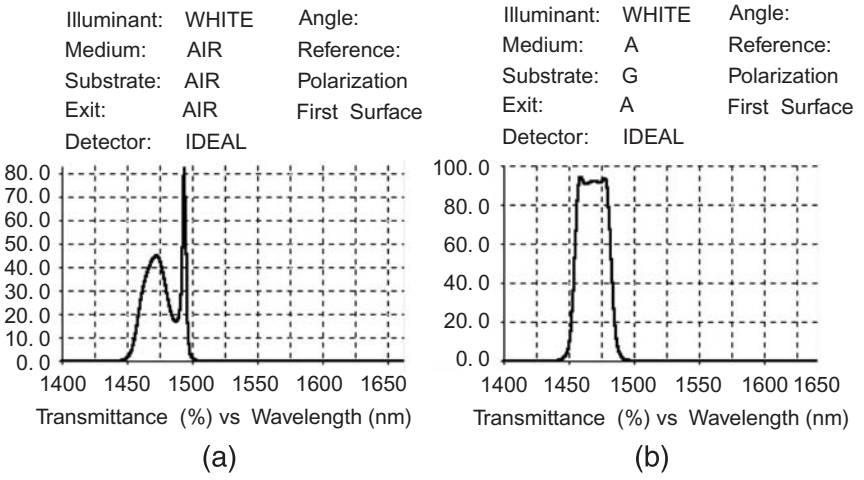

Figure 7.9 (a) Thelen's design: 20 deg in air. (b) My design: 20 deg in air.

7.3 Steps Leading to the Selected Design

When three quarterwave layers are placed in the structure, a simple test with TFCalc shows the proper match for ripple and angle. First, determine the need to remove ripple by examining the spectrum with an all-quarterwave design. Add enough cavities and structure for the filter to have the proper blocking and bandwidth. A five-cavity design follows:

$$(LH)^2\ LL\ (HL)^2$$
$$(HL)^2\ H\ LL\ (HL)^2\ H\ L$$
$$HLHLH\ LL\ (HL)^2\ H\ L$$
$$(HL)^2\ H\ LL\ (HL)^2\ H$$
$$(LH)^2\ LL\ (HL)^2.$$

Ripple is about 4%. For the central etalon (middle layer), substituting a single three-quarterwave-layer design: HL3HLH LL $(HL)^2$ HL will have the same

reflection profile at normal incidence as the design shown (<1%) in Fig. 7.7, but at 20 deg the filter's transmission is distorted. By changing the central etalon to 3H3LHLH LL $(HL)^2$ HL, it becomes a design with the same normal-incidence properties and excellent characteristics at all angles (giving some consideration to polarization). Fewer cavities would not have blocked adequately, and more cavities become more complicated and add unnecessary layers.

No matter how many cavities are analyzed, as far as three-quarterwave placement is concerned the correct procedure is to select a simple three-quarterwave design at normal incidence and then alter it with more three-quarterwaves to lower the sensitivity. Once a set of films is judged to provide good ripple, the same structure can be considered for narrower filters by adding pairs of layers to each cavity (Fig. 7.10).

A narrower design is

$$(LH)^3\ LL\ (HL)^3$$
$$(HL)^3\ H\ LL\ (HL)^3\ HL$$
$$HL3H3LHLH\ LL\ (HL)^3\ HL$$
$$(HL)^3\ H\ LL\ (HL)^3\ H$$
$$(LH)^3\ LL\ (HL)^3.$$

20 layers are added to the original filter. The bandshape factors are the same for each of these filters. Bandshape is the ratio of a bandwidth at any selected $\%T$ to the bandwidth at any common point, say 50%. Results of measuring the bandwidths at various transmission levels are shown in Table 7.1.

Values of "wide" calculated and measured from the bandwidth ratio have the same proportional band factor as "narrow." Families of curves can be easily generated from the analysis of one set of data. Only one set of bandwidth ratios needs to be determined for a situation. The bandwidth at half power is measured,

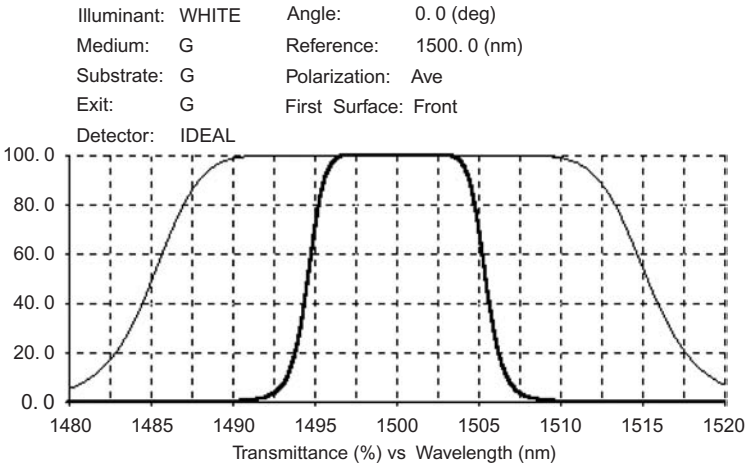

Figure 7.10 Comparison of original (thin line) to narrower filter (thick line).

Table 7.1 Bandwidths (bw) at various transmission levels.

	Narrow		Wide
	Measured	Bandwidth ratio	Measured or calculated
80%bw	17.7 nm	~ **89**% of $\frac{1}{2}$	43.5 nm
50%bw	19.9	–	48.7
10%bw	24.1	**121**% of $\frac{1}{2}$	59

and the other points are derived. Altering the three-quarterwave structure changes the exact ratios, but the changes are typically minor. To achieve filters with bandwidths between these two filters, the spacer for the wider filter can be increased from 2 to as much as 10. For fine tuning, three-quarterwaves are inserted into each cavity at the same distance from the spacer. For example, an optimized design is

$$(\mathrm{LH\ 3L\ HLH})\ 6\mathrm{L}\ (\mathrm{HL})^3$$
$$(\mathrm{HLH\ 3L\ HLH})\ 6\mathrm{L}\ (\mathrm{HL})^3\ \mathrm{HL}$$
$$(\mathrm{HL3H\ 3L\ H3LH})\ 6\mathrm{L}\ (\mathrm{HL})^3\ \mathrm{HL}$$
$$(\mathrm{HLH\ 3L\ HLH})\ 6\mathrm{L}\ (\mathrm{HL})^3\ \mathrm{H}$$
$$(\mathrm{LH\ 3L\ HLH})\ 6\mathrm{L}\ (\mathrm{HL})^3.$$

Virtually any bandwidth can be achieved by using this method; however, the central cavity may need to be fine-tuned for angular and tooling sensitivity. An alternate approach is to switch from a filter with a low-index spacer to a filter that has one more layer in each reflector and has a high-index spacer. The same techniques that improved the bandshape will give the desired result (Table 7.2). A five-cavity design (Fig. 7.11) with sharp slopes and low ripple is

$$(\mathrm{HLH3L5HL})\ 4\mathrm{H}\ (\mathrm{LH})^3\ \mathrm{L}$$
$$(\mathrm{HL})^4\ 4\mathrm{H}\ (\mathrm{LH})^4\ \mathrm{L}$$
$$(\mathrm{HLH3LHL7HL})\ 4\mathrm{H}\ (\mathrm{LH})^4\ \mathrm{L}$$
$$(\mathrm{HL})^4\ 4\mathrm{H}\ (\mathrm{LH})^4\ \mathrm{L}$$
$$(\mathrm{HLH3L5HL})\ 4\mathrm{H}\ (\mathrm{LH})^3.$$

Table 7.2 shows the results of using the curser to measure the bandwidths at various transmission levels.

Table 7.2 The number of layers can be quite large, and the filter still needs blocking.

	Measured	Bandwith ratio
80%bw	9.75 nm	~92.9% of $\frac{1}{2}$
50%bw	10.5	
10%bw	12.25	116.7% of $\frac{1}{2}$

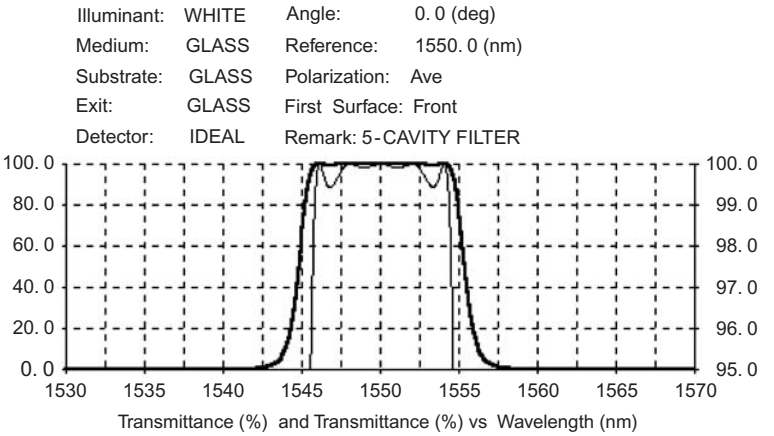

Figure 7.11 An 81-layer 5-cavity high-index spacer filter. The thin line is a zoom view using the right scale.

7.4 Very Wide Filters

Variations of the design philosophy are necessary to provide high-quality wide filters. For etalon filters with fewer than seven layers, the outer filters have little or no effect when the less-than-four-layers rule is applied for similar halfwave structure forms. For improved ripple, a nine-cavity design with reasonable ripple can have the form

6HL
3HL HHLHL
3HL 4HLHL
H3L 4HLHL
H3L 4HLHL
H3L 4HLHL
3HL 4HLHL
3HL HHLHL
8H.

A 33-layer, 7-cavity filter with a 10% bandwidth is designed with this structure:

6HL
HL HHLHL
3HL HHLHL
H3L HHLHL
3HL HHLHL
HL HHLHL
6H.

This filter has less than 1% ripple. Blocking range can be an issue for these filter forms. The transmission curve for the above design is shown in Fig. 7.12.

7.5 Semiclassical Filters

Classical filters have reflectors that contain an equal number of layers (plus a coupler) with spacers that are identical for each etalon section. Semiclassical filters allow the spacers to be varied in thickness. The basic structure of semiclassical filters is (HLHL HH LHLHL)^4. Ripple is reduced by alterations to the inner structure. Minowa and Fujii[7] describe a technique of adding halfwaves to the halfwave spacers to reduce ripple for three- and four-cavity filters. One possible design with low reflection in the bandpass is as follows:

(HLHL HH LHLHL) (HLHL 6H LHLHL) (HLHL 6H LHLHL)
(HLHL HH LHLH).

The performance of these filters at *any* angle is poor. Although the approach is correct, the design needs work in order to obtain high performance.

7.6 Alternative Approach

A five-cavity wideband filter (Fig. 7.13), using my techniques has the design

(HLHL HH LHLHL)
(3H3LHL HH LHLHL)
(3HLH3L 4H LHLHL)
(3H3LHL HH LHLHL)
(HLHL HH LHLH).

The idea is to make the inner filters *more* complex than the outer filters. The same approach is used as in the previous filter (Fig. 7.12). Once a stack length is selected to achieve the basic bandwidth, some three-quarterwaves are added to reduce ripple; then move and alter the number of three-quarterwaves to allow good bandshape with angle and errors.

7.7 Other Ripple-Removal Approaches

The most successful design approach is Thelen's use of microwave prototyping to match the cavity lengths to a Chebyshev formula for equi-ripple.[6] The technique has been applied by Baumeister to design filters with as many as 21 cavities.[8] The cavity lengths are adjusted to fit a profile by adding equivalent layers that fix the mathematical model: this produces filters that have low or no ripple in the bandpass. A typical design is Ref 1 LL Ref 2 LL Ref 3 LL Ref 4 LL Ref 5 for

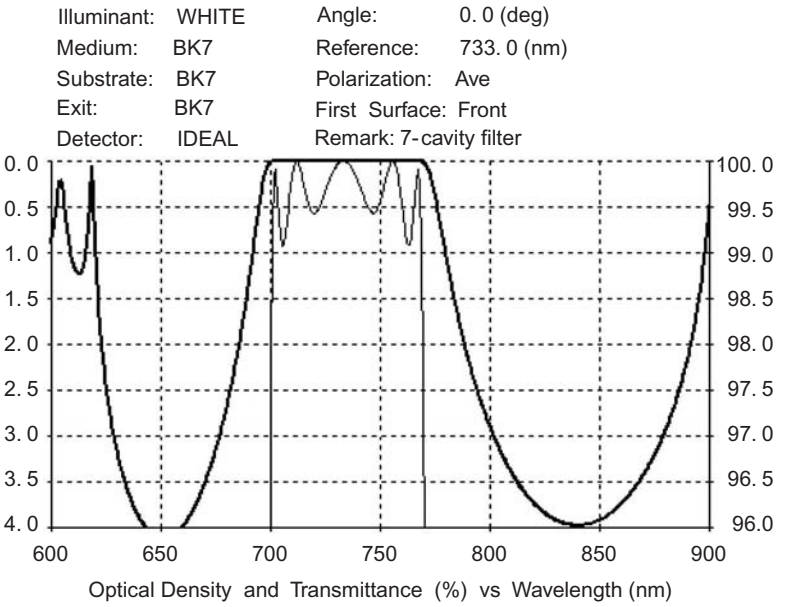

Figure 7.12 A seven-cavity filter. The thick line is optical density. The thin line is transmittance. To increase the blocking range on the high side, designs with no high-order-number layers and many nonquarterwave layers can be utilized; these will be described later in Chapter 8.

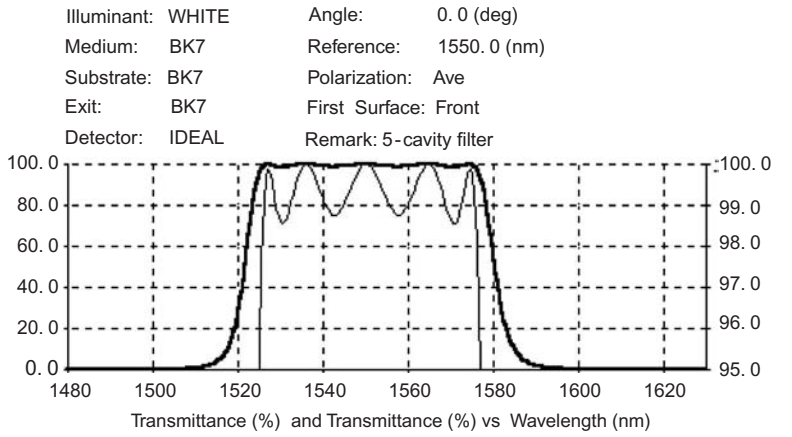

Figure 7.13 The thick line represents a five-cavity high-index spacer filter; the thin line is zoom-in transmittance.

a four-cavity filter. The reflectors still consist of HL pairs, but an extra layer of an intermediate index (B) is added to the stacks to smooth out the transmission zone. For example, a typical 17-layer reflector has the design $[(HL)^4B\ (LH)^4]$. Baumeister would calculate the voltage standing wave ratios (VSWRs) for this

reflector and then do another series of calculations to obtain constants for the best match. He typically produces filters that look like the ones that I design.

7.8 Microwave Filters with Equivalent Layers (My Technique)

The best filters have outer cavities with fewer pairs of layers; the computer can choose the proper equivalent layers after you place the layers in the structure. The index value of the Herpin layers changes slightly for different positions between the pairs of layers. For a conventional filter, I put layers in the outer position. Actual placement of the Herpin layers in the stack may be different in one position to reduce the number of non-optically monitored layers for real filters. High-quality designs can be achieved with a little hard work and insight. The idea is to have the Herpin layers obtain index values between the main index values; when enough pairs of layers are positioned between the "halfwaves," this will be the case.

A 71-layer, 6-cavity design is as follows:

L HL H 6L HL HL
HL HL H 6L HL HL HL
NL HL HL H 6L HL HL HL
ML HL HL H 6L HL HL HL
NL HL HL H 6L HL HL HL
HL H 6L HL HL.

H has an index of 2.22, and L has an index of 1.45. M is a layer with an index of 1.7, and N is a layer with an index of 1.537. There is no need to put equivalent layers in the outer stacks for this example. To find the values of N and M, TFCalc will optimize the selected targets, and then I alter the targets and examine the behavior of the design when stimulated to various values. The design falls into place when the proper targets are used. Minor changes in the targets will significantly alter the shape of the reflectance curve (Fig. 7.14). TFCalc now comes with a built-in prototype to address this, but I do not know how well it performs. It will only calculate for an *odd* number of cavities. The equivalent layers are inserted in the low-sensitivity areas, as I suggest. Most likely, the locations of the Herpin layers will need altering before filters are made from these designs. One of the TFCalc tools converts parts of the design to three quarterwaves in order to avoid Herpin layers. When I tried it, too many layers were added; I prefer to do my own designing. The program is fast, however, and does help to obtain an approximate answer. An example is shown in Fig. 7.15.

Targets of low reflection are every 0.7 nm for 1534–1560 low $\%R$. N becomes 1.56, and M is 1.694 for no reflection. This is not the widest filter possible with low $\%R$. If we change only the outer targets to 1532 nm and 1562 nm, we obtain the results shown by the thin line in Fig. 7.16(a): optimization gives ~30 dB $R_{\max}$ over

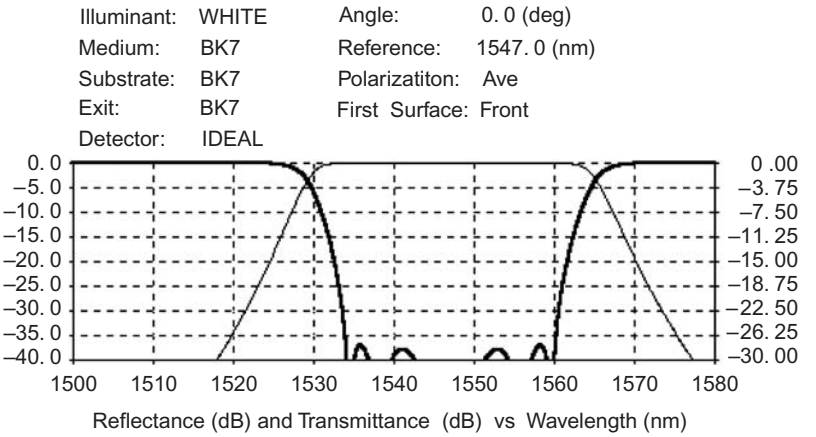

Figure 7.14 A six-cavity microwave filter design. The thin line is transmittance. Reflection (thick line) is virtually nonexistent.

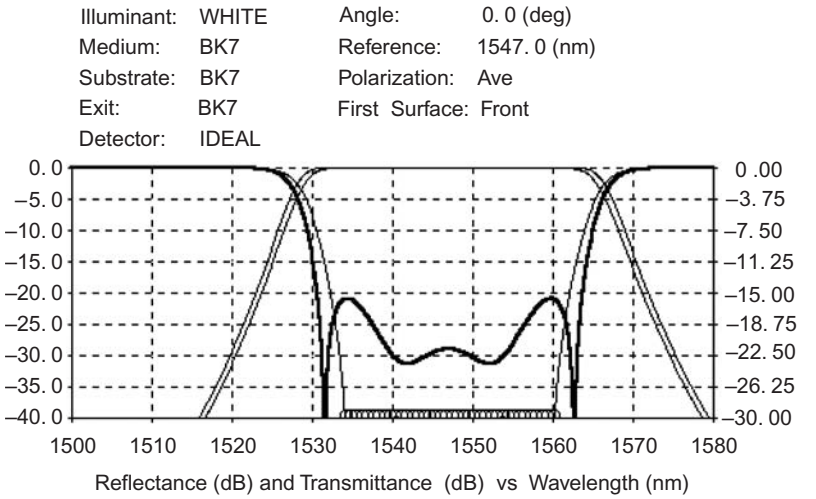

Figure 7.15 A 6-cavity filter, N = 1.52, M = 1.67, has a wide bandpass with a 20 dB reflection. The thick line is reflectance; the thin line is transmittance. The thin outer lines are the original design.

range; Herpin layers are 1.508 and 1.6366. If we change the outer targets to 1533 nm and 1561 nm, we obtain the results shown by the thick line in Fig. 7.16(b): optimization gives ~35 dB R_{max} over range; Herpin layers are 1.537 and 1.67. Herpin layers are 1.55 and 1.685; 38 dB is R_{max}. The bandwidth of the filter in the low-reflection zone is slightly reduced every time the decibel value increases; bandshape also changes slightly. The best slope factor occurs when the ripple is the worst. At some point the slope becomes important, and the number of cavities necessary to block a filter will need to be increased for improvement.

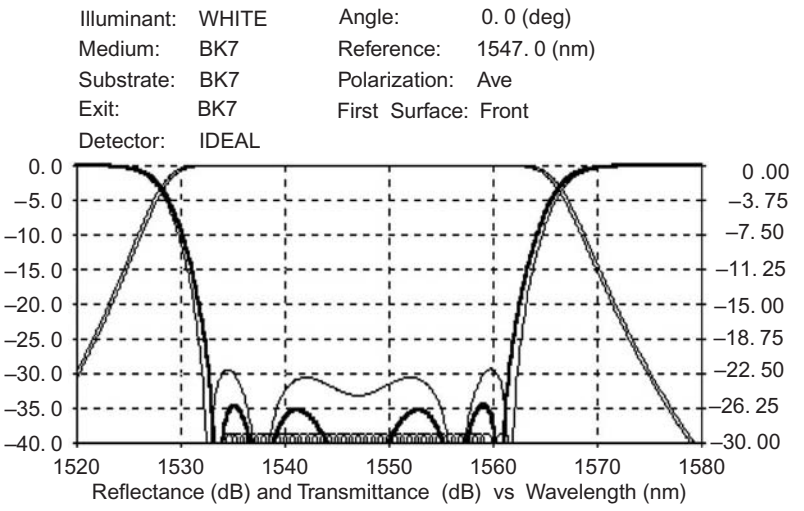

(a)

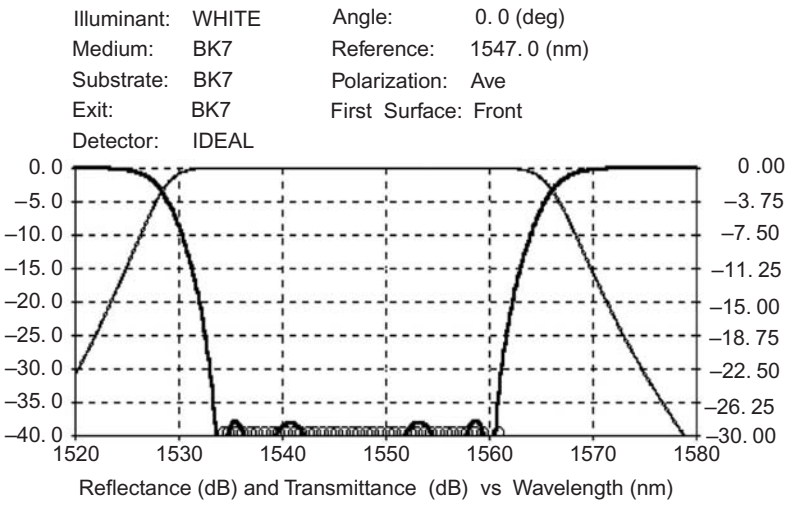

(b)

Figure 7.16 (a) and (b) optimized as per discussion. The thick line is reflectance; the thin line is transmittance.

Suppose that the filter needs to be blocked to a narrower bandwidth than the 71-layer, 6-cavity design. The following design would serve:

L HL H 6L HL HL
HL HL H 6L HL HL HL
NL HL HL H 6L HL HL HL
ML HL HL H 6L HL HL HL
NL HL HL H 6L HL HL HL
HL H 6L HL HL.

Adding targets of $<3\%T$ (15 dB) at 1525 and 1570 nm and optimizing ruined the possible bandshape for this basic design. Another set of Herpin layers needs to be added, but the filter still contains six cavities. The filter shown in Fig. 7.17 has 75 layers:

L HL H 6L HL HL
P L HL HL H 6L HL HL HL
N L HL HL H 6L HL HL HL
M L HL HL H 6L HL HL HL
N L HL HL H 6L HL HL HL
P L HL H 6L HL H L.

The plot optimizes with N = 1.634 and M = 1.3814, and P = 1.516; thin outer lines are the original design. The circles at −15 dB transmission are the specification. See also Fig. 7.18. To reduce the reflection in the transmission zone, slightly reduce the wavelength range. Changing the first and last reflection targets to 1535.3

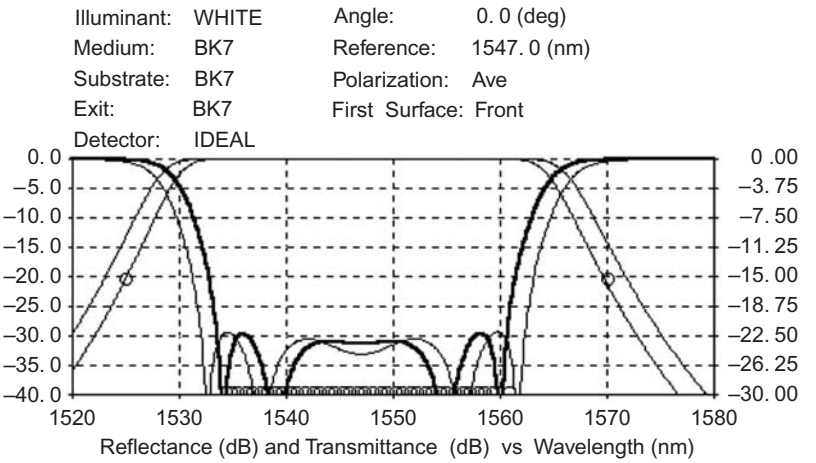

Figure 7.17 New filter design (thick line).

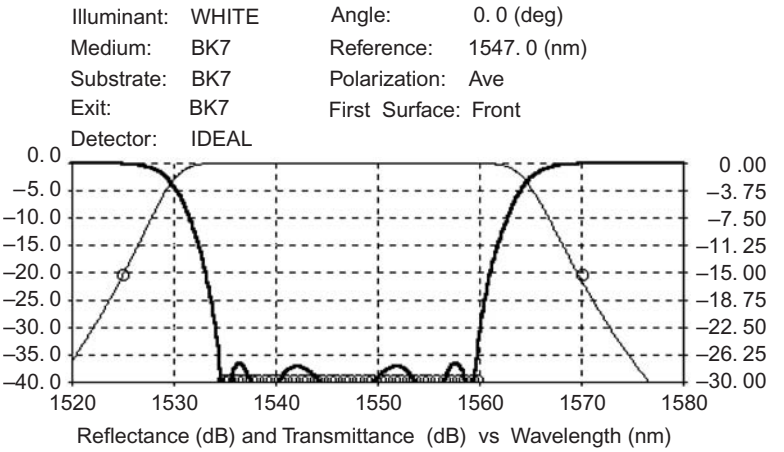

Figure 7.18 Refined filter design.

and 1559.7 nm, respectively, and reoptimizing allows for good performance. This 75-layer filter (Fig. 7.19) has Herpin layers: N = 1.5 and M = 1.63, and P = 1.43 for Ta_2O_5 and quartz. If a wider top is required with the same blocking, then another cavity must be added. The squareness of the seven-cavity filter is clearly superior to that of the six-cavity type.

7.8.1 Approach

I used the same targets as in Fig. 7.19 to find the Herpin layers. After the first refinement there was somewhat high reflection in the 1538-nm area. I altered the target tolerances for three wavelengths and then optimized the design.

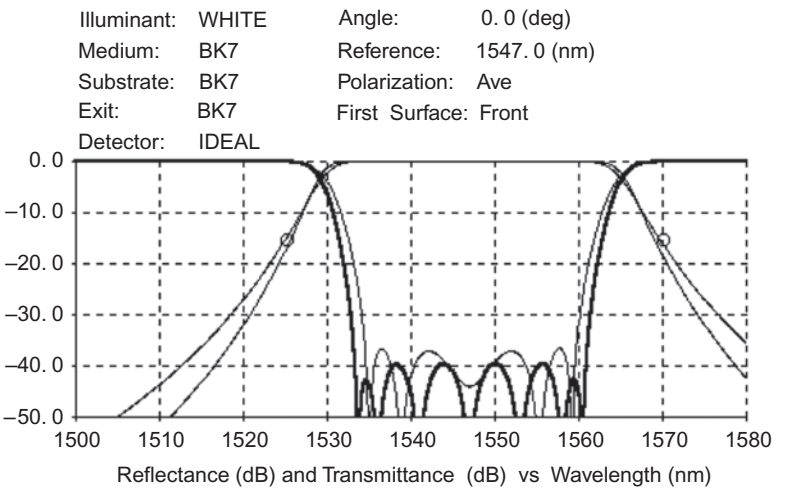

Figure 7.19 Six-cavity (thin line) and seven-cavity (thick line) filters; new scaling shows differences.

7.8.2 Design technique

A cavity is added to the center of the filter using the following reflector type:

M L HL HL H 6L HL HL HL.

The design becomes

L HL H 6L HL HL
P L HL HL H 6L HL HL HL
N L HL HL H 6L HL H L HL
M L HL HL H 6L HL HL HL
M L HL HL H 6L HL HL HL
N L HL HL H 6L HL HL HL
P LHL H 6L HL HL.

When this design is optimized, the "P" Herpin value was 1.47. The LPL combination is essentially three quarterwaves of L at the coupling layer point. The PL pairs are removed with no change in performance after reoptimizing; the values of N and M change slightly.

Final design of the 85-layer, 7-cavity filter:

L HL H 6L HL HL
HL HL H 6L H LHL HL
N L HL HL H 6L HL HL HL
M L HL HL H 6L HL HL HL
M L HL HL H 6L HL HL HL
N L HL HL H 6L HL HL HL
HL H 6L HL HL

$$N = 1.576 \; M = 1.777.$$

For Ta_2O_5 and quartz multilayers, N = 1.5 and M = 1.67.

After the Herpin layers are found, they must be converted to the equivalent HLH or LHL nonquarterwave layers and then compounded into the design; monitoring the layers may be difficult. The next chapter will show the details of equivalent stack monitoring. The filter in Fig. 7.14 was altered slightly by antireflecting to air after changing the index values for the wavelength dispersion at 600 nm. See Fig. 7.20 for an example. Blocking and slopes are similar to conventional filter stacks.

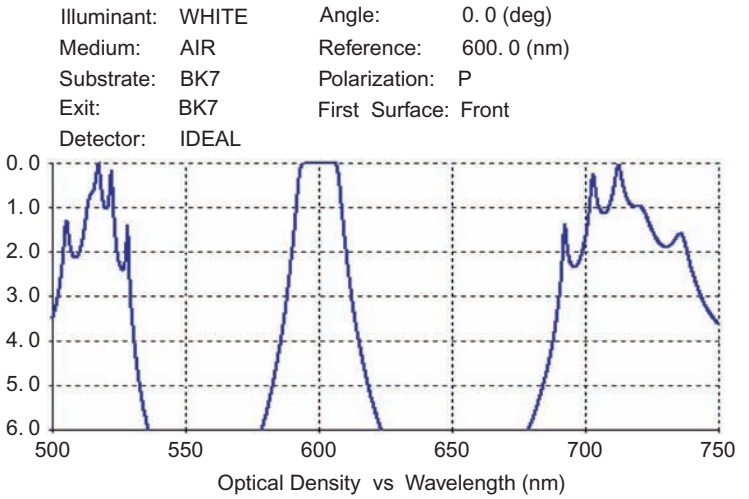

Figure 7.20 A six-cavity Herpin filter matched to air centered at 600 nm.

7.9 Blocking of All-Dielectric Filters

If only the high- or low-side wavelengths need to be extended to meet a specification, a long- or a short-pass filter is effective (Fig. 7.21). For instance, a filter with a wavelength of 1625 nm blocks only a short distance on the low side.

The first four and last four layers are optimized as a 1625-low-side blocker. Optical monitoring is described in the next chapter. The 55-layer bandpass filter is appended to the blocker to complete the blocked assembly (Fig. 7.23). The filter shape in Fig. 7.24 falls off like a classic four-cavity filter, and the blocker's

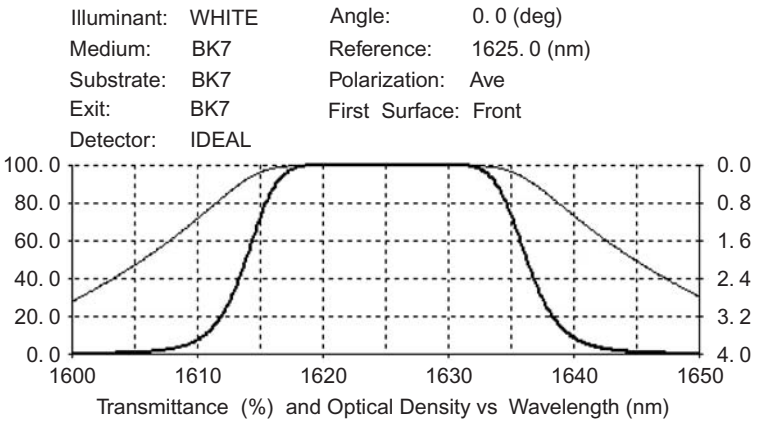

Figure 7.21 A 55-layer, 4-cavity filter. Thin line is OD. The thick line is transmittance. Blocking on the low-wavelength side extends to 1410 nm for $0.01\%T$ (4OD). To further block at 1200 nm, a long-pass filter can be used with the bandpass (Fig. 7.22).

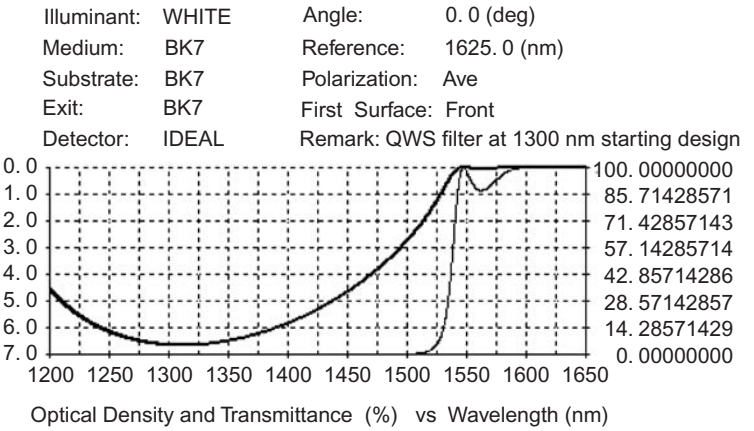

Figure 7.22 A 42-layer long-pass filter. The thick line is OD; the thin line is transmittance.

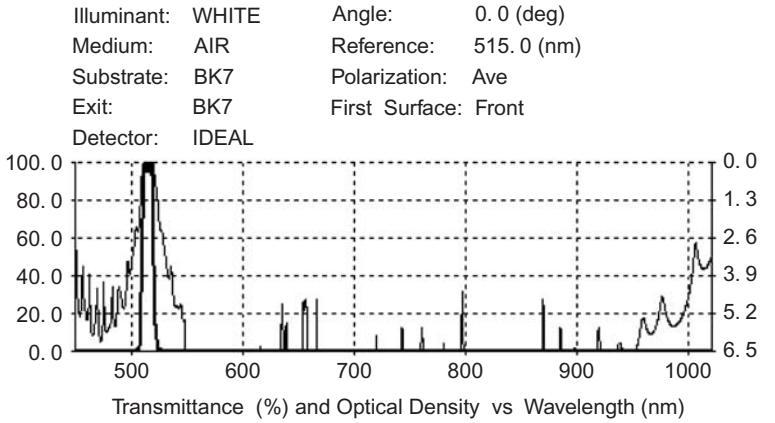

Figure 7.23 A 157-layer, 3-cavity filter with 3 high-side blockers. The thick line is transmittance. The thin line is OD.

nonquarterwave layers retain the rolloff. The basic filter form before optimization is

(aT bQ) 0.79(TQ)^{18} (aT bQ)^3 (TQ3TQ2TQTQTQ) ((TQ)^3 2T (QT)^3 Q)^2 (TQ3TQ2TQTQTQ) (aT bQ) 1.3(TQ)^{20} (aT bQ aT),

where each a and b can assume any fractional value of a quarterwave selected by the optimization program. T isTiO_2 and Q is quartz.

7.10 Conclusion

Bandpass filters can be designed to have virtually any bandwidth and ripple. Herpin filters have fewer layers than quarterwave filters. Blocking of any type of filter with

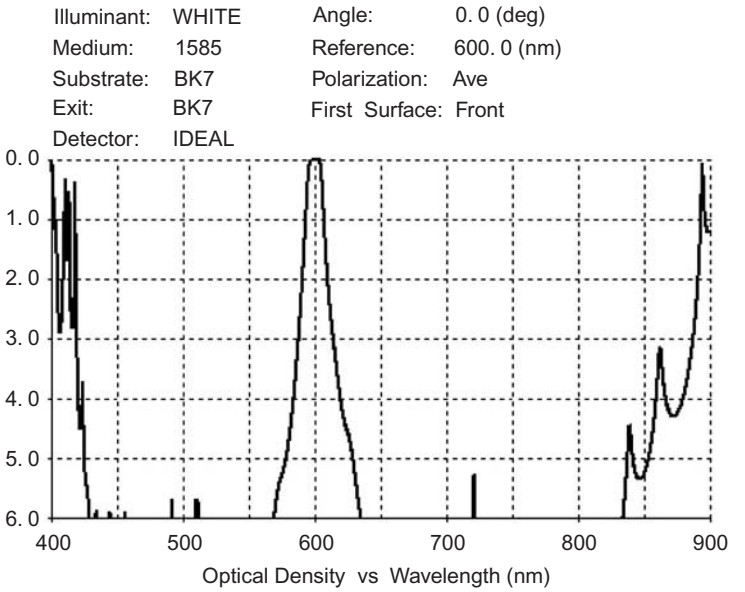

Figure 7.24 A 135-layer, 4-cavity filter with stack blockers on each side of the bandpass.

an all-dielectric filter adds many layers to the structure and can be quite frustrating. Blocking of the filters is an area that needs further consideration.

References

1. T. Edogan, L. Wang, and G. Clarke, "Optical filter and fluorescence spectroscopy system incorporating the same," U.S. Patent 6,809,859 (2004).
2. D. H. Cushing, "Band Shape Improvement Techniques." *Proc. SPIE* **4094** pp. 65–73 (2000) [doi:10.1117/12.404749].
3. D. H. Cushing, "Bandpass filter for 40 Gbit/s," *46th Annual Proceedings of the Society of Vacuum Coaters*, pp. 323–327 (2003).
4. D. H. Cushing, "Manufacturable Filter for CWDMs," *47th Annual Proceedings of the Society of Vacuum Coaters*, pp. 383–387 (2004).
5. A. J. Thelen, in *Optical Interference Coatings*, OSA Technical Digest (Optical Society of America, Washington DC, 2001) pg. TuC1-3 in paper TUC1.
6. A. J. Thelen, *Design of Optical Interference Coatings*, McGraw-Hill, New York (1989).
7. J. Minowa, and Y. Fujii, *High Performance Bandpass Filter for WDM Transmission*, Chapter 10, McGraw-Hill, New York (1989).
8. P. W. Baumeister, "Optical Coating Technology," 5–82, *SPIE Press*, Bellingham, WA (2004). [doi:10.1117/3.548071].

Chapter 8
Optical Monitoring

8.1 Introduction

All-dielectric filters require transmissive optical monitoring. Other methods can be used successfully for AR coatings and edge filters of most types. The basic optical system consists of a collimated beam from a light source emitting in the spectral area of the desired filter that (usually) passes through the substrate and out of the vacuum into a spectrometer. The detector can be a photodiode or a phototube. When a layer is complete, the signal is processed by a computer program to automatically stop the deposition. Alternatively, the signal is fed to a meter or a lock-in amplifier, and a vacuum system operator observes the signal and manually cuts the layers. There are a number of automatic deposition systems available. Ten years ago I used the Leybold system satisfactorily for quarterwaves; a quartz crystal monitor controlled the rate of deposition. The process could use either method as the primary control for any layer. Resolution of the spectrometer must be at least 70% of the bandwidth of the desired filter and collimation of the light beam must be such that the angles through the substrate do not degrade the signal. The beam diameter should be as small as possible so that any nonuniformity of the filter is within the bandwidth of the monochrometer. If any of these factors are not adhered to, the signal will not follow the computed monitor chart.

If only quarterwave layers are used, some of the layers in the filter design will not change transmission value appreciably, but these layers are necessary for the filter's final shape. See Fig. 8.1. The filter design shown in Fig. 8.2 is

$$\begin{gathered}\text{HLH 3L H 2L (HL)}^3\\ \text{(HL)}^3\ \text{H 2L (HL)}^4\\ \text{(HL)}^3\ \text{H 2L (HL)}^4\\ \text{HLH 3L H 2L (HL)}^2\ \text{1.27H 1.39L.}\end{gathered}$$

The last two layers of the design antireflect the filter to air. The H layer must be cut at a particular transmission point; the last layer's transmission is maximized. The filter has well-defined peaks except for the coupling layers, which change value slightly over 1%. Most automatic systems use a different method to *estimate* the thickness of the coupling layers. Another way to improve travel for those layers involves changing the first two layers to nonquarterwaves. If the first layer is altered to 1.2-quarterwave thickness, the next layer can be optimized for ~100% final T

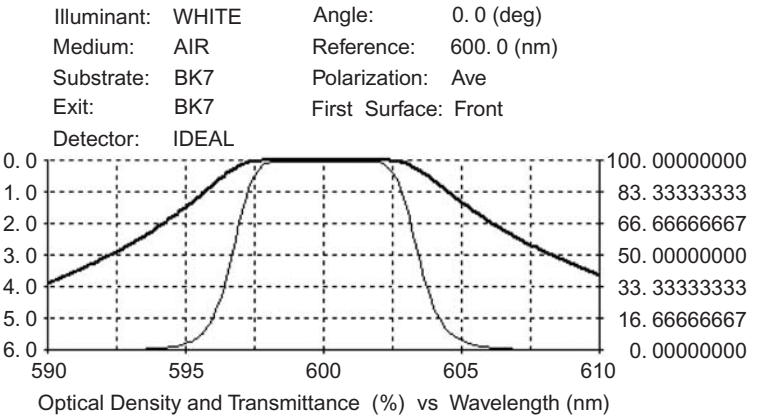

Figure 8.1 Bandpass for a four-cavity filter. The thick line is OD; the thin line is transmittance.

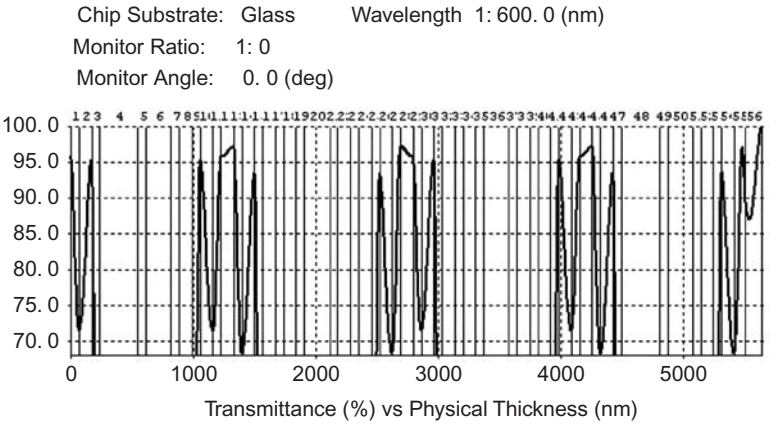

Figure 8.2 A monitor chart for the quarterwave design.

in the band. The layer will be at the maximum $\%T$ point; a quarterwave monitor easily locates this thickness (Fig. 8.3). The coupling layers now travel more than 4%, which is sufficient for the optical monitor to be useful.

8.2 Adding a Low-Side Blocker

As discussed in Chapter 7, a long-pass filter can be used with the bandpass to extend the blocking zone. It is desirable to monitor the layers at the wavelength of the bandpass. The thickness of some of the layers at the beginning and end of the blocker will affect the AR coat for the bandpass; further alterations of the starting layers improve the monitoring of the blocker. The 1625-nm filter in Figs. 7.20 and 7.21 is examined in Figs. 8.4 and 8.5, respectively.

The monitoring curve for the first 44 layers shows that for the selected thicknesses a fairly constant cutoff point is established for the bulk of the blocker.

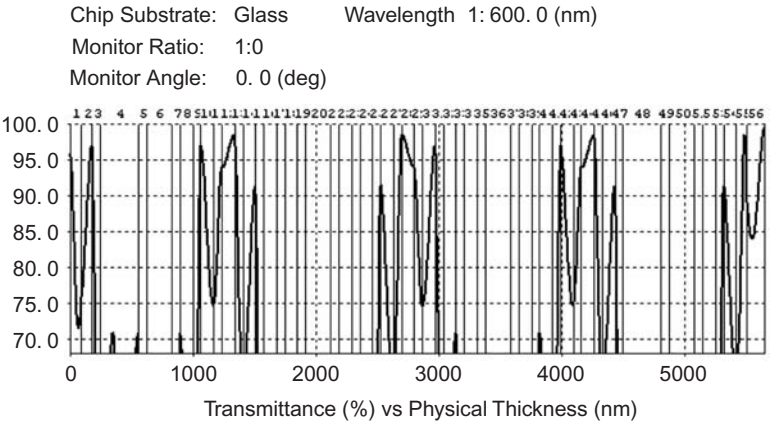

Figure 8.3 A monitor chart for the nonquarterwave design.

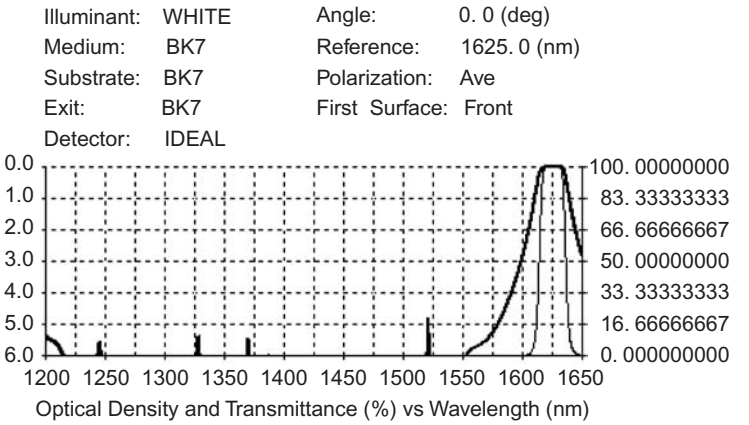

Figure 8.4 A 1625-nm filter blocked to 1200 nm. The thick line is OD; the thin line is transmittance.

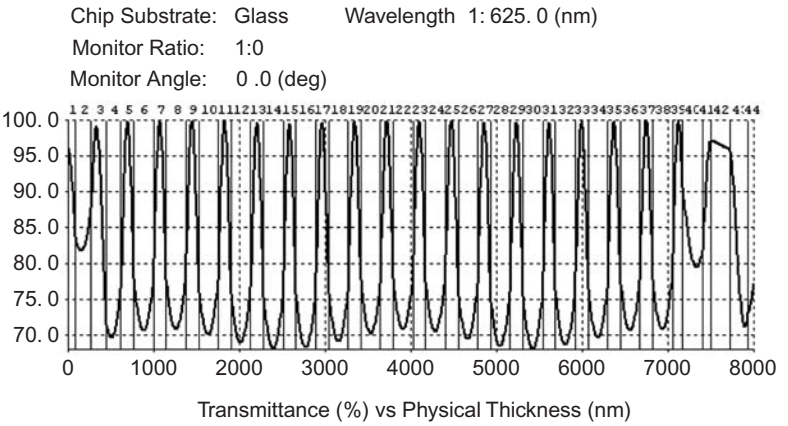

Figure 8.5 The first 44 layers of a monitoring curve for a blocked bandpass filter.

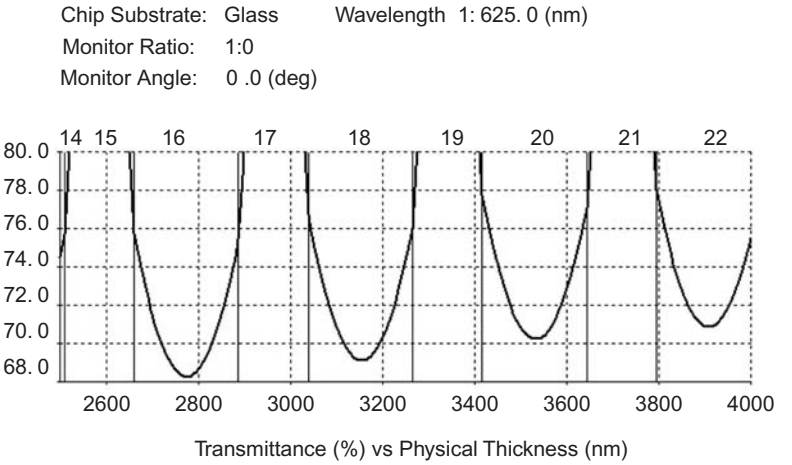

Figure 8.6 Section of the monitor chart in Fig. 8.5 for a long-pass blocker.

The first four layers are selected to keep the signal level within a reasonable bound and provide low ripple in the bandpass when combined with three nonquarterwave layers at the end of the blocking filter (layers 39–41). Guo et al.,[1] Willey,[2] and others have suggested this method of level monitoring. Layer 43 starts the bandpass. The thickness of layer 43 is *selected* to be 1.2 quarterwaves. The thickness of layer 44 (0.91 quarterwaves) is optimized to provide close to 0%R in the bandpass. This area of the chart in Fig. 8.6 shows the detail of cutoff points for some of the layers; travel for the low-index layers is sufficient for automatic control, if available.

8.3 Long-Pass Filters

One example of a long-pass filter contains 38 layers of niobium oxide and quartz. The filter is derived from a halfwave stack at 500 nm; the first nine layers and the last six layers are optimized to give >99%T at 1150–1800 nm (Fig. 8.7). The monitor is set at 1220 nm, where the final filter is quite transparent. The first layer is thin compared to the wavelength and may become a guess (Fig. 8.8). See the papers by Willey[2] for more information about correcting for errors in cuts as film is added.

8.4 Short-Pass Filters

Short-pass filters are monitored much the same as long-pass filters, but the low-wavelength side is the monitor point. A filter with 48 layers made with TiO_2 and SiO_2 that started as a QWS at 800-nm has the spectral performance shown in Fig. 8.9. The maximum transmission is limited by absorption in the TiO_2 films. The first and last 15 layers are nonquarterwaves; monitoring the filter growth of this 800-nm QWS at 685 nm in the final pass zone is fairly painless (Fig. 8.10). An interesting note—if all of the quarterwave layers are removed, the pass zone does

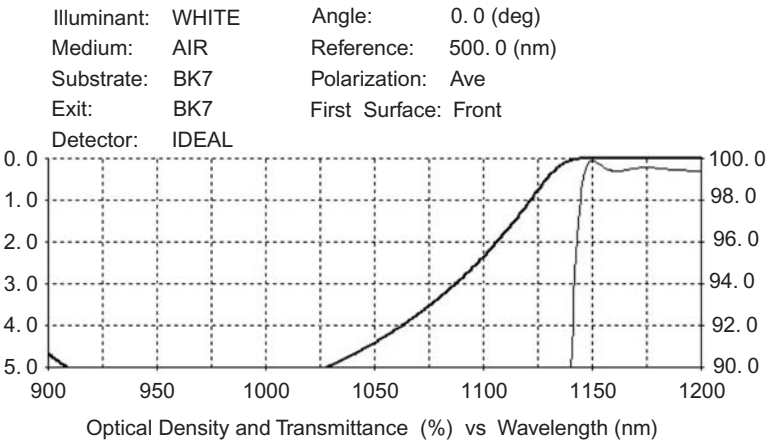

Figure 8.7 A long-pass filter. The thick line is OD; the thin line is transmittance.

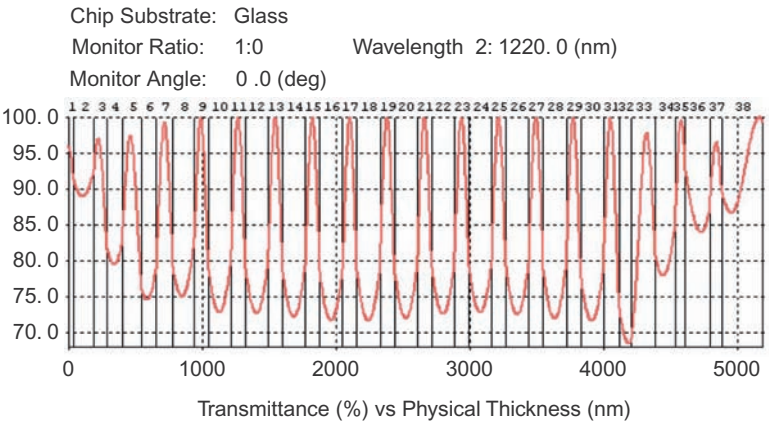

Figure 8.8 A monitor curve.

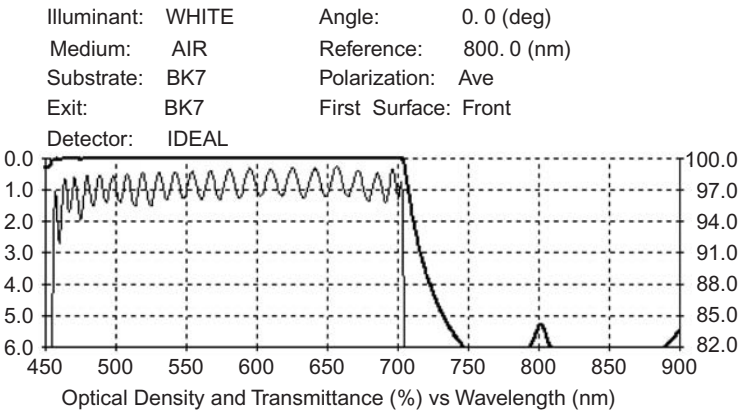

Figure 8.9 A 48-layer short-pass filter. The thick line is OD; the thin line is transmittance.

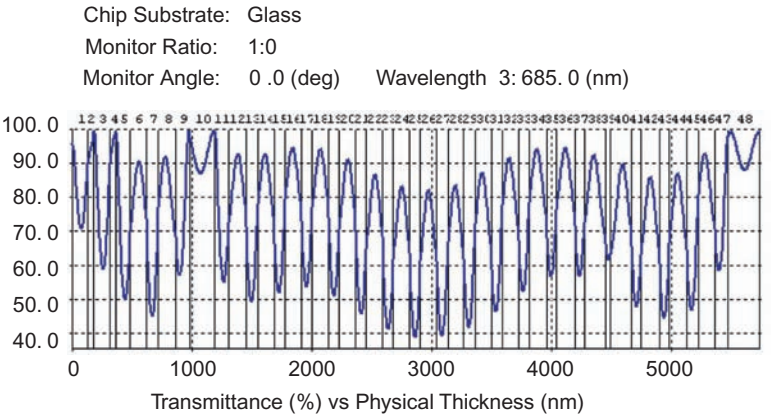

Figure 8.10 A monitoring curve for a 48-layer short-pass filter.

not change. To further demonstrate the monitoring method, the number of layers in the filter was reduced to 30 (Fig. 8.11). The targets for ripple were reduced slightly and the first 9 and last 12 layers were optimized. The monitoring curve at the same wavelength is shown in Fig. 8.12. A similar, easy-to-follow cutoff set is produced.

8.5 Herpin Equivalents

The design for a six-cavity filter requires only three Herpin layers:

$$\begin{gathered}
\text{HA H 4L (HL)}^2 \\
\text{HL H 2L (HL)}^3 \\
\text{HL HL H 2L (HL)}^3 \\
\text{HD HL HL H 2L (HL)}^3 \\
\text{HE HL HL H 2L (HL)}^3 \\
\text{HL H 4L HL H.}
\end{gathered}$$

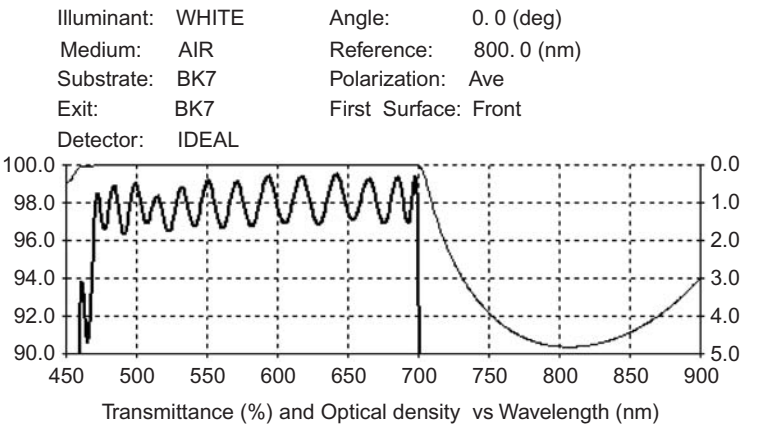

Figure 8.11 A 30-layer short-pass filter. The thick line is transmittance; the thin line is OD.

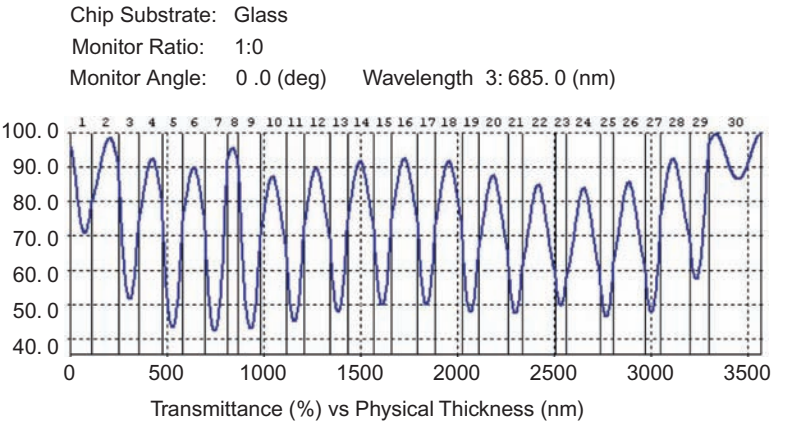

Figure 8.12 A monitoring curve.

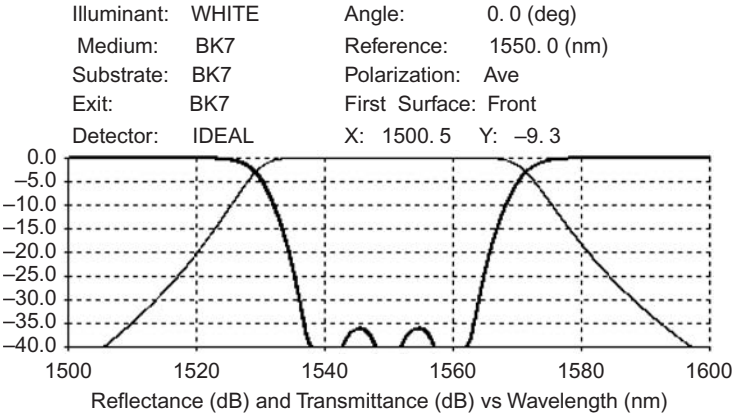

Figure 8.13 A 65-layer bandpass filter with <0.15%R. The thick line is reflectance; the thin line is transmittance.

The Herpin equivalent index values are A 2.0, D 1.815, and E 1.93, which yield the low-reflection bandpass shown in Fig. 8.13 when H is 2.21 and L is 1.45 for a filter structure in a glass medium. If these index values could be realized, the filter could be assembled with an optical quarterwave monitor. Let us assume that the index values are not possible. Some design programs allow the equivalent to be calculated with HLH or LHL combinations when the value falls between H and L. Typically, these layer sets can replace the Herpins with no alterations of the filter profile. The combinations are nonquarterwave sets.

8.6 Using TFCalc

Layer 2 was chosen as an HLH stack because it is between two H layers; the thicknesses of 0.42H, 0.148L, and 0.42H were allowed to replace the layer. The layers were then consolidated with no change in layer count. The optical monitor

changed drastically, as shown in Fig. 8.14. The first layer is now 1.42 quarterwaves and needs to be cut at about 79%T. Layer 2 is only 0.14 quarterwaves thick; the travel is quite small, and the cutoff point is 82%T. Layer 3 travels through a maximum and is cut at the next *minimum*. Small errors will have little effect on the bandpass because the compensation from quarterwave monitoring is still in effect.

Layer 32 is calculated similarly, and the thicknesses are 0.34H, 0.03L, and 0.34H, which are incorporated into the design. Monitoring of coupling layer 30 is simple; transmission changes from 98 to 93%. Layer 31 is now 1.34 quarterwaves and must be cut at 80.5%T after passing through a minimum. Layer 32 is only 0.3 quarterwaves thick; the cutoff point is 86%. Layer 33 is 1.34 quarterwaves, and after a maximum is passed the deposition is stopped at the minimum near 62%T. Calculating the stack for layer 46 has similar consequences to the layer-2 scenario; the preceding coupling layer has plenty of travel. Layer 45 is cut at 83%T, and layer 46 is stopped at 85.5%T. As done previously, the final layer for the Herpin set is stopped at a minimum after a maximum (Fig. 8.15).

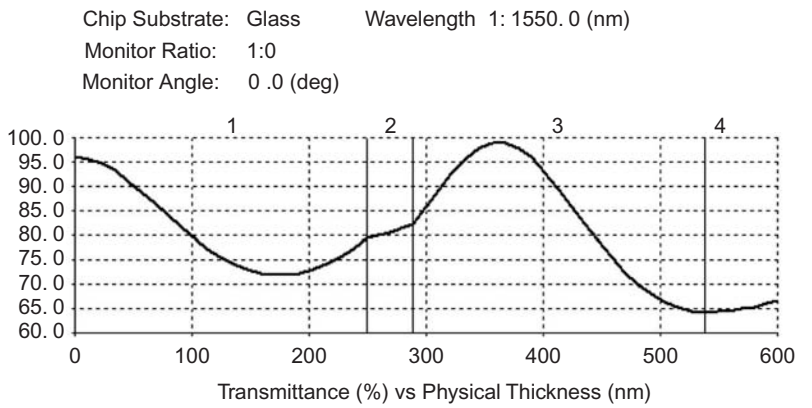

Figure 8.14 A monitoring trace for the first three layers.

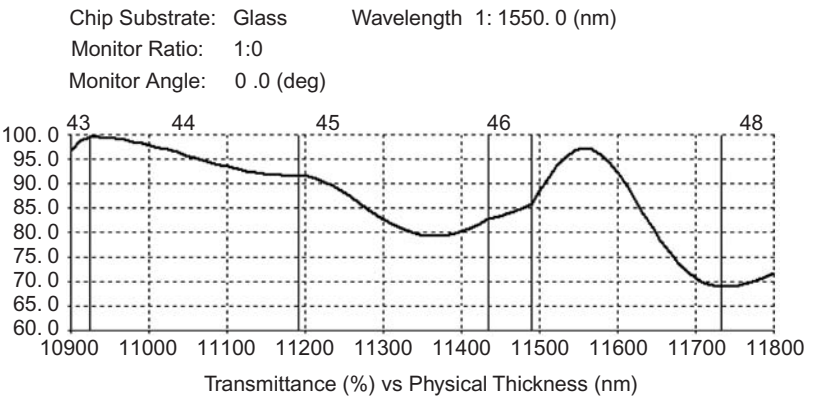

Figure 8.15 The third Herpin set.

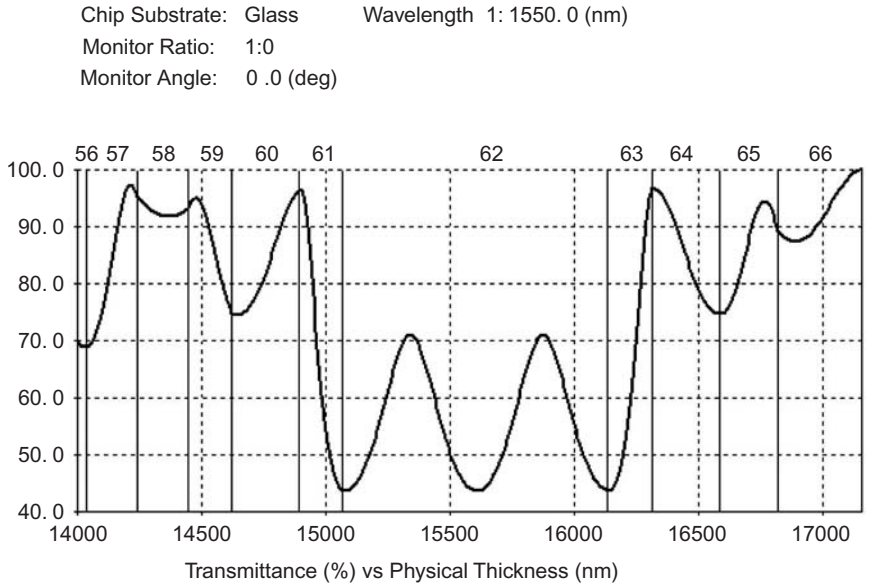

Figure 8.16 The final layers after adjustments.

Layer 58, the final coupling layer, moves only about 1.5%. To obtain more travel, the layer before it can be changed to a thicker layer such as described in the earlier discussion of all-dielectric filters. This filter is to be used in air so the end of the design requires addition of a layer of quartz. The thickness of each of the last two layers will be about 1.3 quarterwaves before optimizing. Layer 57 is set arbitrarily at 1.15 quarterwaves. Layers 58, 65, and 66 are optimized for low reflection in air. The monitor plot showed off-peak cuts on the last few layers, so I adjusted layer 63 to end the layers on the peaks (Fig. 8.16).

Layer 57 is cut after the peak at 95%T. Layer 58, the coupling layer, goes down 4% and is then cut at 93%T. The next layer initially peaks but is stopped sharply at the minimum. Layer 63 is altered to 1.03 quarterwaves to allow cutting at the maximum %T. The AR set at the end has layers of 1.36H and 1.25L.

References

1. P. Guo, S. Y. Zheng, C. N. Yen, and X. Ma, *Appl. Opt.* **28**, 2876–2885 (1989).
2. R. R. Willey, *Practical Design and Production of Optical Thin Films*, Marcel Dekker, New York (1996).

Chapter 9
Fully Blocked Visible Filters

9.1 Introduction

As noted in the previous chapter on all-dielectric filters, blocking unwanted radiation requires many layers and substantial design time. An alternate solution used throughout the industry today is to block low-wavelength leaks with either colored glass or a layer of epoxy containing dissolved dyes, and then block the high-side leaks with a metallic interference filter (M filter).[1] Here, I will briefly review the history of silver filters and describe ways to integrate the metal filters with all-dielectric filters.

In 1942, Geffcken was issued a patent for the first silver filters.[2] They were constructed by depositing two layers of silver separated by a fluoride layer. Schott North America, Inc. manufactures filters this way with two or three silver layers. When the dielectric layer(s) that separates the silver layers is ~one-halfwave thick, the films allow light to pass through; otherwise the light is reflected.

9.2 1M Filters

Adding *pairs* of dielectric layers to a silver film can either increase or decrease reflection of the layer, depending on the layer sequence and thickness. A single layer added to a thin metal layer reduces reflection and increases transmission. For silver, a dielectric layer of about three-fourths quarterwaves has the maximum effect. A filter designed for a wavelength at 500 nm consists of a stack–metal–stack (see Fig. 9.1).

Design: Glass $(HL)^3$ [0.77L 41nmAg 0.75L] $(LH)^3$ air.

The thickness of the layers between the brackets is selected to produce ~0% reflection at the design wavelength (band) from each direction for the complete filter; the indices used are 2.0 and 1.45. The dispersive optical constants of silver are derived from those reported by Johnson and Christy.[3] The thickness of the low-index odd-numbered layers next to the silver layer phase match the stacks to the silver layer. All of the designs shown in this chapter are deposited on BK7 glass and matched to air. 1M filter characteristics: $\%T$ is very high at ~90%; blocking is not deep at ~1%; bandwidth is narrow; and peak is not symmetrical about the center design wavelength.

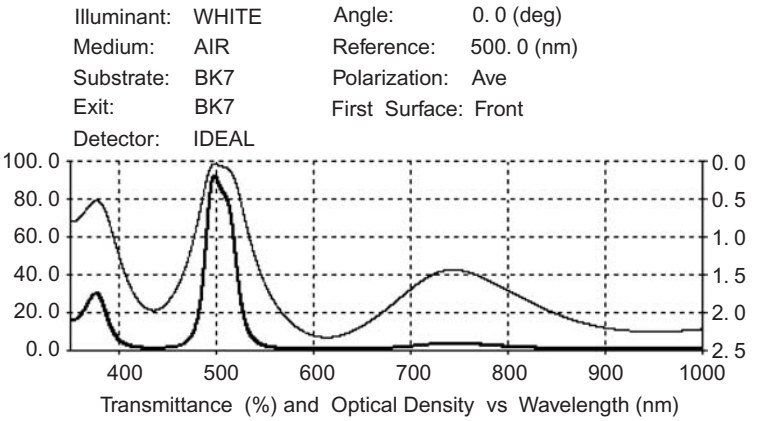

Figure 9.1 A 15-layer 1M filter for 500 nm. The thick line is transmittance; the thin line is OD.

9.3 2M Filters

By adding a "halfwave" dielectric layer and another silver layer adjacent to the first silver layer, a 2M filter evolves. This changes the shape of the bandpass considerably (Fig. 9.2). This design has much better blocking than 1M filters. The same materials are used with fewer pairs of dielectrics to obtain a wider bandwidth.

Design: stack – matched layer – [silver – halfwave with phase-matched layer – silver] – matched layer – stack.

Design: Glass $(HL)^2$ [0.75L 44nmAg 1.45L 55nmAg 0.73L] $(LH)^3$ air.

The thickness of the silver layers and the adjacent layers are optimized to reduce reflection to zero at the center wavelength. Bandwidth is 28 nm, and transmission is 73%; blocking reaches about five densities. If more transmission is necessary,

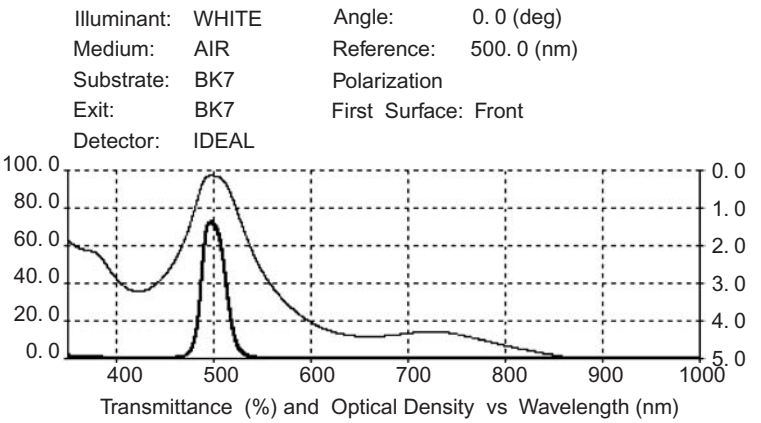

Figure 9.2 A 13-layer 2M filter for 500 nm. The thick line is transmittance; the thin line is OD.

the silver layers must be thinner, and the matching dielectric stacks require fewer pairs of layers. Naturally, the filter would then have less blocking.

9.4 3M Filters

Adding a pair of layers (a dielectric and a metal) to the inner structure broadens the filter with better blocking when the silver layers are thinned out (Fig. 9.3).

Design: glass $(HL)^2$ [0.76L 37nmAg 1.46L 51nmAg 1.47L 41nmAg 0.765L] $(LH)^2$ air.

This bandpass has a correctable small skew; correction would cause a slight overall reduction in transmission. Bandwidth is 50 nm, and transmission is 73%; blocking is better than six densities. This is only an approximation of the process; the program does not show that the metal layers start as islands. Transmission reduces at first (see Fig. 9.4), and then the interference takes effect; this monitoring curve is used as a guide for the cut-off point of the layers. Additional layers can increase blocking.

3M filters can be integrated with all-dielectric filters. Filters can be deposited on glass and designed to work in air. The low-index material is quartz with an index of 1.45; the high-index material can be either zinc sulphide or titanium oxide, both with an index of 2.25. Silver is the metal. The filter is deposited on one side of the substrate and the blocker starts on the opposite side. This is a normal method used by manufacturers to assemble filters (Fig. 9.5).

All-dielectric filter design: $[(HL)^3\ (LH)^3\ L]^2\ (HL)^3\ (LH)^2$ L 1.3H 1.3L.

Blocking filter design: H 1.72L 22.5nmAg 1.39L 40nmAg 1.44L 47.5nmAg 1.735L HLH.

The OD plot shows where the all-dielectric filter stops working on each side of the bandpass (Fig. 9.6). A colored glass filter is needed to block the low-side leak.

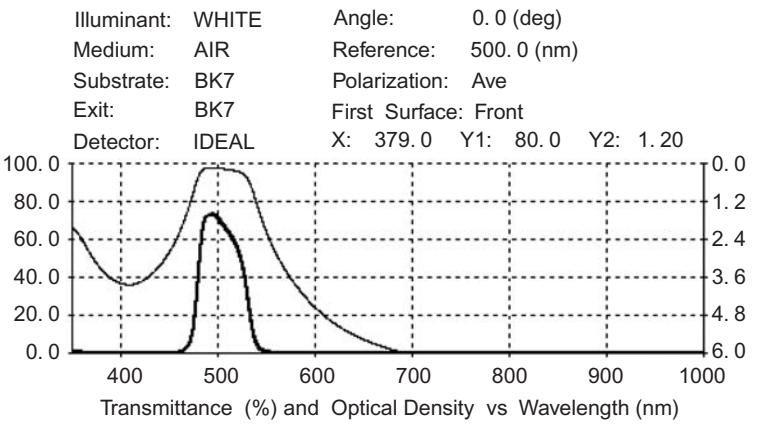

Figure 9.3 A 13-layer 3M filter for 500 nm. The thick line is transmittance; the thin line is OD.

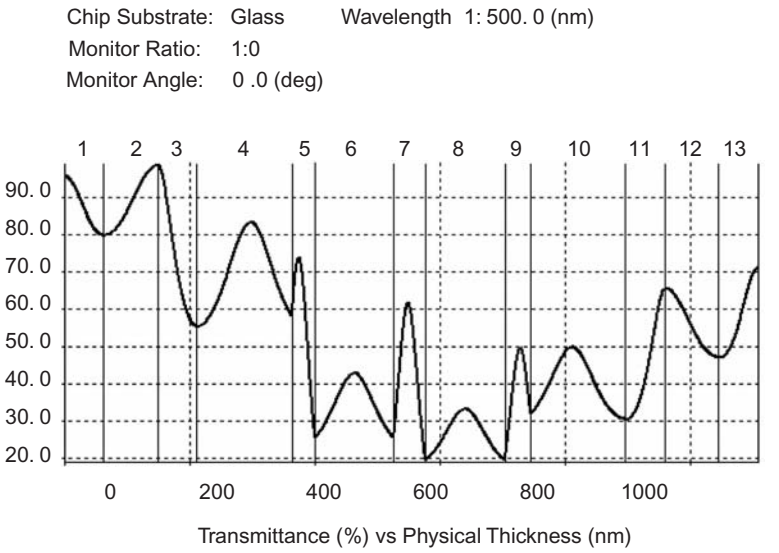

Figure 9.4 A monitoring curve for a 3M filter.

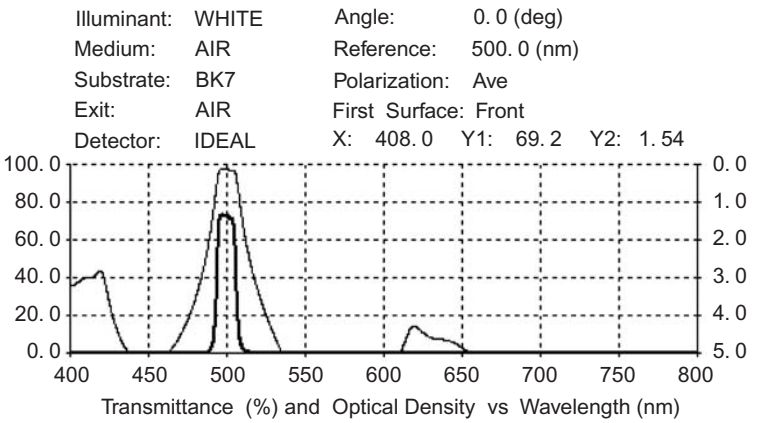

Figure 9.5 Complete filter assembly. The thick line is transmittance; the thin line is OD.

Typically, the industry uses soft chemicals and deposits on window-type glass. The parts are then cemented to the colored glass and cut to the final shape. If the all-dielectric filter is deposited *on* the metal filter as shown in Fig. 9.6, new leaks emerge due to interference between the filters. A separate all-dielectric blocking filter can be deposited on the opposite side to reduce the leak, but I designed a new filter structure to manage the leak; fewer layers are required to achieve good performance.[4–6] After adding an all-dielectric filter section to the metal filter it evolves into a 27-layer filter with good spectral characteristics (Fig. 9.7).

Design: H 1.81L 30nmAg 1.46L 50nmAg 1.46L 47nmAg 0.743L HLL HLHLH L HLHLH LL HL H.

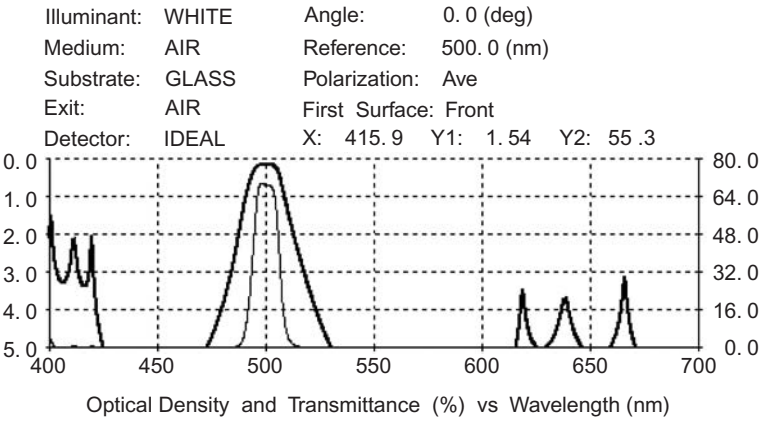

Figure 9.6 Layers on one side only. The thick line is OD; the thin line is transmittance.

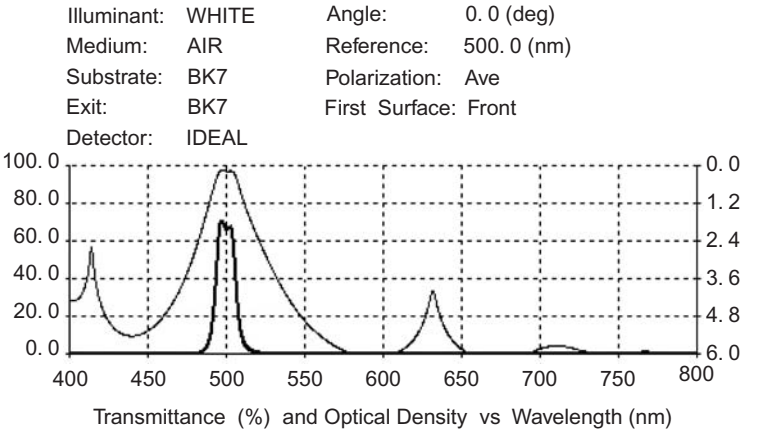

Figure 9.7 Integrated silver filter spectral response. The thick line is transmittance; the thin line is OD.

The first section produces what I call an enhanced filter. The layer following the final silver layer is a low-index matching quarterwave rather than a halfwave. For this design, one high-index quarterwave is added followed by an etalon halfwave. The reflector is then added to obtain the highest $\%T$. A filter curve at this point would have a two-cavity shape with a bandwidth of ~20 nm (Fig. 9.8). Examining the monitoring curve shows a metal filter that also acts as a reflector for the two-cavity filter. Layer 16 is the coupling layer. At this point another etalon is added to complete the filter. More cavities may be added to sharpen the edges of the filter; ripple is also introduced. See References 4–6 for examples.

The filter still has a high-side leak; adding another pair of silver and dielectric layers will reduce the leak substantially with a small loss in transmission. However, I still found the leak objectionable and found an improved design[6] (Fig. 9.9). A short-pass filter is first deposited and spectrally placed such that the blocking zone covers the leak. Layer count is empirically determined to provide five densities of

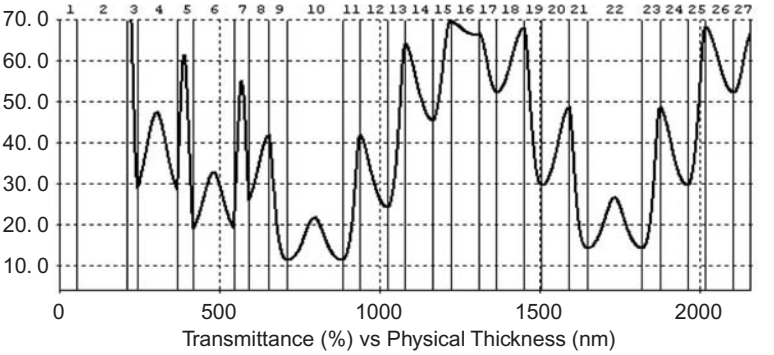

Figure 9.8 A monitoring curve for a two-cavity filter.

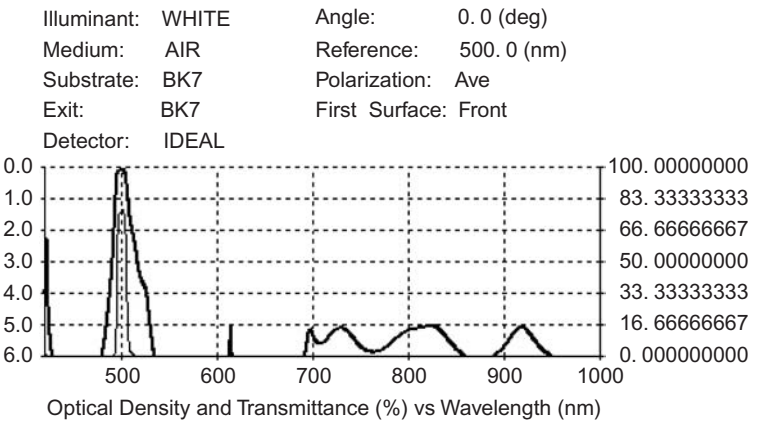

Figure 9.9 A 56-layer filter. The thick line is OD; the thin line is transmittance.

blocking. The design is optimized to give more transmission simultaneously by reducing the overall thickness of the silver layers.

The following 56-layer filter transmits ~79%: 1.18H 2.24L 1.9H 1.2L 1.18H 1.17L 1.16H 1.16L 1.15H 1.15L 1.15H 1.15L 1.15H 1.14L 1.13H 1.46L 34nmAg 1.6L 42nmAg 1.53L 43nmAg 0.78L HL 2H $(LH)^3$ L $(HL)^3$ 2H $(LH)^3$ L $(HL)^2$ 2H LHL 1.11H 1.63L.

Layers 16–21 can be monitored with a quartz crystal. The bandpass is optically monitored except for the coupling layers, and the last two layers are for antireflection. The bandpass may be deposited first by reversing the design and reoptimzing:

HLHL 2H $(LH)^2$ L $(HL)^3$ 2H $(LH)^3$ L $(HL)^3$ 2H LH 0.783L 43nmAg 1.53L 43.5nmAg 1.55L 37.5nmAg 1.4L 1.13H 1.15L 1.16H 1.16L 1.16H 1.155L 1.17H 1.16L 1.17H 1.16L 1.16H 1.16L 1.155H 1.14L 1.62H.

Bandshape is excellent, and the filter is image quality when deposited on AR-coated colored glass (Fig. 9.10). Blocking is as shown in Fig. 9.9. Further

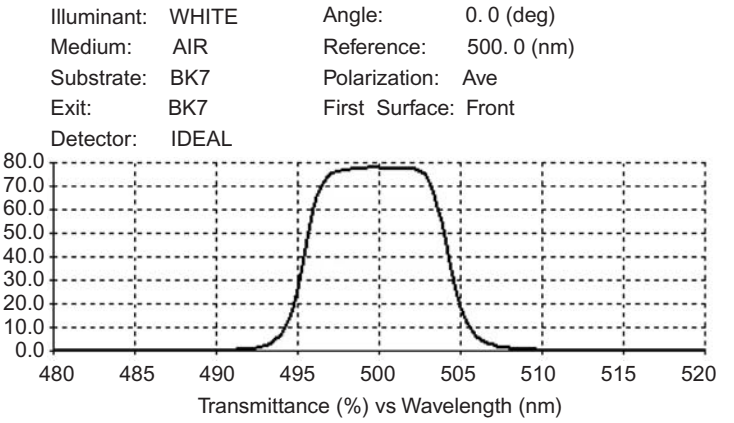

Figure 9.10 Transmission profile for a 55-layer filter.

development of the bandpass structure improves the low-side leak; silver has a natural bandpass in the near-UV region. Absorbing materials and/or special designs[7] are required to completely remove the low-side leak for higher-wavelength filters.

The performance shown in Fig. 9.11 is for a 55-layer filter. The dielectric layers are composed of TiO_2 and SiO_2. There are 3 silver layers; all 55 layers are nonquarterwave. The bandshape is between classical three and four cavities; the filter is image quality. The 49-layer starting design first deposited the three-cavity bandpass:

$(HL)^2\ (LH)^2\ L$
$(HL)^3\ (LH)^3\ L$
$(HL)^3$ LH.798L 40.2nmAg 1.56L 37.1nmAg 1.56L 40.5nmAg 1.39L 1.19H 1.18L 1.17H 1.18L 1.17H 1.16L 1.14H 1.05L 1.47H 0.976L 1.33H 1.39L 1.18H 1.83L 0.37H.

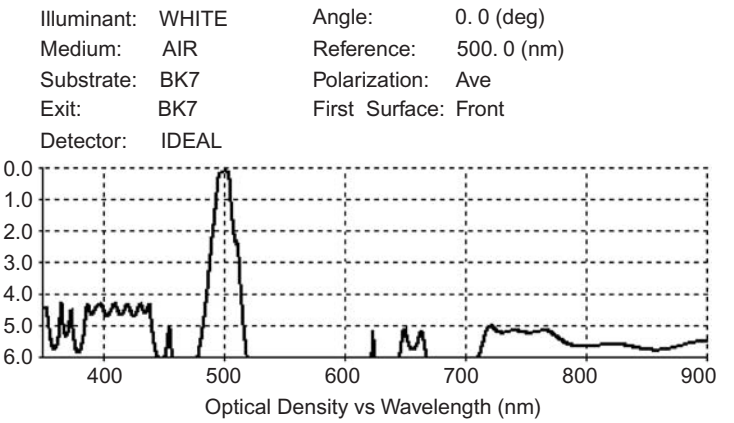

Figure 9.11 A fully blocked filter.

Additional layers are inserted on both sides of the design when the optimization program stops improving the bandshape. The index profile for the final filter is shown in Fig. 9.12. A filter designed for a wavelength of 600 nm requires more layers to achieve a bandwidth of 10 nm. The layout is similar to the 500 nm filter before optimizing:

$(HL)^2$ 4H $(LH)^2$ L
$(HL)^3$ 4H $(LH)^3$ L
$(HL)^3$ 4HLH.798L 40.2A 1.56L 37.1A 1.56L 40.5A 1.39L 1.19H 1.18L 1.17H 1.18L 1.17H 1.16L 1.14H 1.05L 1.47H 0.976L 1.33H 1.39L 1.18H 1.83L 0.37H.

The 61-layer image-quality filter after optimizing all layers is shown in Fig. 9.13. The layer index profile highlights the three-cavity nature of the filter (Fig. 9.14).

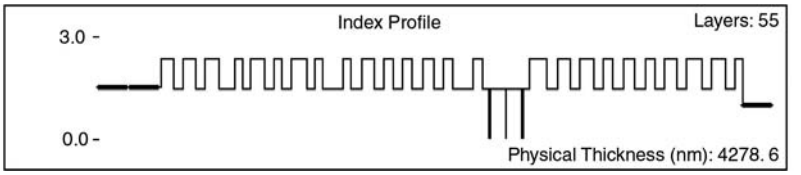

Figure 9.12 A fully blocked filter profile.

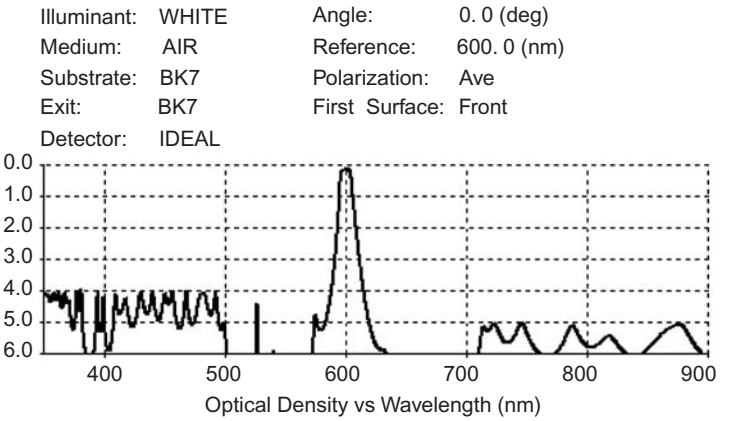

Figure 9.13 The 61-layer image-quality filter after optimizing all layers.

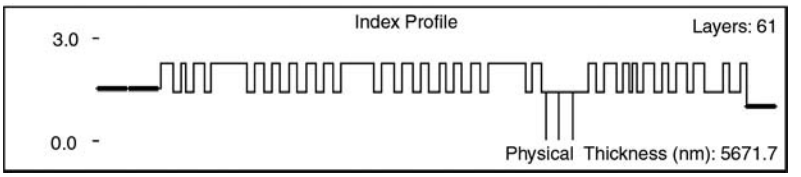

Figure 9.14 A 600-nm filter index profile.

References

1. D. Cushing, "Silver filter development for blocking all dielectric interference filters," *SVC Winter News Bulletin* (2006).
2. W. Geffcken, "Interference light filter," German Patent No. 716153 (1942).
3. P. B. Johnson and R. W. Christy, "Optical constants of the noble metals," *Phys. Rev. B,* **6**, 4370 (1972).
4. D. H. Cushing, "A new approach to blocked multi-cavity filters," *49th SVC Annual Technical Conference Proceedings*, 239–243 (2006).
5. D. H. Cushing, "Filter set for the visible spectrum," *49th SVC Annual Technical Conference Proceedings*, 712–715 (2006).
6. D. H. Cushing, "Bandpass filter with improved blocking," *50th SVC Annual Technical Conference Proceedings*, 480–484 (2007).
7. A. Piegari and J. Bulir, "Variable narrowband transmission filters with a wide rejection band for spectrometry," *Appl. Opt.* **45**, 3768–3773 (2006).

Chapter 10
Fully Blocked Ultraviolet Filters

10.1 Introduction

Generally, UV filters offered by U.S. manufacturers have poor bandshape and low transmission. In this chapter, I design UV filters with high transmission (>40%) and deep blocking (>6 OD). This newer approach is based on my previously published work.[1–6] The filters use hafnium oxide and magnesium fluoride or silicon dioxide dielectrics, and aluminum is the selected metal; the substrate is quartz, and the designs are matched to air. The dispersive indices used are based on previous work and also the literature (see Chapter 2.) HfO_2 and MgF_2 or SiO_2 are deposited by e-beam deposition on substrates at ~80 °C. The highest reflection metal films utilize thermal deposition. To apply the aluminum layers and obtain good optical constants, a vacuum in the 6–10 Torr range and metal deposition rates of 2–4 nm/sec are proposed. The temperature of the substrate is lowered by cooling the filter *in situ* for one hour in a gas atmosphere after depositing the initial dielectric layers; this process may be necessary even if IAD is used to stabilize the films (the substrate becomes warm). Following the metal layers, the balance of layers is deposited at high temperature and/or with IAD.

High-density blocked filters with 10-nm bandwidth are designed in this chapter. The thickness of the dielectric layers are in quarterwave units; the metal layers are specified in nanometers. The back surface requires a low-reflection coating. Other bandwidths can also be achieved with the method that is used.

10.2 Metal Portion Starting Design

The starting design is a 15-layer 4M (four-metal layer) enhanced filter using MgF_2. The design is developed from ideas presented at OIC in 2001 in Banff.[2]

Filter design: 13nmAl 1.42L 30nmAl 1.45L 25nmAl 1.54L 20nmAl 0.78L H 2L HLHLH yields a 10-nm bandpass with 30%T for a design wavelength of 250 nm. Blocking is six optical densities starting at ~360 nm.

This design is derived from 11 layers: 13nmAl 1.42L 30nmAl 1.45L 25nmAl 1.54L 20nmAl 1.78L HLH; an augmented filter. An augmented filter design is shown in Fig. 10.1; the bandwidth is 18 nm. While I was technical director (1971–1990) at MicroCoatings Inc., my staff fabricated many filters with these structures.

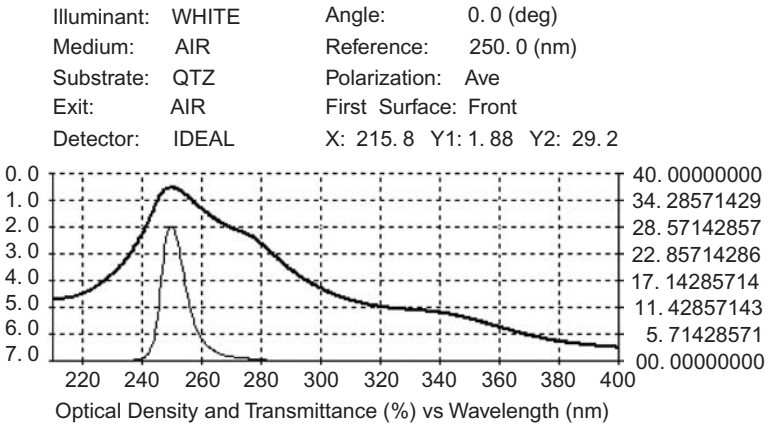

Figure 10.1 Spectral characteristics for an augmented filter. The thick line is OD; the thin line is transmittance.

Since the bandshape of filters like that in Fig. 10.1 is poor, a two-cavity Fabry–Perot all-dielectric filter is deposited before adding the above filter.

Design: $[(HL)^2\ HH\ (LH)^2\ L]^2$. The last layer is phase matched to the metal filter to provide a flatter top with low reflection (Fig. 10.2).

The all-dielectric filter only blocks for short ranges on both sides of the center wavelength. The combination is illustrated in Fig. 10.3. This filter has better performance than catalog filters but can be improved by adding a short-pass segment (Fig. 10.2) to remove the crossover leak. The thickness of the layers is optimized to improve the blocking, as shown by Piegari and Bulir.[7] I used HfO_2 that has some absorption to show realistic transmission. Figure 10.4 exemplifies the bandshape improvement for the 52-layer combination.

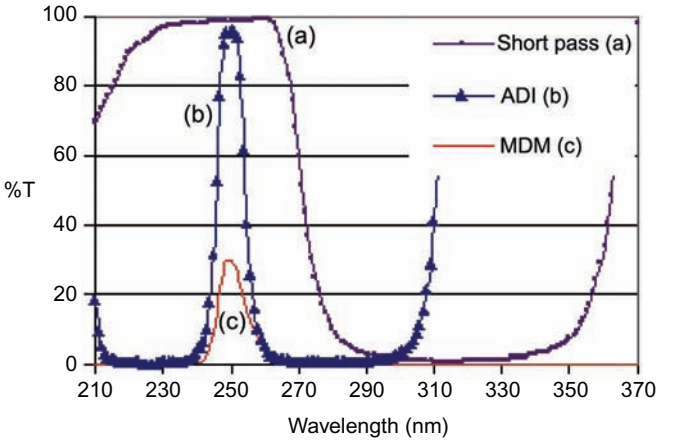

Figure 10.2 Starting components: (a) short-pass filter; (b) Fabry–Perot filter; and (c) metal–dielectric–metal (MDM) filter.

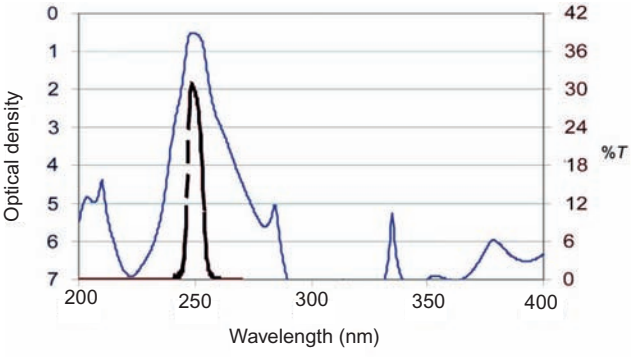

Figure 10.3 First deposit a Fabry–Perot filter, then the 15-layer metal filter (35 layers total). The thin line is OD; the thick line is transmittance.

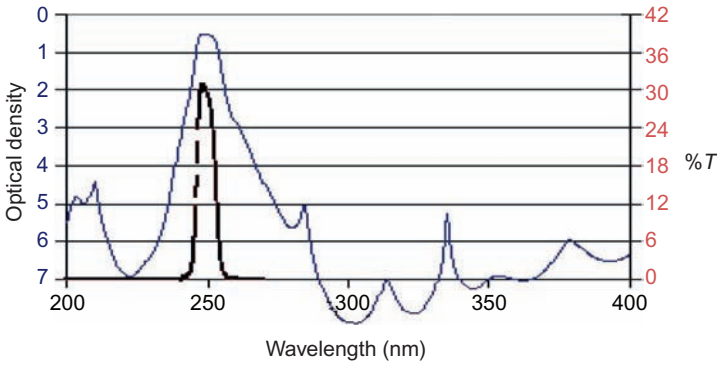

Figure 10.4 A 52-layer filter used as the basis for a new design. The thin line is OD; the thick line is transmittance.

Design of the 52-layer filter:

$$(HL)^2\ HH\ (LH)^2\ L$$

$$(HL)^2\ HH\ (LH)^2\ 1.02L$$

12.5Al 1.43L 23Al 1.49L 23.6Al 1.51L 20Al
1.41L 1.22H 1.28L 1.27H 1.49L 1.6H 1.35L 1.22H 1.25L 1.18H 1.2L 0.97H 1.07L
1.62H 0.7L 1.23H 1.17L 1.23H 0.91L 1.61H 1.23L 1.07H 1.01L 0.47H 0.97L.

The next step is to remove the minor leaks and improve the shape and transmission with optimization. The high-side blocking target is >6 densities for wavelengths >285 nm; target transmission is initially >40% at 253.6 nm; and low-side blocking target is >5OD. Thin layers are removed as the optimization proceeds. The entire filter is allowed to have nonquarterwave-thickness layers to achieve better performance (Fig. 10.5). This design is stable; it may be reduced to 47 layers with no penalties. A thickness error of ±2% on all layers still produces useful filters.

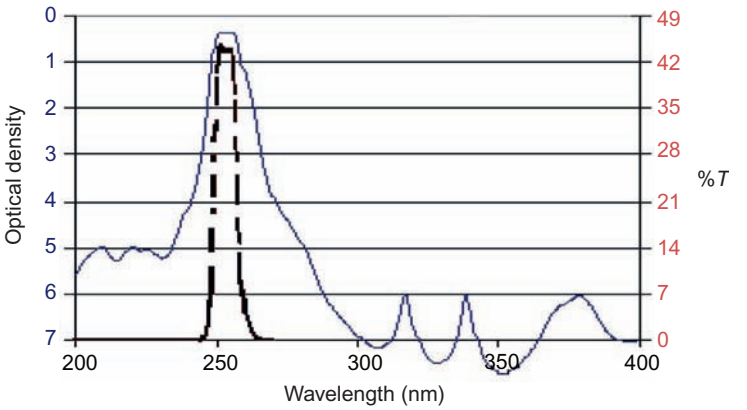

Figure 10.5 Design after optimization has 47 layers, all nonquarterwaves. The thin line is OD; the thick line is transmittance.

Design of the 4MDM 47-layer filter: 1.25H 1.19L 1.26H 1.29L 1.2H 1.13L 1.08H 1.16L 1.24H 1.26L 1.17H 1.16L 1.1H 1.1L 1.04H 1.07L 1.06H 1.18L 1.59H 1.05L 22nmAl 1.53L 22.6nmAl 1.52L 22.9nmAl 1.59L 15.8nmAl 1.14L 1.73H 1.16L 1.07H 0.97L 0.65H 0.88L 1.04H 1.13L 1.16H 1.33L 1.38H 1.29L 1.21H 1.22L 1.22H 1.31L 1.93H 0.5L 1.71H.

10.3 Other Wavelengths

Similar results were achieved for variations of this filter when calculated for the wavelengths 240 and 265 nm. In Fig. 10.6, two layers are added to the bandpass for the wavelengths 280–310 nm to extend the low-side blocking. Bandshape for these filters is between the conventional ratios expected from three- and four-cavity filters. An OD level of six is reached at ~1.16 times the center wavelength. In spite of the absorption present in the hafnium oxide filters for wavelengths as low as

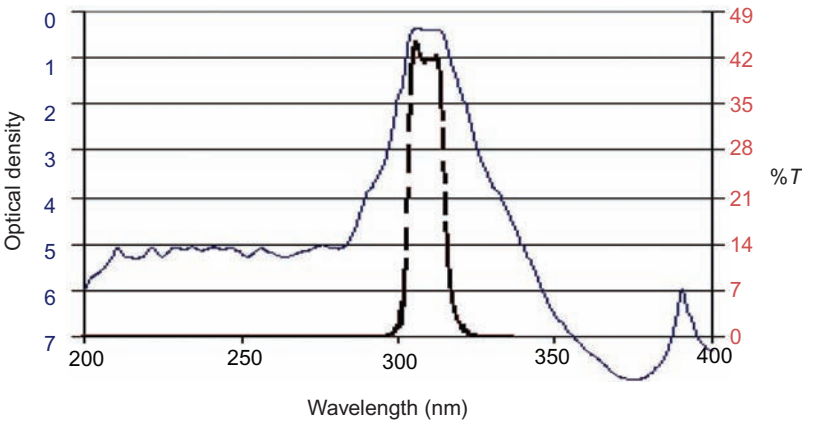

Figure 10.6 A 49-layer filter for 310 nm. The thin line is OD; the thick line is transmittance.

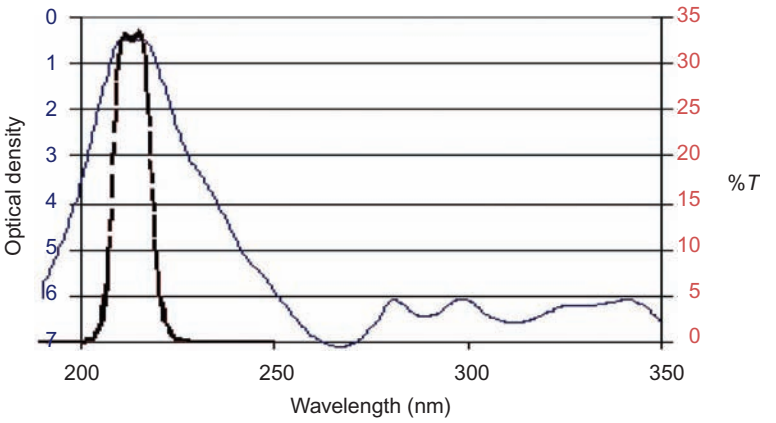

Figure 10.7 A 214-nm filter. The thin line is OD; the thick line is transmittance.

214 nm, reasonable transmission is provided. The curve shown in Fig. 10.7 is for a 37-layer design; 32% transmission is expected.

Thickness of layers: 0.9H 1.86L 1.15H 1.38L 1.09H 1.29L 1.05H 1.39L 0.93H 1.5L 21.6nmAl 1.41L 23.6nmAl 1.43L 23nmAl 1.42L 23.7nmAl 1.43L 0.85H 1.51L 0.94H 1.35L 0.91H 1.23L 0.82H 1.38L 0.91H 1.66L 0.87H 1.5L 0.81H 1.48L 0.46H 1.68L 0.46H 2.15L 0.65H.

10.4 More Cavities

Adding a 10-layer Fabry–Perot bandpass to the beginning of the 49-layer 310-nm filter and altering the bandshape targets increases the cavity count. After optimization the filter has a more square shape with the same out-of-band blocking and the same transmission as the other filters. Spectral performance is indicated in Fig. 10.8. The low-side ripple is removed by adding more optimization targets; more cavities can be added to make the filter even sharper.

10.5 Higher-Transmission Filters

Obtaining a higher-transmission filter is possible by removing a metal–dielectric pair from the 47-layer 253.6 nm filter and reducing the blocking requirements. After optimization, the filter has 58%T with three decades of blocking on the low side and >4.5 decades on the high side (Fig. 10.9).

Design after optimization: 1.34H 1.28L 1.2H 1.21L 1.25H 1.25L 1.17H 1.13L 1.11H 1.21L 1.23H 1.23L 1.19H 1.15L 1.07H 1.04L 1.01H 1.14L 1.53H 1.23L 19nmAl 1.54L 21nmAl 1.55L 18nmAl 1.14L 1.62H 1.25L 1.11H 1.03L 0.59H 0.89L 1.1H 1.21L 1.24H 1.37L 1.32H 1.3L 1.25H 1.27L 1.94H 1.28L 1.21H 0.87L 1.94H.

When another pair of metal–dielectric layers is removed, the bandshape for the 10-nm bandpass is skewed, so I designed a wider-band filter; a 34-layer 2MDM

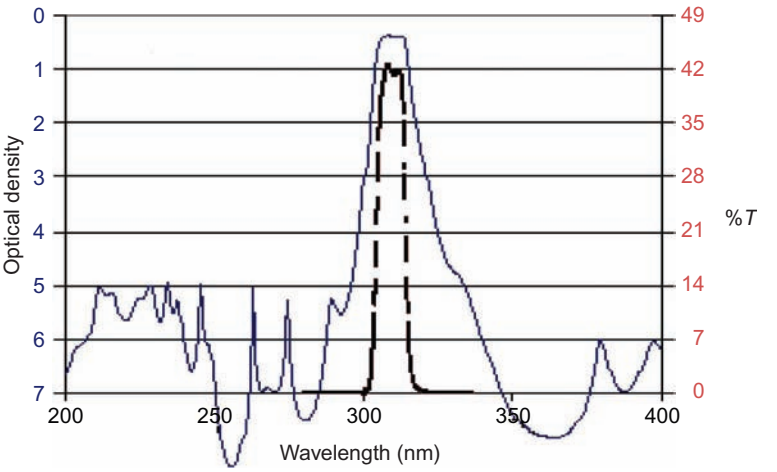

Figure 10.8 A 59-layer filter with fast slopes. The thin line is OD; the thick line is transmittance.

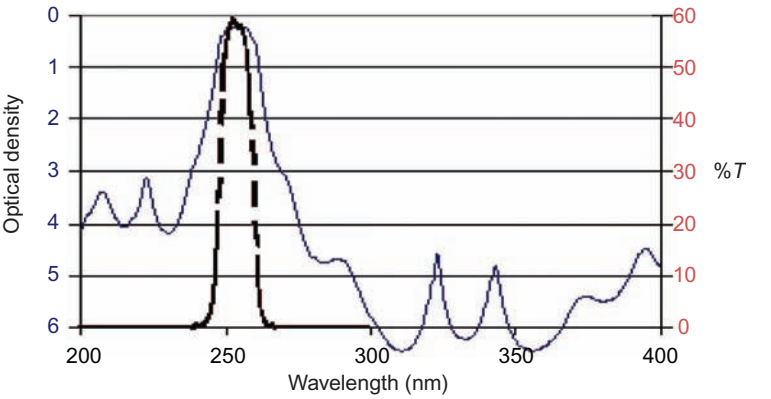

Figure 10.9 A 45-layer 3MDM filter with ~10 nm bandwidth. The thin line is OD; the thick line is transmittance.

filter with a bandwidth of 15 nm blocks to three densities while transmitting 72%, as shown in Fig. 10.10.

A 2MDM design for 253.6 nm: 1.54H 1.89L 1.05H 1.01L 1.00H 1.06L 1.61H 1.3L 19nmAl 1.54L 17.7nmAl 1.86L 1.04H 1.07L 2.34H 1.07L 1.1H 1.15L 1.79H 0.62L 0.95H 1.18L 1.54H 1.11L 1.05H 1.2L 1.54H 0.86L 0.72H 1.86L 0.69H 1.85L 0.47H 2.8L.

Deeper blocked filters are possible with less transmission for these 2MDM and 3MDM filters. Simply optimizing with altered targets produces the best design. For instance, with five-density blocking, the 3MDM 10-nm filter provides 53% transmission.

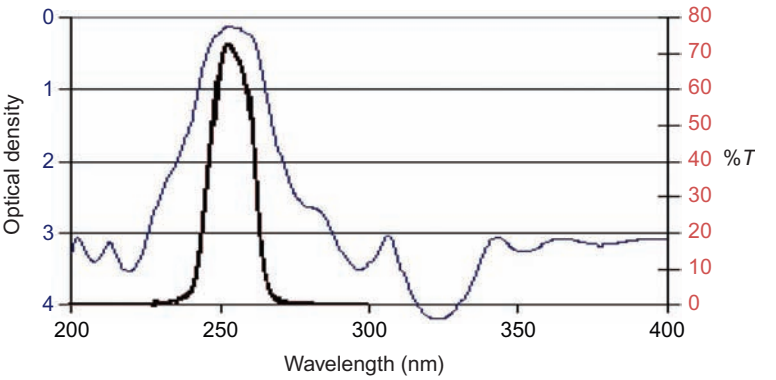

Figure 10.10 A 34-layer 2MDM filter. The thin line is OD; the thick line is transmittance.

10.6 Substituting SiO_2 for MgF_2

UV filters can be designed with low-index layers of quartz instead of MgF_2. However, more layers are required (Fig. 10.11).

Design: 1.11H 1.3L 1.52H 1.11L 1H 0.89L 0.73H 1.9L 0.8H 1.19L 1.1H 1.17L 1.14H 1.19L 1.16H 1.2L 1.14H 1.13L 1.06H 1.07L 1.04H 1.08L 1.07H 1.21L 1.68H 0.82L 21nmAl 1.48L 24nmAl 1.49L 23.5nmAl 1.53L 18.5nmAl 1.79L 1.05H 1.1L 1.07H 1.07L 0.65H 0.5L 1.05H 1.1L 1.11H 1.18L 1.35H 1.39L 1.19H 1.17L 1.15H 1.15L 1.12H 1.13L 1.18H 1.67L 1.22H.

The alteration of the index ratio now requires 55 layers to produce a filter compared with the 47-layer filter shown in Fig. 10.5. Transmission can be increased to 47% when more layers are used.

The filter displayed in Fig. 10.12 has 53 layers: 0.86H 1.06L 1.82H 1.35L 0.725H 0.84L 0.88H 1.4L 1.52H 1.14L 0.98H 1.12L 1.07H 1.25L 1.22H 1.32L

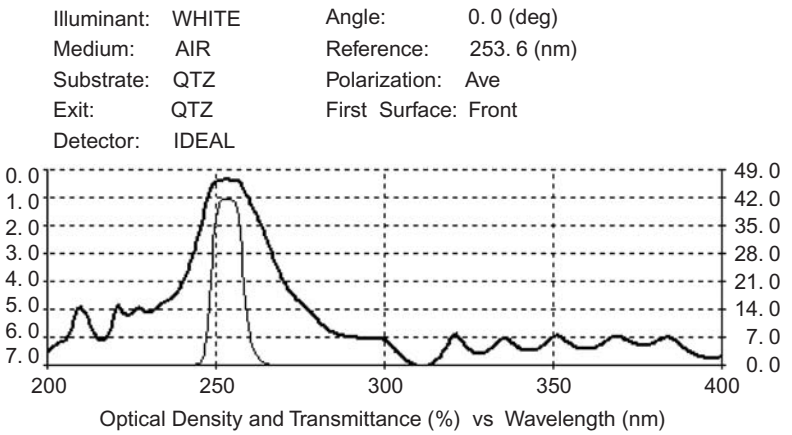

Figure 10.11 A 4MDM filter with SiO_2 low-index layers. The thick line is OD; the thin line is transmittance.

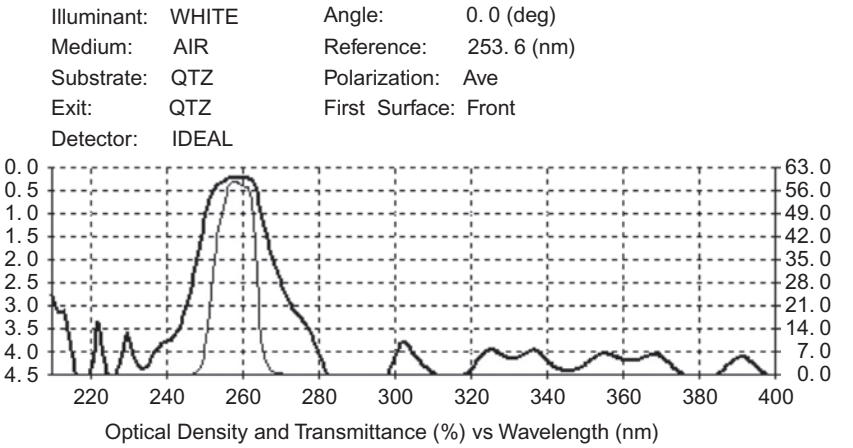

Figure 10.12 A 3M filter with ~63%T. The thick line is OD; the thin line is transmittance.

1.21H 1.17L 1.06H 1.07L 0.93H 1.06L 0.99H 1.34L 1.57H 1.1L 16.7nmAl 1.59L 20nmAl 1.575L 17.1nmAl 1.13L 1.6H 1.34L 1.12H 1.15L 0.97H 0.34L 1.0H 1.08L 1.01H 1.25L 1.41H 1.21L 1.15H 1.62L 1.02H 1.14L 1.02H 1.11L 0.98H 2.03L 1.07H.

The filter in Fig. 10.9 contains MgF_2 and has 45 layers with 58%T. A filter with even more transmission is possible with less blocking (Fig. 10.13). Removing a metal and quartz layer pair and optimizing for a 10-nm filter with three densities of blocking and many trials yields a filter with ~ 70%T.

Design: 1.28H 1.33L 0.94H 1.23L 1.52H 1.05L 1.05H 1.27L 1.14H 1.03L 0.93H 0.91L 0.98H 1.89L 1.04H 1.08L 1.07H 1.01L 0.98H 1.15L 0.96H 0.52L 0.94H 1.14L 1.64H 1.34L 18.4nmAl 1.55L 19.9nmAl 1.64L 1.25H 1.16L 1.14H 2.1L

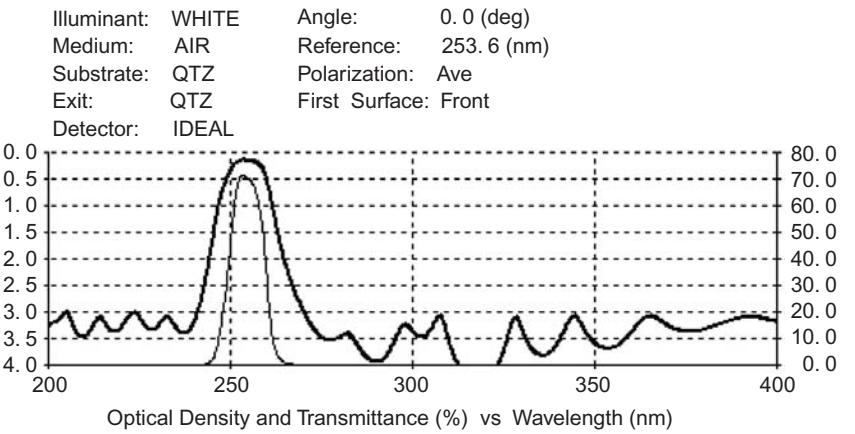

Figure 10.13 A 52-layer 2M filter with a 10 nm bandwidth using quartz layers. The thick line is OD; the thin line is transmittance.

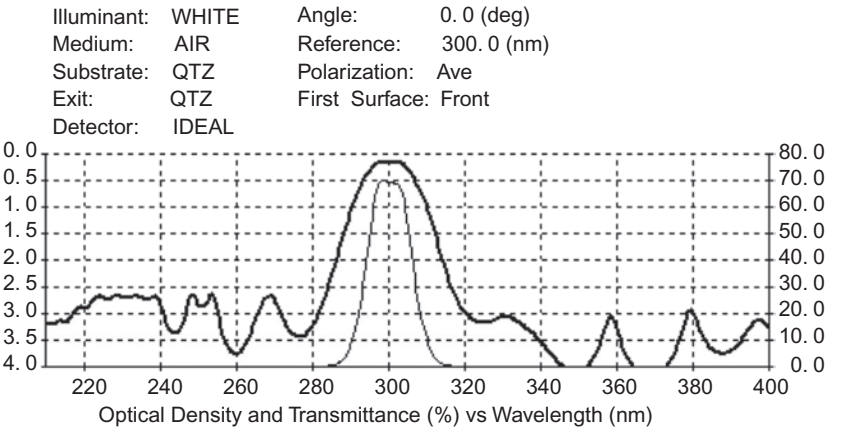

Figure 10.14 A 49-layer 300 nm filter. The thick line is OD; the thin line is transmittance. The bandwidth of this filter is 13 nm. Blocking is complete on the high-wavelength side to three optical densities and less than 0.4$\%T$ on the low side. The filter has ~70$\%T$.

0.88H 1.29L 1.44H 1.2L 0.97H 0.90L 0.94H 1.68L 1.36H 1.08L 1.06H 1.6L 1.15H 0.9L 0.82H 0.22L 0.6H 2.42L.

Filters for other wavelengths are similarly designed (Fig. 10.14).

Design: 1.28H 1.46L 1.68H 0.76L 1.23H 3.53L 1.46H 1.67L 0.89H 0.96L 1.15H 1.85L 1.0H 1.0L 1.55H 0.95L 0.82H 0.78L 0.9H 1.04L 1.03H 1.86L 18nmAl 1.63L 18.75nmAl 1.68L 1.04H 1.21L 1.27H 0.75L 0.76H 0.85L 0.9H 0.86L 1.63H 0.79L 1.35H 1.32L 0.98H 1.01L 1.28H 1.38L 1.06H 0.95L 0.95H 1.3L 1.13H 1.4L 1.28H.

With the proper layer configuration, ultraviolet filters can be designed to provide both high transmission and deep blocking with excellent bandshape. Many more layers could be utilized than used in current practice, and designs with many more layers than above can be produced; the results are worth the extra effort. These are image-quality filters.

References

1. D. Cushing, "Completely blocked ultraviolet filters," in *Optical Interference Coatings on CD-ROM*, *OSA Technical Digest*, TuD6 (2007).
2. D. Cushing, "Narrow band UV MDM filter for the new millennium," in *Optical Interference Coatings*, *OSA Technical Digest*, TUA8 (2001).
3. D. Cushing, "A new approach to blocked multi-cavity filters," *49th SVC Annual Technical Conference Proceedings*, 239–243, 712–715 (2006).
4. D. Cushing, "Bandpass filter with improved blocking," *50th SVC Annual Technical Conference Proceedings;* 480–484 (2007).
5. D. Cushing, "Optical filters for high resolution ultraviolet imaging systems," *Proc. SPIE* **932**, 148–152 (1988).

6. D. Cushing, "Ultraviolet narrowband filters with both high transmittance and superior rejection for imaging situations," *Proc. SPIE* **1158**, 346–350 (1989).
7. A. Piegari and J. Bulir, "Variable narrowband transmission filters with a wide rejection band for spectrometry," *Appl. Opt.* **45**, 3768–3773 (2006).

Chapter 11
Nonpolarizing Reflection Filters

Bandpass and edge filters are examined in this chapter. Filters are designed to be used at a 45-deg angle in air. Reflective bandpass filters are discussed first; they are designed to *absorb* the radiation that is not reflected as a bandpass. Two types of designs are shown. For low wavelengths a long-pass dielectric filter deposited on a dark mirror performs well. The filters described in Chapter 6 are used as the starting designs for these dichroic reflective color filters.

Bandshape cannot be easily improved beyond the performance shown for the following designs. Multicavity filters are not allowed. The filters are designed to function only in the visible spectrum area (for the most part), and further blocking is possible with more layers and less contrast. To achieve low polarization, two sets of targets, one for each polarization mode, are provided for the spectral zone affected (Fig. 11.1).

Design: 20nmI 0.52qwQ 1.57qwT 1.83qwQ 19nmI 1.97qwT 0.26qwQ 1.32qwT 3.18qwQ 1.24qwT 0.59qwQ 0.38qwT 1.9qwQ 2.66qwT 1.92qwQ 0.27qwT 0.47qwQ 1.23qwT 2nmI 0.72qwT 1.18qwQ referenced to 490 nm.

The bandwidth is about 60 nm and displays little polarization in both the reflective and absorptive regions. The filter's properties are uncontrolled above 800 nm. The purpose of the filters is color control. The wavelength may be altered for this configuration of layers to produce different colors; the layer thicknesses are then slightly adjusted to keep low reflectance in the blocking region of interest. A green filter with 21 layers shows similar shape and blocking characteristics (Fig. 11.2).

Design: 20nmI 0.87qwQ 1.55qwT 1.53qwQ 21nmI 2.16qwT 0.42qwQ 0.7qwT 2.02qwQ 0.27qwT 1.0qwQ 1.63qwT 0.1qwQ 1.26qwT 3.0qwQ 0.18qwT 0.24qwQ 0.88qwT 0.31qwQ 0.39qwT 1.12qwQ referenced to 558 nm.

If the highlighted layer is changed to metal, the filter has less polarization as in Fig. 11.1. A broad bandpass filter for the blue–green region containing up to four metal layers is more appropriate for most of the spectrum (Fig. 11.3).

Design: 20nmI 0.86qwT 2.78qwQ 8.6nmI 2.24qwQ 7.2nmI 1.82qwT 0.29qwQ 1.36qwT 1.79qwQ 0.26qwT 0.51qwQ 1.34qwT 1.36qwQ 2.57qwT 0.29qwQ 0.25qwT 0.35qwQ 1.39qwT 1.74qwQ 2nmI 0.52qwQ 0.16qwT 1.54qwQ referenced to 550 nm.

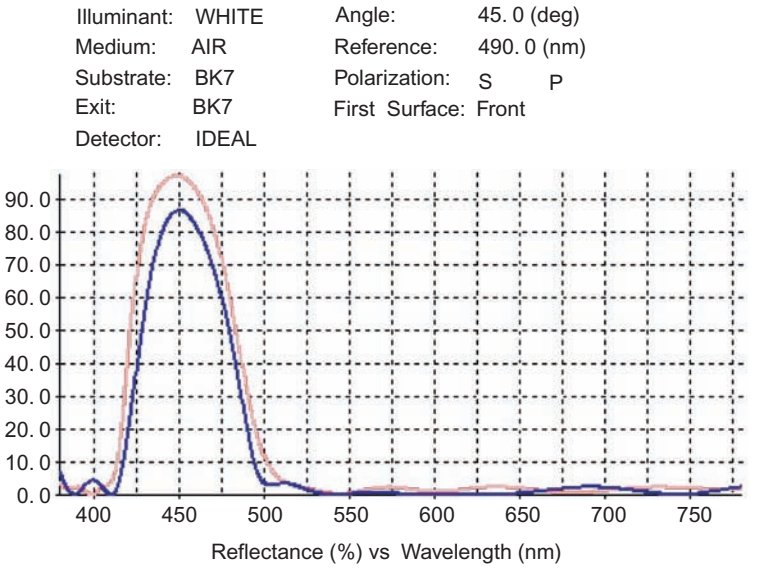

Figure 11.1 A 21-layer, blue reflector filter. The higher curve at 450 nm is S-polarized reflectance; the lower curve is P-polarization.

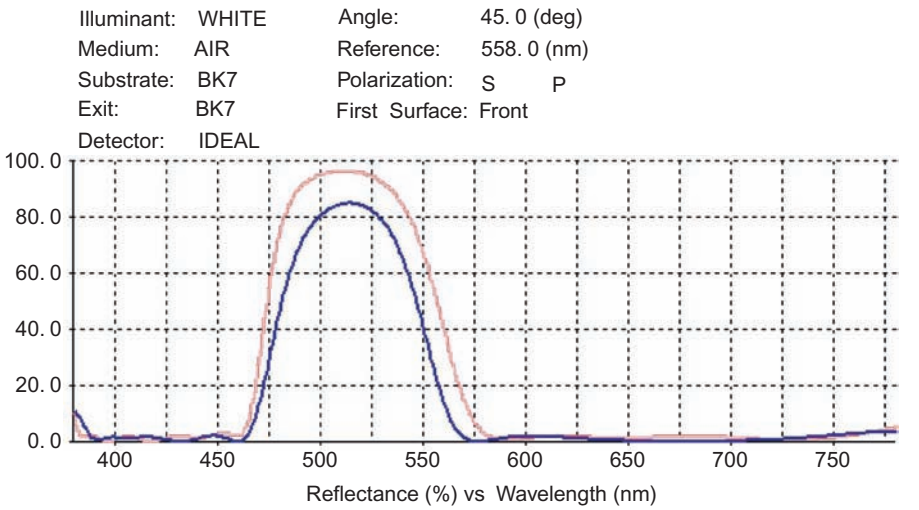

Figure 11.2 A 21-layer refined design for a higher-wavelength notch. The higher curve at 500 nm is S-polarized reflectance; the lower curve is P-polarization.

For the orange region two designs are shown to compare features. The first orange filter is a bandpass similar to the figure in Fig. 11.3, but with three metal layers. Blocking is not as good overall, but it is reasonable for the low-wavelength spectral area; the bandpass is quite pronounced and has virtually no polarization (Fig. 11.4).

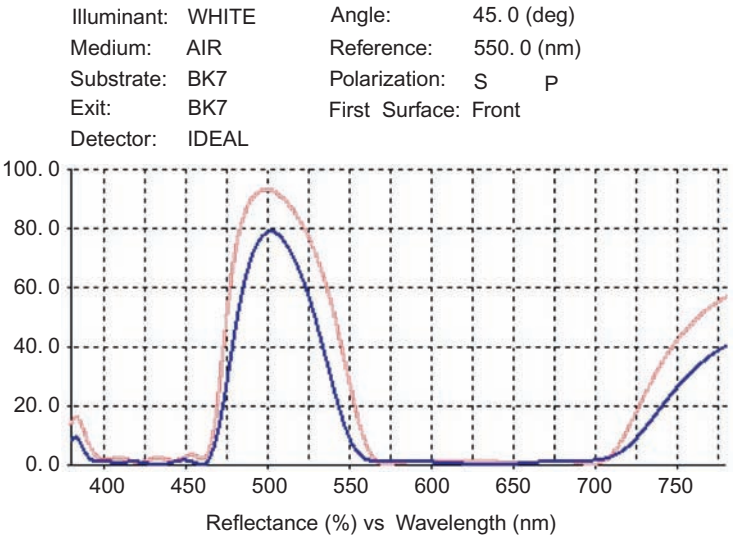

Figure 11.3 A 24-layer green reflector featuring four metal layers. The higher curve at 500 nm is S-polarized reflectance; the lower curve is P-polarization.

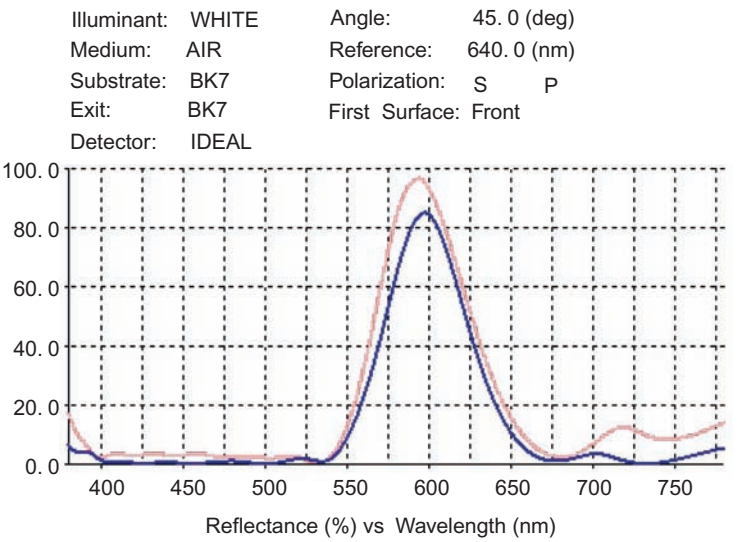

Figure 11.4 A 21-layer orange filter with three metal layers. The higher curve at 600 nm is S-polarized reflectance; the lower curve is P-polarization.

Design: 30nmI 0.2qwQ 0.65qwT 1.0qwQ 15.4nmI 0.39qwT 0.23qwQ 1.53qwT 0.36qwQ 1.34qwT 1.15qwQ 1.37qwT 0.18qwQ 1.13qwT 1.32qwQ 0.95qwT 1.31qwQ 1.82qwT 0.93qwQ 8nmI 2.31qwQ referenced to 640 nm.

These filters are basically (multiple) etalon filters optimized to have no polarization. A notch-type filter similar to the design of Fig. 11.2 is optimized with 21 layers (Fig. 11.5).

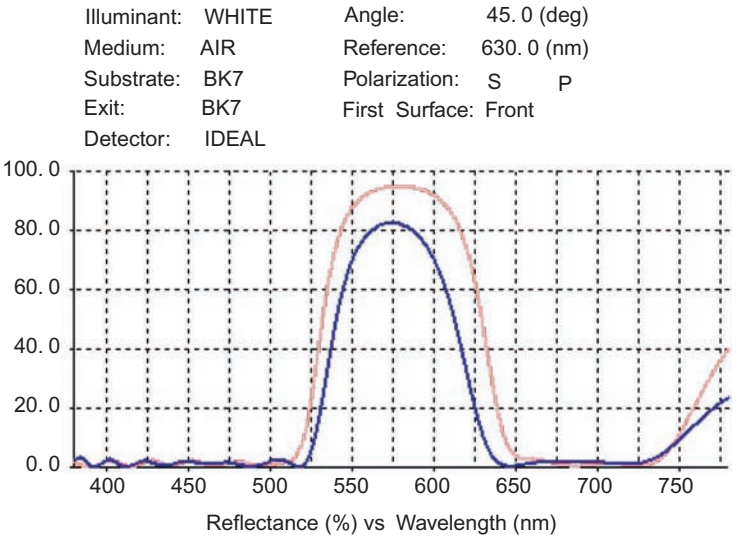

Figure 11.5 A three-metal-layer yellow notch filter. The higher curve at 600 nm is S-polarized reflectance; the lower curve is P-polarization.

Design: 20nmI 0.31qwT 0.96qwQ 2.0nmI 0.35qwT 2.61qwQ 12.5nmI 1.88qwT 0.32qwQ 1.45qwT 1.17qwQ 0.08qwT 1.78qwQ 1.33qwT 0.07qwQ 1.22qwT 1.4qwQ 1.45qwT 0.13qwQ 2.74qwT 0.73qwQ referenced to 630 nm.

Blocking is improved, but some thin layers are necessary to wring out the best performance. Although none of these designs shown are targeted for color, the targets can be color coordinates and luminosity. Narrower filters can also be designed; they may need more or thicker (three-quarterwave) layers (Fig. 11.6). This filter contains 17 layers, including three metal layers, with a start similar to the design shown in Fig. 11.4. The bandwidth is about 35 nm, and the filter was obtained with higher-order films included in the design. This filter is useful for a heads-up display (HUD) system. Cathode ray tubes (CRTs) need filtering to remove the sunlight; therefore, this filter performs a dual function. The light generated from a green CRT is reflected strongly while sunlight coming from the opposite direction is absorbed. The reflected signal can now be directed to a cockpit window. The design can be altered to work for larger angles and larger fields of view. If the surface has focusing power, the coating can still be applied.

Design: 21nmI 1.98qwT 6.1nmI 1.57qwT 3.29qwQ 0.98qwT 3.28qwQ 0.9qwT 3.31qwQ 0.87qwT 3.27qwQ 1.02qwT 4.01qwQ 0.29qwT 16.4nmI 0.75qwT 1.19qwQ referenced to 574 nm.

A red filter centered for the 633-nm laser can be used in a field of view of +/−4 deg (Fig. 11.7).

A design with a bandwidth of 25 nm for the red reflector: 30nmI 0.8qwQ 16nmI 0.62qwT 1.62qwQ 2.66qwT 1.58qwQ 0.44qwT 1.48qwQ 1.27qwT 0.15qwQ

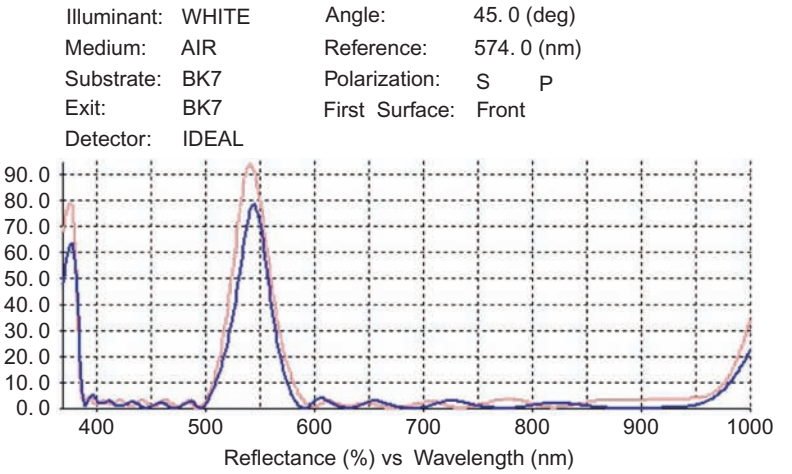

Figure 11.6 A narrow-band filter for 543-nm wavelength. The higher curve at 540 nm is S-polarized reflectance; the lower curve is P-polarization.

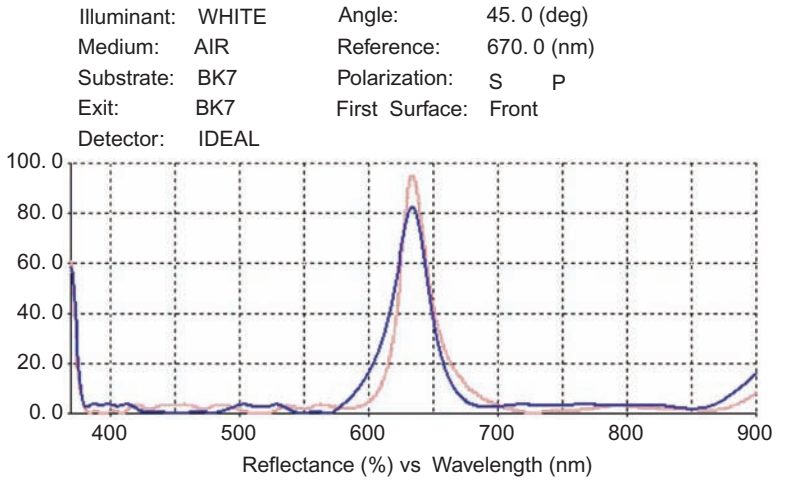

Figure 11.7 A 25-layer red reflector. The higher curve at 630 nm is S-polarized reflectance; the lower curve is P-polarization.

1.34qwT 1.22qwQ 1.01qwT 1.17qwQ 1.39qwT 0.1qwQ 1.01qwT 1.56qwQ 1.34qwT 2.01qwQ 0.82qwT 0.86qwQ 10nmI 0.68qwQ referenced to 670 nm.

The design method can be extended to the ultraviolet spectrum. The high-index material used in the following design (Fig. 11.8) will be HfO_2.

Design: 11nmI 0.9qwH 1.02qwQ 9nmI 1.18qwH 1.61qwQ 0.29qwH 1.4qwQ 0.86qwH 0.76qwQ 1.06qwH 1.16qwQ 0.49qwH 1.57qwQ 0.8qwH 0.53qwQ 1.43qwH 1.95qwQ 7.3nmI 0.36qwH 1.49qwQ referenced to 280 nm.

Blocking extends to ~800 nm. If a second identical filter is positioned in series with the above filter, the average filter performance is very good (Fig. 11.9). The

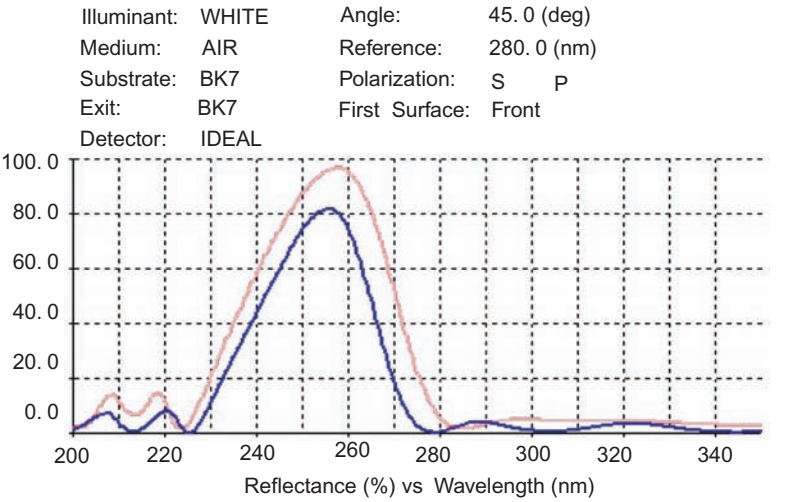

Figure 11.8 A 21-layer reflection filter that includes three metal layers. The higher curve at 260 nm is S-polarized reflectance; the lower curve is P-polarization.

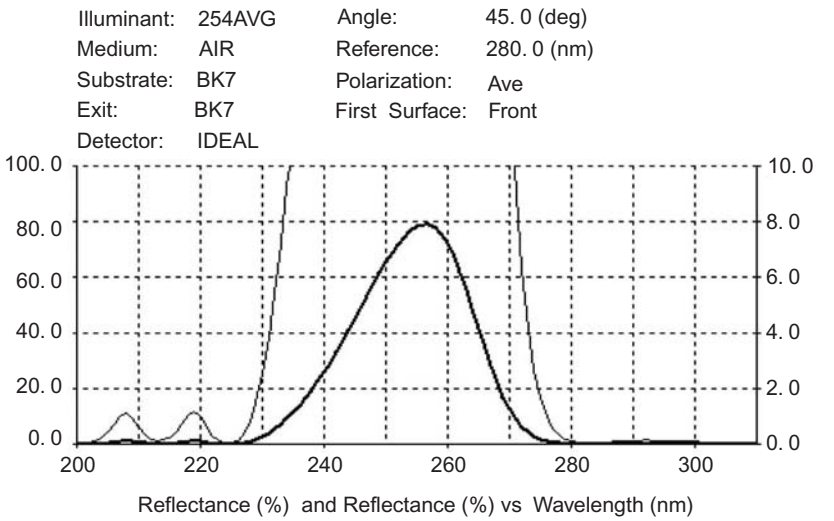

Figure 11.9 Two 254-nm filters in series. The thick line is reflectance; the thin line is zoom-in reflectance.

half-bandwidth is ~20 nm, and the high-side blocking is better than 0.03% to 800 nm (Fig. 11.10). The leaks near 300 nm are <0.2% average. Good performance is accomplished with either Ta_2O_5 or Ti_3O_5 high-index materials at wavelength 365 nm (Fig. 11.11).

Design: 0.81qwH 20nmI 0.91qwH 12.3nmI 1.45qwH 0.68qwQ 1.01qwH 0.51qwQ 1.63qwH 0.42qwQ 1.03qwH 1.2qwQ 0.23qwH 1.95qwQ 0.64qwH 2.05qwQ 9.1nmI 0.26qwH 1.49qwQ referenced to 400 nm.

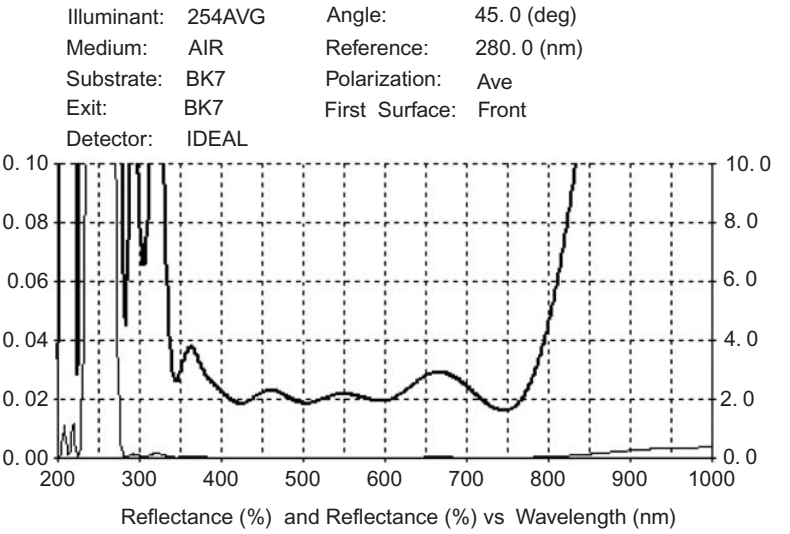

Figure 11.10 The average blocking of two filters in series. The thick line is reflectance; the thin line is zoom-in reflectance.

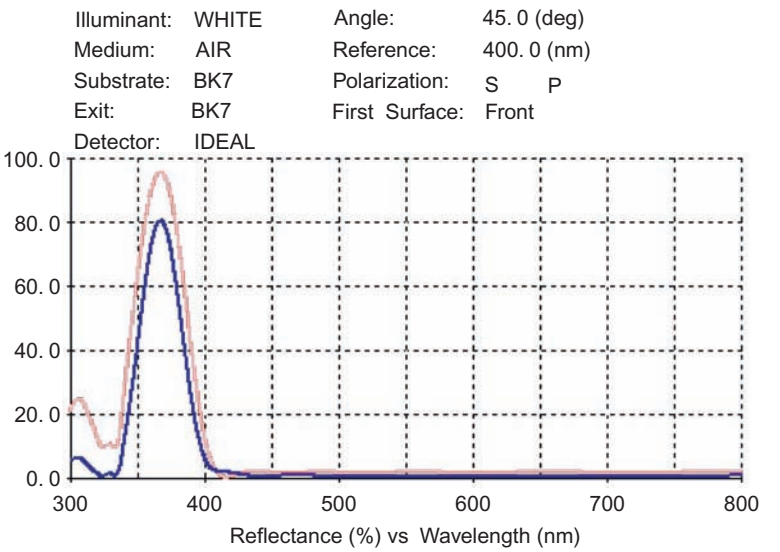

Figure 11.11 A 19-layer filter. TiO_2 is the high index. The higher curve at 370 nm is S-polarized reflectance; the lower curve is P-polarization.

This mirror would be useful to isolate the black light at 365 nm for fluorescence studies. The low-wavelength radiation is uncontrolled; lower-wavelength reflectors require Ta_2O_5.

Chapter 12
Nonpolarizing Transmissive Filters

12.1 Introduction

Bandpass and edge filters are examined in this chapter and are designed for use at a 45-deg angle. These are slab filters; therefore, the second surfaces of transmissive filters require a nonpolarizing reflection-reducing coating (Fig. 12.1). A design with nine layers using three materials provides excellent performance. The bulk of the design uses TiO_2 and SiO_2 with one layer of MgF_2. The coating retains hardness by covering the MgF_2 layer with a 20-nm-thick SiO_2 layer. Fewer layers are effective for a narrower spectral range.

Design: 0.22qwT 0.43qwQ 1.05qwT 0.11qwQ 0.74qwT 2.2qwQ 1.93qwT 0.82qwM 0.22qwQ all layers in qw units at 520 nm.

About 10% of the S-polarized light is reflected without a coating.

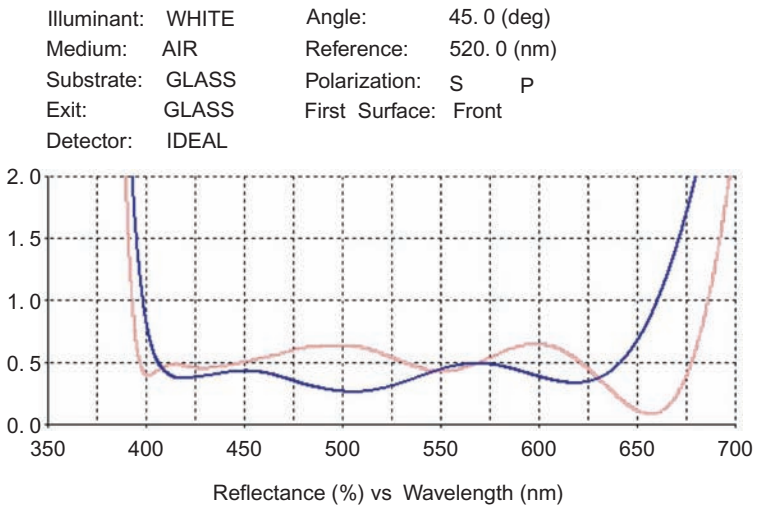

Figure 12.1 An AR coating. The higher curve at 500 nm is S-polarized reflectance; the lower curve is P-polarization.

12.2 Broadband Filters

In 1998, I presented a paper[1] about filters for an RGB system that separates the red, green, and blue spectral zones; the filters are immersed in a glass prism medium. Slab filters are simpler to achieve; the bandpass portion is a multicavity MDM filter with nonpolarizing spacers. Costich[2] was the first person to write about the use of these types of spacers. These bandpass filters are second order; the first-order leaks are covered with MDM filters that polarize, so the design is a compromise. I updated the materials to include energetic deposition with an ion source. To design the filter shown in Fig. 12.2 the thicknesses of silver, TiO_2, and SiO_2 are optimized.

Green filter design: 0.93qwT 15nmAg 1.49qwT 17nmAg 1.67qwT 17nmAg 1.49qwT 28nmAg 1.58qwT 0.32qwQ 1.38qwT 34nmAg 1.41qwT 0.37qwQ 1.43qwT 28nmAg 1.58qwT 0.53qwQ 1.13qwT 8nmAg 1.35qwT for 520 nm.

To remove the leak in the infrared spectrum, six layers are added to the filter of about a halfwave thickness each. First, the six layers are deposited followed by the filter. Optimization changes the layer thicknesses slightly. The final filter is shown in Fig. 12.3.

Six layers are added to the Fig. 12.2 design: 2.03qwT 2.2qwQ 2.13qwT 1.76qwQ 2.21qwT 1.76qwQ 0.73qwT 14nmAg 1.57qwT 19nmAg 1.57qwT 19nmAg 1.48qwT 31.5nmAg 1.65qwT 0.3qwQ 1.35qwT 36nmAg 1.49qwT 0.48qwQ 1.25qwT 28nmAg 1.35qwT 0.78qwQ 1.1qwT 6.5nmAg 1.28qwT for 520 nm.

Lower-wavelength filters are easily obtained using this general design. Higher-wavelength filters have a low-wavelength leak to reconcile. Colored glass or a long-pass filter may need to be added to complete the filter. All-dielectric filters are described in the referenced articles but are difficult to block and contain many layers.[1–6]

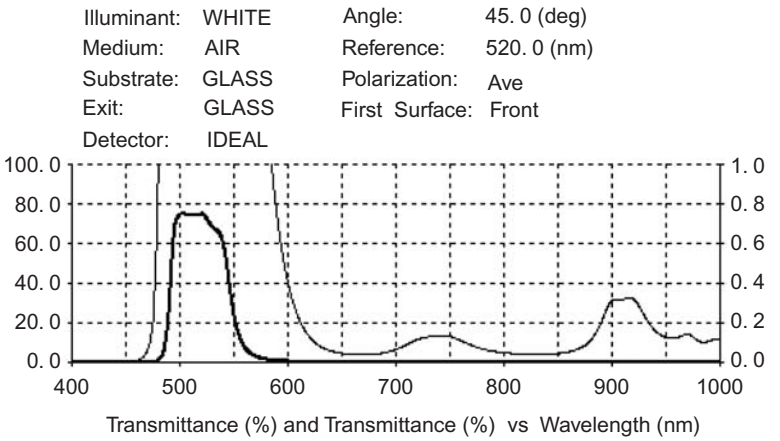

Figure 12.2 A 21-layer filter. The thick line is transmittance; the thin line is zoom-in transmittance.

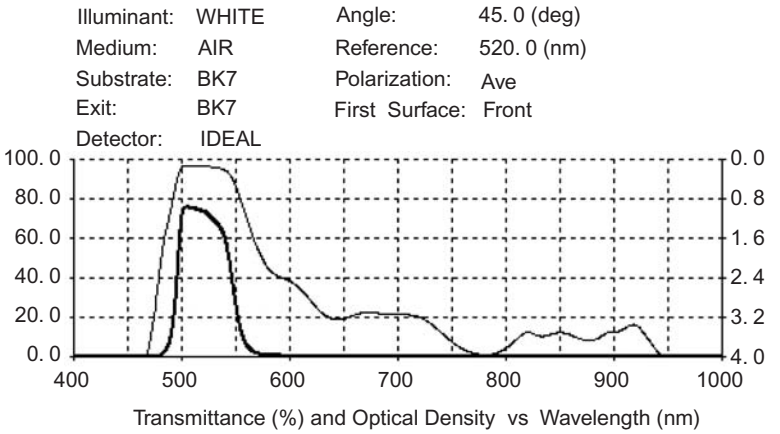

Figure 12.3 Six layers are added to improve the blocking and the bandpass. The thick line is transmittance; the thin line is OD.

12.3 Long-Pass Filters

Thelen[4] devotes a chapter in his book to designing nonpolarizing filters, and Macleod[3] includes a chapter about tilted coatings. I published an article about long-pass filters in 2005 that is still a current useful approach.[8] Using the design methods outlined by Thelen, I selected a broadband 39-layer filter of the type $(2H\ 1.65L)^{19}$ 2H as a prototype reflector with long-wavelength passing properties (Fig. 12.4). Indices selected are VT = 2.1; VQ = 1.5, and the substrate (BK7) index is ~1.52. This ratio of thicknesses produces very little polarization at the band edge. The design is then optimized using TFCalc to improve the transmission from the band edge to 800 nm (Fig. 12.5). A wider bandpass is possible, but for high final $\%T$ over the selected range many more layers are required (see Fig. 12.12 for more details).

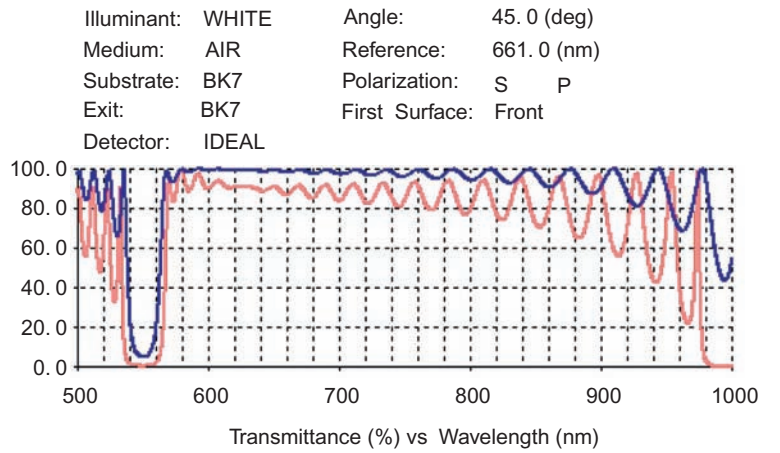

Figure 12.4 Starting design: a 39-layer filter measured at 45 deg. The higher curve is P-polarized transmittance; the lower curve is S-polarized transmittance.

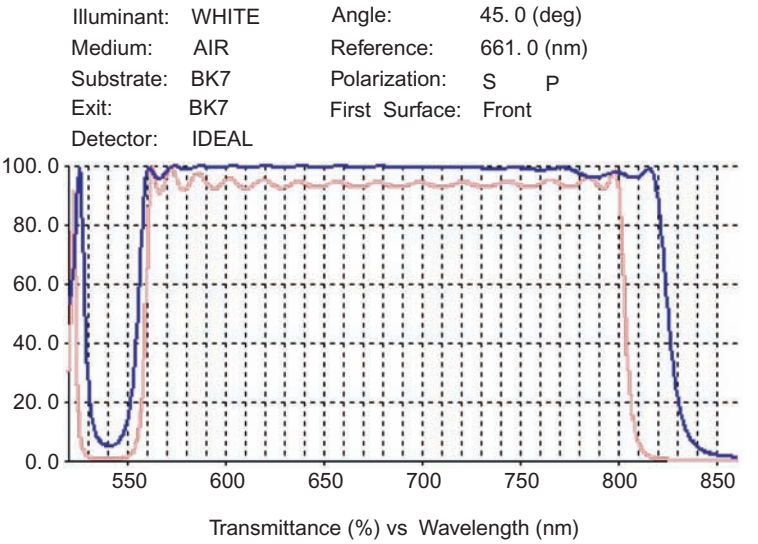

Figure 12.5 The same 39-layer design after optimization. The higher curve is P-polarized transmittance; the lower curve is S-polarized transmittance.

Curves are extended into the infrared spectrum to show the bandpass nature of the coating. In the transmission zone the filter looks like an uncoated glass slab. P-polarized transmittance is near 100%; S-polarized transmittance is ~91%. Notice the reduced transmission zone beyond 800 nm and the large transmission loss for S-polarized light (~91%T). Also note that the reflection zone near 540 nm is quite narrow. These problems will be remedied with the addition of the blocking filter. Layers of a ~quarterwave long-pass filter for a slightly shorter wavelength is appended to the above design (Fig. 12.6). The selected blocking filter has 21 layers with the same materials: VT = 2.1; VQ = 1.5. The 50% point for S-polarized light is the same wavelength as that of the final filter. The blocker improves the transmission of the final filter in addition to extending the P-polarized blocking zone to ~450 nm (Fig. 12.7).

If the materials have absorption, there are spike losses in reflection that do not show in transmission, and the use of many *reflection* targets is necessary to fix this problem (Fig. 12.8). More layers smooth out the blocking, and filters can be blocked further on the low-wavelength side with additional layers. A 74-layer filter composed of TiO_2 and SiO_2 has more than a 98% average reflection from the bandpass to 380 nm (Fig. 12.9). The design started with two 22-layer blockers added to the dichroic filter. Since the materials are absorbing, the targets need to specify reflectively (Fig. 12.10).

Hafnium oxide is used as the high-index material for the ultraviolet spectral range. The cutoff wavelength can be positioned at ~220 nm and higher. If necessary, additional blocking layers may be included in the design to extend the reflection zone. A filter for a telecom application designed to separate (combine) the 1250–1350 nm range from the 1400–1600 nm range is designed by utilizing the

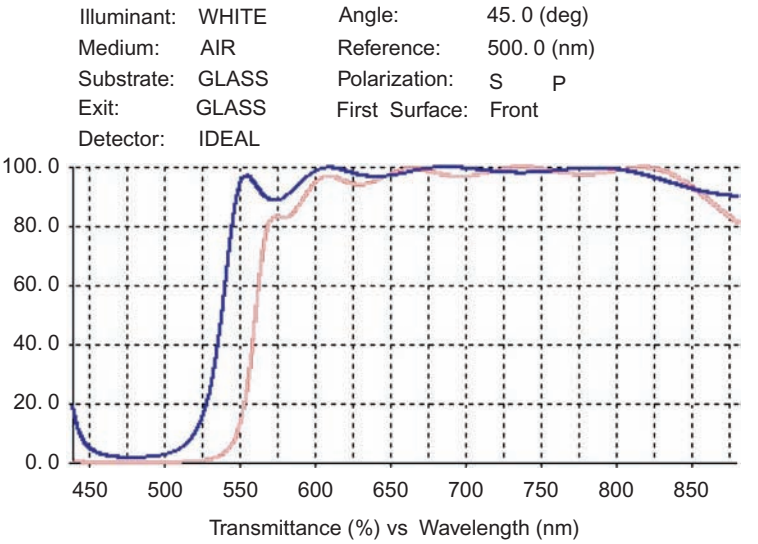

Figure 12.6 The added blocker. The higher curve at 550 nm is P-polarized transmittance; the curve is S-polarized transmittance.

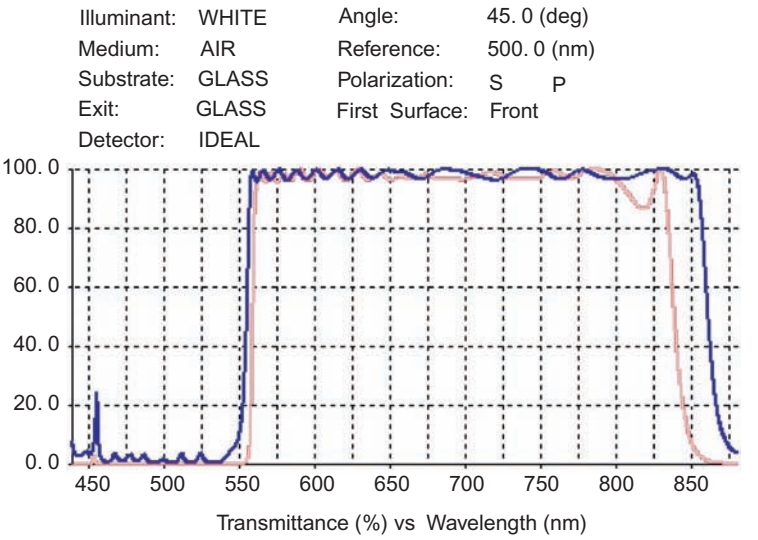

Figure 12.7 A 60-layer filter. The higher curve is P-polarized transmittance; the lower curve is S-polarized transmittance.

starting materials combination. Requirements are stringent for this possible fiber-to-the-premises (FTTP) filter. A 99% efficiency is expected for both wavelength streams (Fig. 12.11).

Filters with very fast slopes are required for Raman spectroscopy; many layers are needed to achieve this. A filter with a wide bandpass has the following starting design: $(2.3qwTa\ 2.21qwQ\ 2.21qwTa\ 2.2qwQ)^{27}$. After optimization,

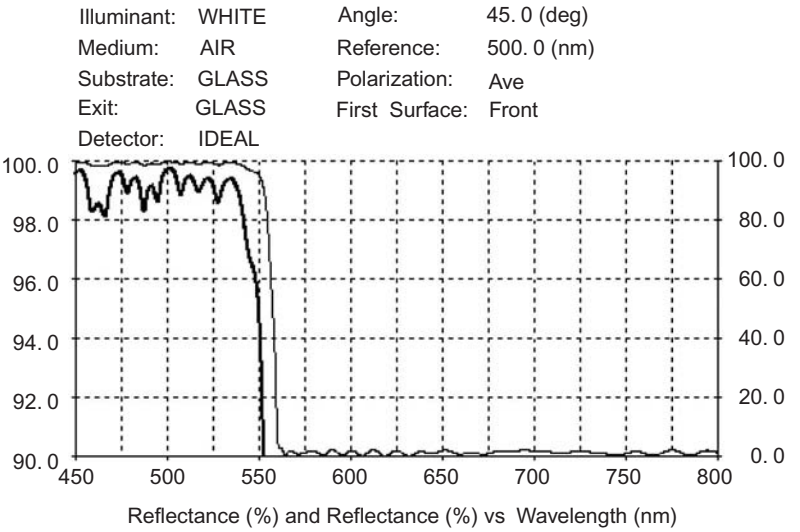

Figure 12.8 A 64-layer filter made with Ta_2O_5 and SiO_2. The thin line is reflectance; the thick line is zoom-in reflectance.

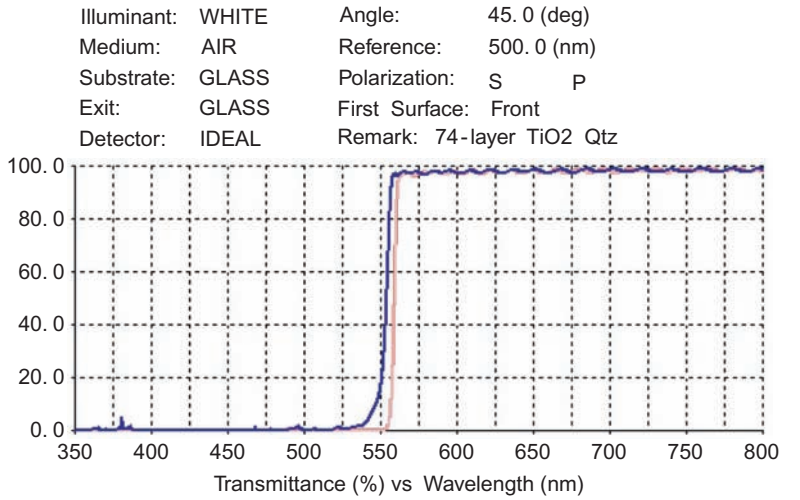

Figure 12.9 A TiO_2 quartz nonpolarizing color separator. The higher curve is P-polarized transmittance; the lower curve is S-polarized transmittance.

this 108-layer long-pass filter reflects more than 98% of the available light and transmits well over 90% average from 640 nm to beyond 1000 nm for a 633-nm laser reference (Fig. 12.12). No blocking filters are required to achieve the slope.

Blocking of the laser wavelength (~1%T avg.) is improved by adding a quarterwave-stack starting design at ~80% of the wavelength between the substrate and the filter; transmission is also improved to about 95%. Most of the losses are due to absorption. If the high-index material is changed to HfO_2, the same design can be used in the ultraviolet spectrum. The slope is very fast, and fewer layers can

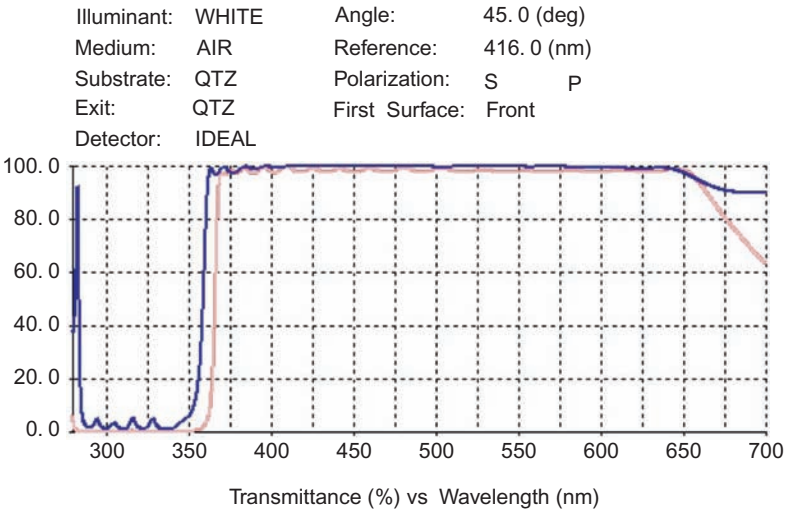

Figure 12.10 A 44-layer UV dichroic. The higher curve is P-polarized transmittance; the lower curve is S-polarized transmittance.

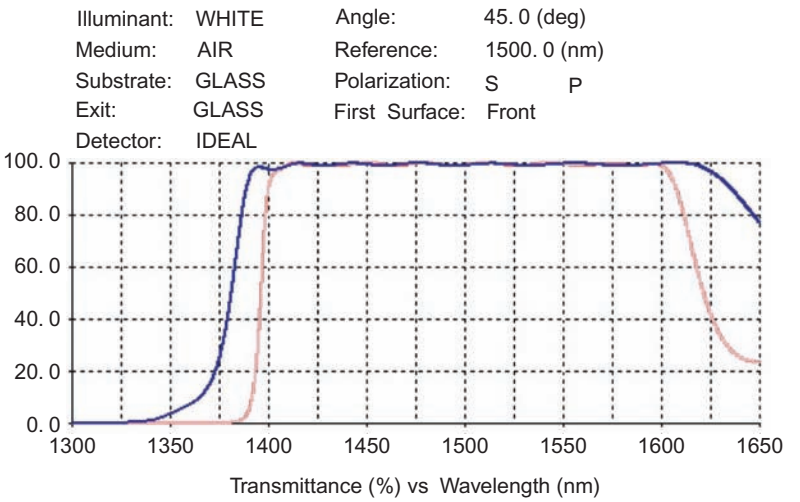

Figure 12.11 A 56-layer telecom filter for H = 2.1 and L = 1.5. The higher curve is P-polarized transmittance; the lower curve is S-polarized transmittance.

accomplish the long-pass criteria (Fig. 12.13). A 92-layer filter has a separation of 0.8 nm between polarization modes and the transmission zone extends to 400 nm. Filters with more layers designed from a starter of the type used for Fig. 12.12 feature transmission to 450 nm for a ~300-nm reflector.

12.4 Short-Pass Filters

The chapter of Thelen's book[4] also shows designs for short-pass filters. I selected one to use as the starting design for my short-pass filter.[9] The problem with

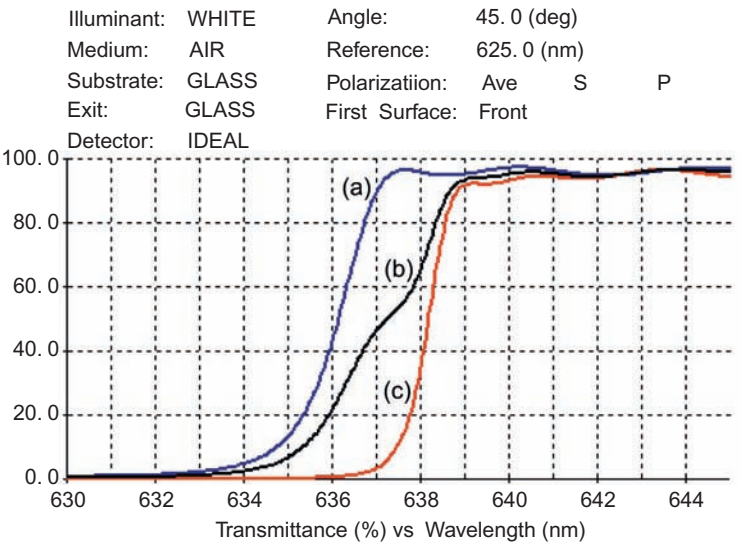

Figure 12.12 The cutoff of a 128-layer long-pass Raman filter. (a) The higher curve is P-polarized transmittance; (b) the middle line is for average transmittance; (c) the lowest line is S-polarized transmittance.

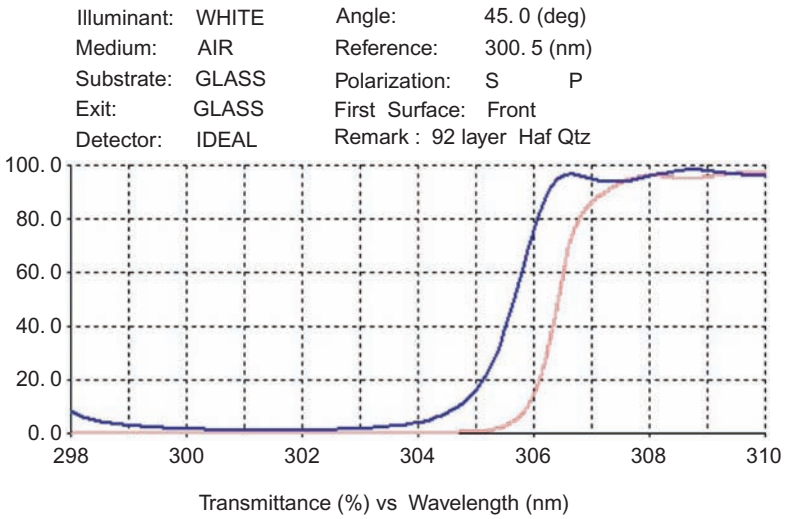

Figure 12.13 Raman long-pass filter for the UV region. The higher curve is P-polarized transmittance; the lower curve is S-polarized transmittance.

Thelen's designs comes from a lack of blocking, both for depth and distance. A blocking filter can be added to make a hybrid filter that allows a short-pass filter to have a reasonable spectral shape. Also, the blocking band for short-pass filters may be extended through the addition of more blocking filters. Many layers are necessary to achieve good spectral characteristics at 45 deg (Fig. 12.14).

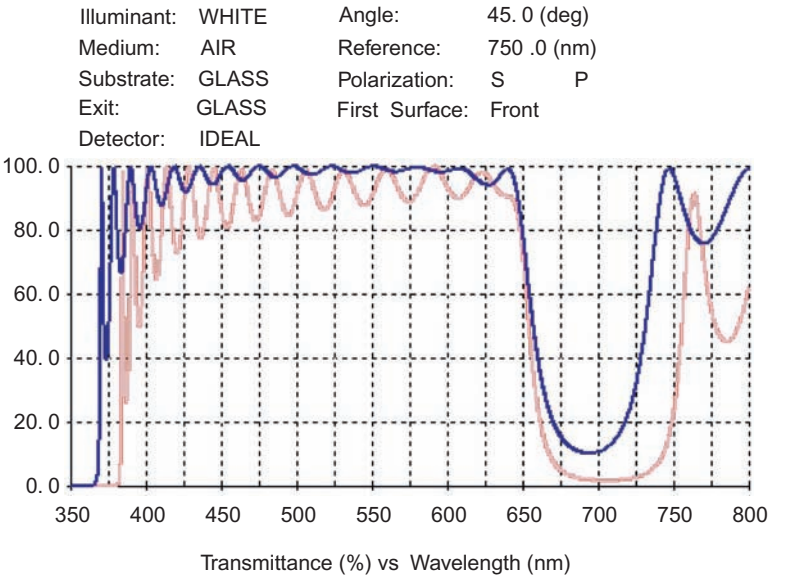

Figure 12.14 A 60-layer starting design. The higher curve is P-polarized transmittance; the lower curve is S-polarized transmittance.

From Thelen's book[4], one of the best layer combinations is in his figure 9.21: $(.3202H\ .3908L\ .6445H\ .6445L)^{15}$.

Although the slope is fast for the high-transmission edge, there is a lack of power in the P-polarization blocking. The curves look like a partially opened zipper. After smoothing the transmission zone through any optimization program, the blocking will be further degraded. Coating with tantalum pentoxide and silicon dioxide in an ion-beam sputter system is recommended. A high degree of thickness accuracy is possible for this method; adding a conventional blocker provides a superlative filter. A 650 nm cutoff filter is shown in Fig. 12.15.

Initial design: $1.08\ [(HL)^{12}\ H\ .5L]^1\ (.3202H\ .3908L\ .6445H\ .6445L)^{13}$.

A few more layers were added later for smoothing. This filter contains 80 layers of Ta_2O_5 and SiO_2 for 99% reflection at 700–800 nm and high transmission at 415–645 nm. The design was first deduced with 2.1 and 1.5 index films, and then the design was changed to the dispersive materials.

Construction details: A 26-layer blocker is first deposited. Then a 52-layer filter is appended. After optimization, two layers drop out. Low ripple comes from adding two thin layers between the substrate and the blocker and reoptimizing. After altering the materials, the low-wavelength edge shifts to the red. Reoptimization restores the bandpass to the correct position.

An example of a short-pass dichroic using TiO_2 for a high index with a starting design of a 69-layer edge filter and a 20-layer quarterwave blocker shows the high transmission and decent blocking zones that are possible (Fig. 12.16). A number of layers were removed when their thicknesses became less than 10 nm (Fig. 12.17). Adding another blocker to the two filters increases the range

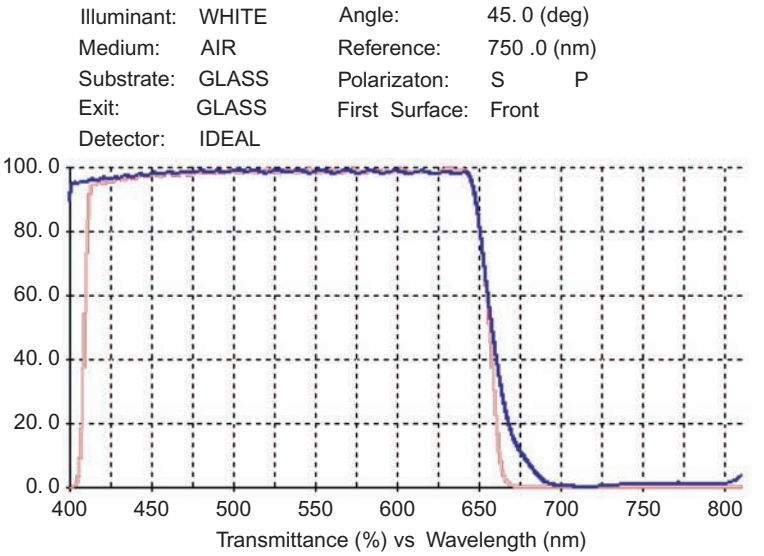

Figure 12.15 A combination short-pass filter. The higher curve is P-polarized transmittance; the lower curve is S-polarized transmittance.

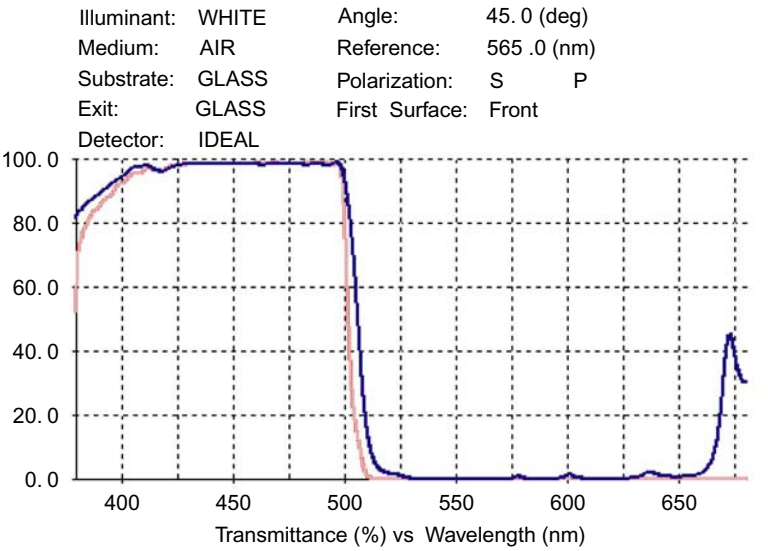

Figure 12.16 A 78-layer dichroic. The higher curve is P-polarized transmittance; the lower curve is S-polarized transmittance.

considerably. Figure 12.18 shows the P-polarized transmission of each filter by illustrating the point at which each filter does its work. For a reasonable blocking level the overlap point is at about 15%T for P-polarized light. The lack of blocking for the basic filter is glaringly shown in this figure. Despite this, the performance of a composite filter is fairly good as a hot mirror. Two thin layers are deposited

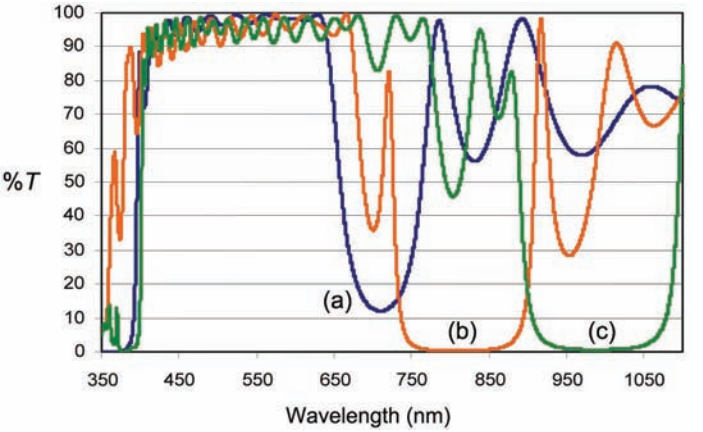

Figure 12.17 A 30-layer filter [line (a) at 950 nm] plus two 22-layer blockers [lines (b) and (c) at 950 nm].

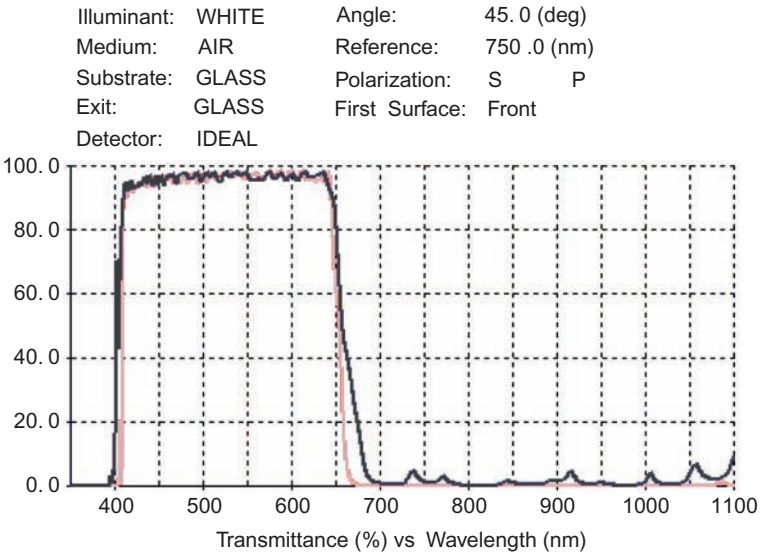

Figure 12.18 A 76-layer filter. The higher curve is P-polarized transmittance; the lower curve is S-polarized transmittance.

first, preceding the 22-layer blockers and the cutoff filter; these two layers increase the transmission of the filter considerably. The UV region can also be handled with the same approach (Fig. 12.19). Changing to HfO_2 for a high index and positioning the blocker closer to the dichroic yields a filter with essentially no leaks after smoothing. The starting design is a 28-layer blocker added to two thin starting layers (to increase transmission); it is then covered with a 44-layer dichroic. Blocking of higher wavelengths is feasible by adding more blockers. Short-pass filters are less efficient than long-pass filters because the layers are thicker and absorb more available light. If you have a choice, use long-pass filters.

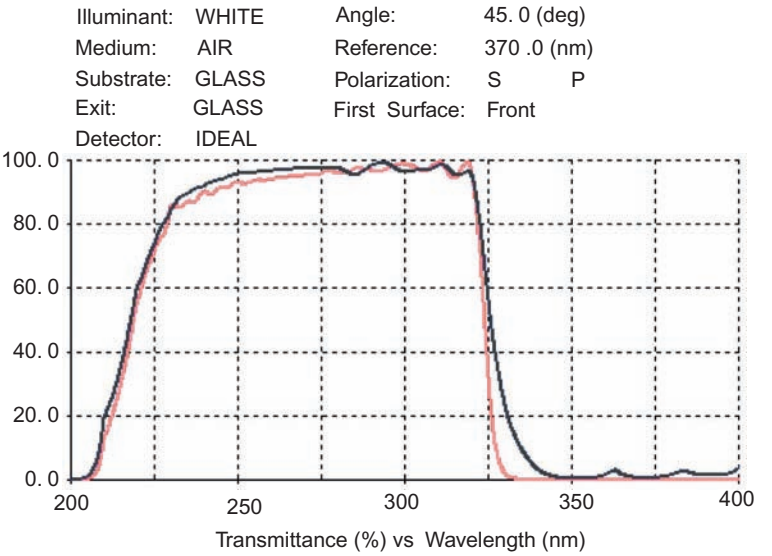

Figure 12.19 A 74-layer filter for the UV spectrum. The higher curve at 250 nm is P-polarized transmittance; the lower curve is S-polarized transmittance.

References

1. D. H. Cushing, "Bandpass filter for forty-five degree angle with low polarization properties," *Proc. Optical Interference Coatings Topical Meeting*, 226–228 (1998).
2. V. R. Costich, "Reduction of polarization effects in interference coatings," *Appl. Opt.* **9**, 866–870 (1970).
3. H. A. Macleod, *Thin Film Optical Filters*, 2nd ed., McGraw-Hill, New York (1986).
4. A. J. Thelen, *Design of Optical Interference Coatings*, McGraw-Hill, New York (1989).
5. P. W. Baumeister, "Bandpass design—applications to nonnormal incidence," *Appl. Opt.* **31**, 504–512 (1992).
6. D. H. Cushing, "Thin film interference filter for 45° angle of incidence inside a glass prism with extremely low polarization dependence," *Proc. 1999 OSA Annual Meeting* Santa Clara, CA (1999).
7. A. J. Thelen, "Non-polarizing interference films inside a glass cube," *Appl. Opt.* **15**, 2983–2985 (1976).
8. D. H. Cushing, "Long pass non-polarizing 45 degree dichroic filter," *Vacuum Technology & Coatings*, June 2005, 36–39.
9. D. H. Cushing, "Low polarization short pass filter for 45 degrees with good blocking characteristics," *Vacuum Technology & Coatings*, Aug 2005, 50–55.

Index

David Cushing was a thin-film consultant who had more than 40 years experience in the optical coating field. At the time of his death in 2009, he was programming and running a 48-inch box coater in the University of Arizona and pursuing independent studies of advanced spectral-design techniques. He authored papers on a variety of filter types and held 7 US patents and a number of world patents, mostly related to WDM filter designs. Former employment included 3 years as Director of Coating R&D at 3M Precision Optics and 10 years at JDS Uniphase Ottawa. He was technical director of OCA (MicroCoatings Inc) from 1971 to 1990. Before that he held various positions in Bairdco (Baird Atomic Inc).